

5-2011

Analysis of Band 4.1B in Integrin-Mediated Cell Adhesion and Signaling

Youngsin Jung

Follow this and additional works at: https://digitalcommons.library.tmc.edu/utgsbs_dissertations



Part of the [Cell Biology Commons](#), and the [Developmental Biology Commons](#)

Recommended Citation

Jung, Youngsin, "Analysis of Band 4.1B in Integrin-Mediated Cell Adhesion and Signaling" (2011). *The University of Texas MD Anderson Cancer Center UTHealth Graduate School of Biomedical Sciences Dissertations and Theses (Open Access)*. 108.

https://digitalcommons.library.tmc.edu/utgsbs_dissertations/108

This Dissertation (PhD) is brought to you for free and open access by the The University of Texas MD Anderson Cancer Center UTHealth Graduate School of Biomedical Sciences at DigitalCommons@TMC. It has been accepted for inclusion in The University of Texas MD Anderson Cancer Center UTHealth Graduate School of Biomedical Sciences Dissertations and Theses (Open Access) by an authorized administrator of DigitalCommons@TMC. For more information, please contact digitalcommons@library.tmc.edu.

Analysis of Band 4.1B in Integrin-Mediated Cell Adhesion and Signaling

By

Youngsin Jung, B.S.

Approved:

Joseph H. McCarty, Ph.D.

Supervisory Professor

Gary E. Gallick, Ph.D.

Georg Halder, Ph.D.

Victoria P. Knutson, Ph.D.

Renhao Li, Ph.D.

Approved:

Dean, The University of Texas

Graduate School of Biomedical sciences

Analysis of Band 4.1B in Integrin-Mediated Cell Adhesion and Signaling

A

DISSERTATION

Presented to the Faculty of

The University of Texas

Health Science Center at Houston

and

The University of Texas

M.D. Anderson Cancer Center

Graduate School of Biomedical Sciences

In Partial Fulfillment

of the Requirements

for the Degree of

DOCTOR OF PHILOSOPHY

by

Youngsin Jung, B.S.

Houston, Texas

May, 2011

DEDICATION

I would like to dedicate this dissertation
to my parents, Hyung Keun Jung and Hea Ran Chang,
who have always been my greatest support,
my sister, Yoon Seo Jung,
who has been cheering me through the life's ups and downs,
my aunt, Young Ran Chang,
who has always believed in me,
and
my grandparents, Seok Rok Chang and In Soon Kim,
who have been my inspiration.

ACKNOWLEDGEMENTS

I express immense gratitude to my mentor, Dr. Joseph McCarty, for his support throughout my Ph.D. training. His guidance has helped me become a better scientist. I would also like to thank the University of Texas-Houston M.D./Ph.D. Program and the Smith Research Foundation for their funding during my training at MD Anderson Cancer Center. I am extremely thankful for the members of my advisory, examining, and supervisory committees, Drs. Gary Gallick, Georg Halder, Victoria Knutson, Renhao Li, Zhimin Lu, and Renata Pasqualini, for taking time from their busy schedules to support my scientific development. I also thank the past and present members of the McCarty lab, including Mohammad Hossain, Aaron Mobley, Jeremy Tchaicha, Jae-Kyung Shin, Steve Reyes, Drs. Adam Hsu and Roman Schinder, for their support.

Analysis of Band 4.1B in Integrin-Mediated Cell Adhesion and Signaling

Publication No. _____

Youngsin Jung, B.S.

Supervisory Professor: Joseph McCarty, Ph.D.

Band 4.1B is a cytoskeletal adaptor protein that regulates various cellular behavior; however, the mechanisms by which Band 4.1B contributes to intracellular signaling are unclear. This project addresses *in vivo* and *in vitro* functions for Band 4.1B in integrin-mediated cell adhesion and signaling. Band 4.1B has been shown to bind to $\beta 8$ integrin, although cooperative functions of these two proteins have not been determined. Here, functional links between $\beta 8$ integrin and Band 4.1B were investigated using gene knockout strategies. Ablation of $\beta 8$ integrin and Band 4.1B genes resulted in impaired cardiac morphogenesis, leading to embryonic lethality by E11.5. These embryos displayed malformation of the outflow tract that was likely linked to abnormal regulation of cardiac neural crest migration. These data indicate the importance of cooperative signaling between $\beta 8$ integrin and Band 4.1B in cardiac development. The involvement of Band 4.1B in integrin-mediated cell adhesion and signaling was further demonstrated by studying its functional roles *in vitro*. Band 4.1B is highly expressed in the brain, but its signaling in astrocytes is not understood. Here, Band 4.1B was shown to promote cell spreading likely by interacting with $\beta 1$ integrin via its band 4.1, ezrin, radixin, and moesin (FERM)

domain in cell adhesions. In astrocytes, both Band 4.1B and $\beta 1$ integrin were expressed in cell-ECM contact sites during early cell spreading. Exogenous expression of Band 4.1B, especially its FERM domain, enhanced cell spreading on fibronectin, an ECM ligand for $\beta 1$ integrin. However, the increased cell spreading was prohibited by blocking $\beta 1$ integrin. These findings suggest that Band 4.1B is crucial for early adhesion assembly and/or signaling that are mediated by $\beta 1$ integrin. Collectively, this study was the first to establish Band 4.1B as a modulator of integrin-mediated adhesion and signaling.

Table of Contents

Approval Signatures.....	i
Title Page.....	ii
Dedication.....	iii
Acknowledgments.....	iv
Abstract.....	v
Table of Contents.....	vii
List of Figures.....	x
List of Tables.....	xiii
Chapter 1: Introduction.....	1
1.1. Cell migration.....	1
1.2. Protein 4.1 superfamily.....	6
1.3. Band 4.1B.....	13
1.4. Integrin family.....	17
1.5. Integrin activation and signaling.....	23
1.6. Integrin signaling and Band 4.1B.....	27
1.7. Integrins, Band 4.1B, and organogenesis.....	29
1.8. Specific aims.....	31
Chapter 2: Materials and Methods.....	33
2.1. Experimental mice.....	33
2.2. Astrocyte isolation.....	34
2.3. Immunoblotting.....	35
2.4. Biotinylation and immunoprecipitation.....	35

2.5.	Immunohistochemistry.....	36
2.6.	Immunofluorescence.....	37
2.7.	Whole-mount immunostaining.....	38
2.8.	Adhesion assays.....	39
2.9.	Statistical analysis.....	40
Chapter 3: Specific Aim I.....		41
3.1.	Introduction.....	41
3.2.	Results.....	42
3.2.1.	Genetic knockouts of $\beta 8$ integrin and Band 4.1B demonstrate lethal phenotypes by E11.5.....	42
3.2.2.	Cardiovascular abnormalities contribute to the lethal phenotype of $\beta 8^{-/-};4.1B^{-/-}$ embryos.....	56
3.2.3.	$\beta 8^{-/-};4.1B^{-/-}$ embryos display abnormal morphogenesis of the outflow tract and myocardium of the heart.....	68
3.2.4.	Neural crest cell migration is impaired in $\beta 8^{-/-};4.1B^{-/-}$ embryos.....	76
3.3.	Discussion.....	81
Chapter 4. Specific Aim II.....		87
4.1.	Introduction.....	87
4.2.	Results.....	88
4.2.1.	Lack of Band 4.1B expression does not affect integrin expression in astrocytes.....	88

4.2.2. Band 4.1B shows time-dependent changes in its subcellular localization.....	94
4.2.3. Band 4.1B and $\beta 1$ integrin co-localize to cell-ECM contact sites.....	100
4.2.4. Band 4.1B is not necessary for cell adhesion to the ECM.....	109
4.2.5. The FERM domain of Band 4.1B enhances cell spreading on fibronectin.....	112
4.3. Discussion.....	118
Chapter 5. Summary and Future Directions.....	123
References.....	132
Vita.....	147

List of Figures

Chapter 1. Introduction

Figure 1.	Cell migration.....	3
Figure 2.	Protein 4.1 superfamily.....	7
Figure 3.	Each conserved domain of Band 4.1B interacts with unique binding partners.....	16
Figure 4.	Integrin family.....	19
Figure 5.	Integrins are involved in various intracellular signaling pathways.....	22
Figure 6.	Talin regulates integrin inside-out activation by interacting with the β subunit cytoplasmic domain.....	24

Chapter 3. Specific Aim I

Figure 7.	The genotypes of embryos are determined by PCR-based gene amplification methods.....	44
Figure 8.	$\beta 8^{-/-}$ and $\beta 8^{-/-};4.1B^{-/-}$ mice develop intracerebral hemorrhage after E11.5.....	48
Figure 9.	Kaplan-Meier survival analysis.....	50
Figure 10.	Adult $\beta 8^{-/-}$ and $\beta 8^{-/-};4.1B^{-/-}$ mice develop hydrocephalus.....	52
Figure 11.	Double knockout embryos develop lethal cardiovascular phenotypes.....	55
Figure 12.	CNS vascular pathologies are seen in $\beta 8^{-/-}$ and $\beta 8^{-/-};4.1B^{-/-}$ embryos.....	57
Figure 13.	$\beta 8^{-/-};4.1B^{-/-}$ mice lack an elaborate vascular network.....	59
Figure 14.	Yolk sac vascular pathologies in $\beta 8^{-/-};4.1B^{-/-}$ embryos.....	61

Figure 15.	The expression of Band 4.1B and $\alpha\beta 8$ integrin in yolk sacs.....	63
Figure 16.	The expression of Band 4.1B and $\alpha\beta 8$ integrin in the embryonic heart.....	66
Figure 17.	Defective heart morphogenesis in $\beta 8^{-/-};4.1B^{-/-}$ embryos.....	69
Figure 18.	Reduced expression of desmin in $\beta 8^{-/-};4.1B^{-/-}$ embryos.....	72
Figure 19.	αV integrin and Band 4.1B proteins are co-expressed in the embryonic heart.....	74
Figure 20.	Abnormal patterns of neurofilament expression in $\beta 8^{-/-};4.1B^{-/-}$ embryos.....	77
Figure 21.	Neurofilament expression patterns are abnormal in $\beta 8^{-/-};4.1B^{-/-}$ trunks.....	79

Chapter 4. Specific Aim II

Figure 22.	Protein 4.1 expression in astrocytes.....	89
Figure 23.	Integrin expression in astrocytes.....	92
Figure 24.	Protein 4.1B and 4.1G, but not 4.1N, localize to cell-ECM contact sites.....	95
Figure 25.	Protein 4.1 sub-cellular localization changes as cell-cell contacts are formed.....	98
Figure 26.	Band 4.1B and $\beta 1$ integrin localize to adhesions during early stages of cell adhesion and spreading.....	101
Figure 27.	Band 4.1B and $\beta 1$ integrin co-localize during early cell spreading.....	104

Figure 28.	Band 4.1B and β 1 integrin co-localize in the neuroepithelium.....	107
Figure 29.	Band 4.1B is not necessary for cell adhesion to the ECM.....	110
Figure 30.	The FERM domain of Band 4.1B enhances cell spreading on fibronectin.....	113
Figure 31.	The Band 4.1B FERM domain promotes cell spreading mediated by β 1 integrin.....	116

List of Tables

Chapter 1. Introduction

Table 1.	Protein 4.1 family.....	10
----------	-------------------------	----

Chapter 3. Specific Aim I

Table 2.	Genotype distribution of mice.....	46
----------	------------------------------------	----

Chapter 1. Introduction

1.1. Cell migration

Cell migration and invasion are crucial for numerous physiological and pathological events, such as embryogenesis, tissue repair, immune response, vascular diseases, and cancer (Costa and Parsons 2010; Nowotschin and Hadjantonakis, 2010; Peri F, 2010; Caswell et al., 2008). Characterizing regulatory signaling pathways of cell motility, therefore, is pivotal to understanding human physiology and pathology. The regulation of cell motility requires the complex coordination of cell-extracellular matrix (ECM) interactions and cytoskeleton organization (Teckchandani et al., 2009).

Adherent cells first begin to migrate by forming protrusions termed lamellipodia and filopodia (Le Clainche and Carlier, 2008). These protrusions are stabilized by adhesions that connect the ECM to the cytoskeleton (Hood and Cheresch, 2002). Integrin cell adhesion receptors are essential for orchestrating adhesion formation, cytoskeleton organization, and cell polarity during migration and invasion (Ridely et al., 2003). After binding to ECM ligands, integrins recruit and/or interact with multiple adaptors and signaling molecules, such as α -actinin, focal adhesion kinase (FAK), tensin, and talin, which in turn bind to actin-binding vinculin and paxillin (Zamir and Geiger, 2001; Calderwood et al., 2000). At the adhesion sites, integrins provide traction for the cell body to move forward by linking the ECM to the cytoskeleton, and also function as mechanosensors that can alter cytoskeletal dynamics (Webb et al., 2002). During migration, adhesions are disassembled at both leading and trailing edges, and integrins are actively recycled.

Proteases degrade various ECM components, including fibronectin, laminin, and collagen (Friedl and Wolf, 2003). Some proteases, such as seprase, MMP1, MMP2, MT1-MMP directly bind to integrins (Dumin et al., 2001; Ellerbroek et al., 2001; Galvez et al., 2002). These processes allow for dynamic regulation of cell's forward motion and new protrusion formation (Ridely et al., 2003) (Figure 1). Invasion also involves adhesion formation, proteolysis of ECM components, and cell movement, although it requires penetration of tissue barriers by cells (Friedl and Wolf, 2003).

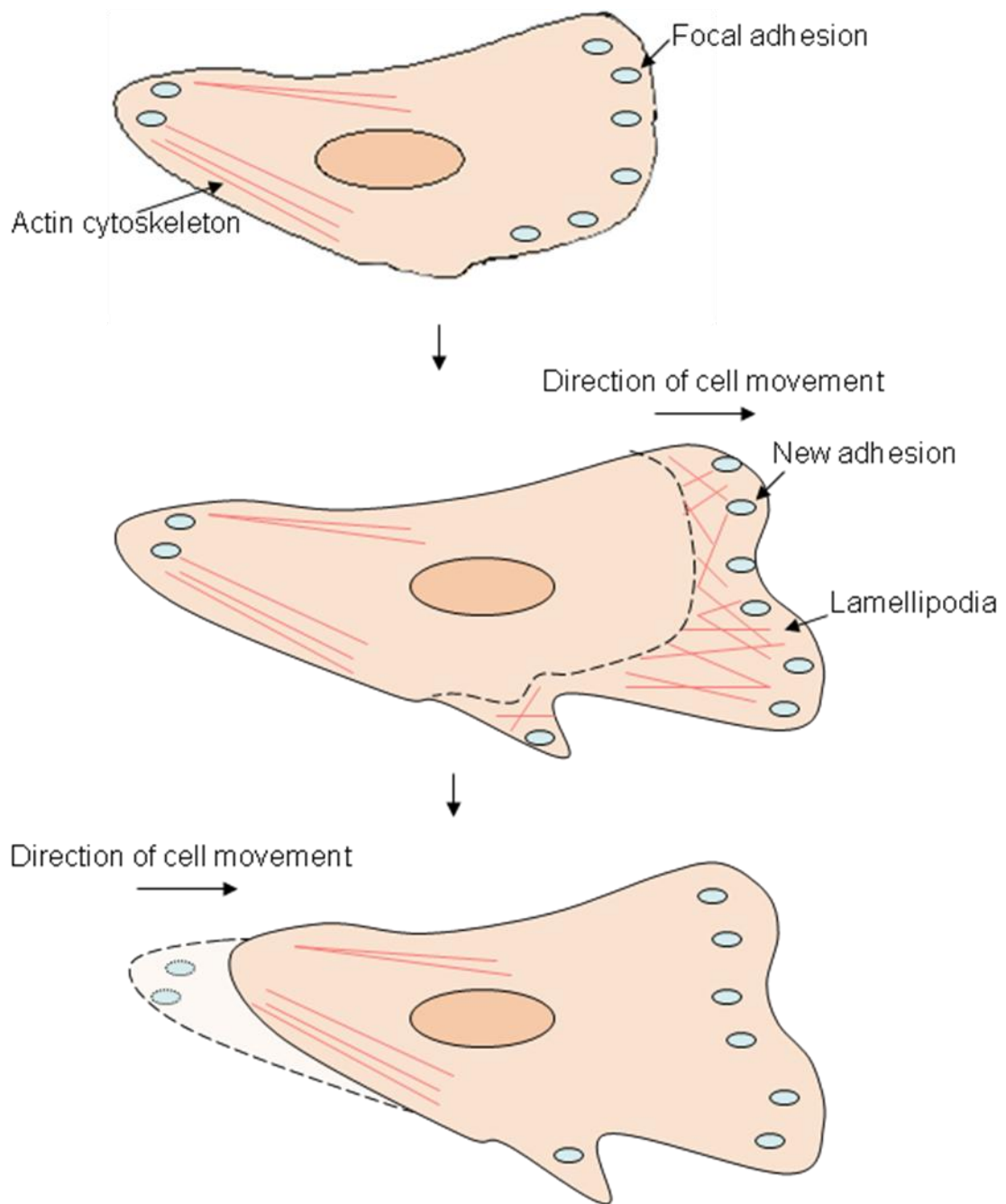


Figure 1. Cell migration.

Figure 1. Cell migration.

Cell migration begins with the formation of lamellipodia. Focal adhesions that connect the ECM to the cytoskeleton stabilize these protrusions. At the site of adhesion formation, integrins provide traction for the forward movement of cell body and alter cytoskeletal dynamics by acting as mechanosensors. Adhesion disassembly at both leading and trailing edges allow tail retraction and new protrusion formation, leading to cell's forward motion (Adopted from Ridley et al., 2003 with permission from AAAS).

In addition to integrins, multiple signaling molecules are involved in cell migration. For example, talin acts as a link between integrins and the actin cytoskeleton and regulates integrin-actin associations (Zhang et al., 2008; Cram et al., 2003). Mice genetically null for talin are embryonic lethal due to defective cytoskeletal organization and cell migration (Monkley et al., 2000). Vinculin is an actin binding protein that localizes to focal adhesions. Fibroblasts that lack vinculin expression showed increased cell migration whereas vinculin overexpressing cells displayed decreased cell migration (Xu et al., 1998; Rodriguez Fernandez et al., 1992). Vinculin is thought to be required to strengthen the linkage between talin and the actin cytoskeleton (Legate et al., 2009). Actin dynamics are regulated by Rho GTPases. RhoA, Rac, and cdc42 modulate cell contractility, lamellipodium formation, and cell polarity, respectively (Fukata et al., 2003; Legate et al., 2009; van Hengel et al., 2008). In addition, FAK is a signaling molecule that is activated early in cell migration and is crucial for focal adhesion turnover that promotes directional cell motility (Mitra et al., 2005)

Band 4.1B is a cytoskeletal adaptor protein that has been postulated to be important for a wide range of cellular processes, including cell motility. In sarcoma cell lines, the decreased expression of Band 4.1B enhanced cell motility and promoted metastatic phenotypes, whereas the re-expression of Band 4.1B in these cells reduced cell migration (Cavanna et al., 2007). However, the mechanisms by which Band 4.1B regulates cell migration are unknown. Determining how Band 4.1B affects these cellular events will lead to novel understanding of cell migration signaling cascades.

1.2. Protein 4.1 superfamily

Band 4.1B belongs to the protein 4.1 superfamily (Parra et al., 2000). All members of this superfamily contain an N-terminal band 4.1, ezrin, radixin, and moesin (FERM) domain (Sun et al., 2002). The protein 4.1 superfamily can be subdivided into five groups based on the protein sequence similarity: protein 4.1 family, ERM proteins, talin-related molecules, protein tyrosine phosphatases (PTPH), and novel band 4.1-like 4 (NBL4) proteins (Figure 2).

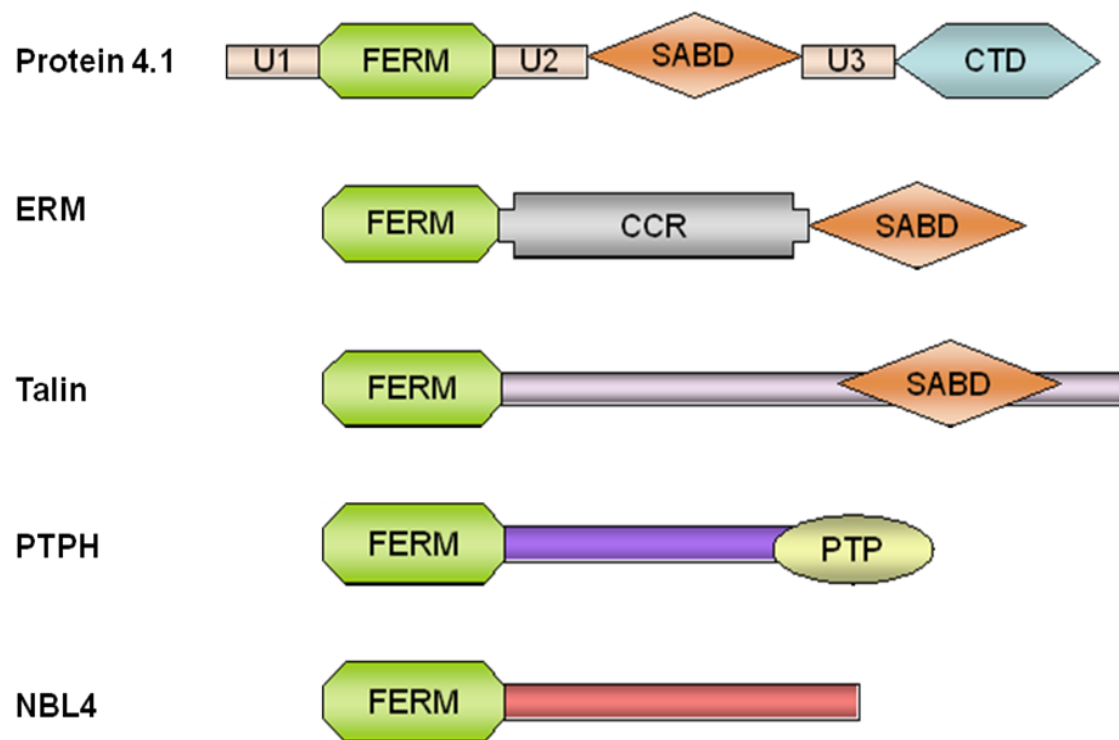


Figure 2. Protein 4.1 superfamily.

Figure 2. Protein 4.1 superfamily.

The members of the protein 4.1 superfamily are characterized by the presence of an N-terminal FERM domain. About 50 members have been identified to date. The members are divided into five subfamilies based on sequence homology: protein 4.1 family, ERM proteins, talin-related molecules, protein tyrosine phosphatases (PTPH), and novel band 4.1-like 4 (NBL4) proteins. FERM, Protein 4.1-ezrin-radixin-moesin domain; ABD actin-binding domain; CCR, coiled-coil region; CTD, carboxyl terminal domain; PTP, protein tyrosine phosphatase; SABD, spectrin-actin binding domain; U1, U2, U3, unique regions (Adopted from Sun et al., 2002 with permission from J Cell Sci).

These proteins not only provide links between the cell membrane and the actin cytoskeleton, but also play roles in cell adhesion, proliferation, motility, cell cycle regulation, and various other intracellular signaling (Diakowski et al., 2006).

The protein 4.1 family consists of Band 4.1R (erythrocyte), Band 4.1G (general), Band 4.1B (brain), Band 4.1N (neuronal), and Band 4.1O (ovary). The name 4.1 was given based on the band position of Band 4.1R, the first member identified, on 2D SDS polyacrylamide gel electrophoresis (Holzwarth et al., 1976). Erythrocyte membrane proteins were separated by SDS-PAGE and named according to their motility on gel electrophoresis. The band with slowest mobility was named band 1, and the fastest migrating band was named band 7. As resolution improved, additional bands were named using decimals. Bands 1-3 and 5-7 were identified as spectrin, ankyrin, anion transport exchanger, actin, G3PD, and stomatin, respectively. However, the name of 4th band remained Band 4.1 (Yawata, 2003).

In addition to the N-terminal FERM domain, the members of the protein 4.1 family contain an internal spectrin actin binding domain (SABD), a C-terminal domain (CTD), and three unique domains (Sun et al., 2002) (Figure 2). The FERM domain, SABD, and CTD are highly conserved among the various members. The 30kDa FERM domain is made of three lobes that form a clover leaf-like structure (Han et al., 2000). The FERM domains of Band 4.1G, Band 4.1B, and Band 4.1N share 74%, 73%, and 71% structural similarities with Band 4.1R, respectively (Sun et al., 2002). This domain interacts with multiple integral membrane proteins, such as glycophorin C, p55, and calmodulin (Gascard and Cohen, 1994; Marfatia et al.,

1994; Nunomura et al., 2000). The 10kDa SABD binds spectrin and actin, as the name suggests (Correas et al., 1986), although Band 4.1N's SABD does not interact with spectrin and actin (Gimm et al., 2002). By forming the spectrin-actin complex, this domain influences membrane stability (Diakowski et al., 2006). The 22/24kDa CTD is crucial for interacting with cell surface proteins, including occludin, zonula occludens-1, and zonula occludens-2 (Mattagajasingh et al., 2000), as well as a translational complex subunit, eIF3-p44 (Hou et al., 2000).

Each member of the protein 4.1 family is encoded by genes located on different chromosomes and has somewhat overlapping tissue expression patterns (Table 1).

Table 1. Protein 4.1 family (Adopted from Sun et al., 2002 with permission from J Cell Sci)

Protein	Chromosome	Tissue Distribution
4.1R	1p36.2-p34	Erythrocytes, brain
4.1G	6q23	Heart, brain, placenta, lung, skeletal muscle, kidney, pancreas, gonads
4.1N	20q11.2-q12	Brain, peripheral nerve
4.1B	18p11.3	Brain, heart, lung, kidney, intestine, testis, adrenal gland
4.1O	9q21-22	Ovary

Four of the members are expressed in the brain, although they are found in different cell populations. For example, Band 4.1N is expressed in virtually all neurons (Walensky et al., 1999) whereas Band 4.1R is localized in granule cells of the cerebellum and dentate gyrus (Walensky et al., 1998). Band 4.1B is found in purkinje cells of the cerebellum, pyramidal cells of the hippocampus, neurons of thalamic nuclei and olfactory bulbs (Parra et al., 2000).

The ERM family is composed of ezrin, radixin, moesin, and merlin. These proteins share approximately 75% sequence homology (Diakowski et al., 2006). The members of the ERM family is characterized by the presence of an N-terminal ERM association domain (N-ERMAD) and a C-terminal actin-binding domain (C-ERMAD) that are separated by an α -helical coiled coil region (CCR) (Sun et al., 2002) (Figure 2). The FERM domains of ERM proteins and merlin share about 30% structural similarities with Band 4.1R (Sun et al., 2002). These proteins have been implicated in connecting the actin cytoskeleton to CD43, CD44, ICAM1-3, Na^+/H^+ exchanger-3, and cystic fibrosis transmembrane regulator (Bretscher et al., 2002). Merlin, also known as neurofibromatosis 2 (NF2) or schwannomin, is a schwannoma suppressor that regulates cell proliferation and motility (Shermen and Gutmann, 2001). ERM protein activation is regulated by conformational changes (Fehon et al., 2010). ERM proteins exist in inactive state where they maintain closed conformation by binding of C-ERMAD to the FERM domain (Gary and Bretscher 1995). Release of C-ERMAD from the FERM domain activates ERM proteins and exposes binding sites in these two domains, including the F-actin binding site in C-ERMAD (Fehon et al., 2010). Each ERM protein has a

phosphorylation site that is important for its activation. Moesin, ezrin, and radixin are phosphorylated on Thr558, Thr576, and Thr564, respectively (Nakamura et al., 1995; Fievet et al., 2004). Multiple kinases have been shown to phosphorylate these Thr residues, including Rho kinase, protein kinase C α (PKC α), PKC θ , NF- κ B-inducing kinase, and lymphocyte-oriented kinase (Matsui et al., 1998; Ng et al., 2001; Belkina et al., 2009; Simons et al., 1998). In addition, other phosphorylation sites have been demonstrated to be involved in ERM activation. Thr235 can be phosphorylated by cyclin-dependant kinase 5 (CDK5) (Yang and Hinds 2003). Furthermore, Tyr145 and Tyr553 on ezrin are phosphorylated by epidermal growth factor receptor (EGFR) (Krieg and Hunter, 1992).

Talin forms an anti-parallel rod-shaped homodimer that contains an N-terminal FERM domain, sharing 20% sequence similarity with Band 4.1R (Anthis and Campbell, 2011) (Figure 2). The FERM domain consists of F1, F2, and F3 subdomains (Moser et al., 2009). The F3 domain is similar to phosphotyrosine binding (PTB) domain, and binds to the integrin cytoplasmic tails, phosphatidylinositol 4-phosphate 5-kinase γ (PIPKI γ), and layilin (Anthis and Campbell, 2011). The rod domain contains binding sites for vinculin and a second integrin binding site (Critchley and Gingras, 2008). The N-terminal FERM domain is 50 kDa and the C-terminal rod is 220kDa (Calderood, 2004). Talin localizes to focal adhesions and the membrane ruffles of migrating cells (Critchley, 2000). Talin plays crucial roles in integrin signaling, focal adhesion formation and organization, and cell migration (Shattil et al., 2010; Critchley, 2009; Zhang et al., 2008; Calderwood and Ginsberg, 2003).

The PTPH family consists of PTPH1 and PTPMEG that contain an N-terminal FERM domain and a C-terminal phosphatase domain (Gu et al., 1991) (Figure 2). The FERM domain of the PTPH proteins has 37% sequence homology with Band 4.1R (Sun et al., 2002). They are involved in regulating cytoskeletal dynamics, cell cycle progression, and cell proliferation (Diakowski et al., 2006). NBL4 also has an N-terminal FERM domain that shares 40% sequence identity with Band 4.1R (Sun et al., 2002) (Figure 2). NBL4 functions as a regulator of cell polarity, proliferation, and migration by being a part of the β catenin/Tcf signaling cascade (Ishiguro et al., 2000).

1.3. Band 4.1B

Band 4.1B, a member of the protein 4.1 family, was originally discovered in non-small cell lung carcinomas. Differentially expressed in adenocarcinoma of lung (DAL-1), a truncated Band 4.1B gene that lacks complete U1 and CTD, and partial U2 and SABD, was found to be absent in these tumors by differential display reverse transcriptase polymerase chain reaction (RT-PCR) (Tran et al., 1999). The full length protein has a molecular mass of 125-145kDa depending on alternative splicing (Tran et al., 1999). Alternatively spliced forms of Band 4.1B are expressed in a tissue specific manner. Band 4.1B is the most abundant member of the protein 4.1 family in the brain. In situ hybridization has shown that 4.1B mRNA is highly concentrated in the cerebellum, hippocampus, thalamic nuclei, and olfactory bulb (Parra et al., 2000). In addition, Band 4.1B is found in the heart, lungs, kidneys, intestine, testes, adrenal glands, and skeletal muscle (Parra et al., 2000).

Subcellularly, this protein is localized to the plasma membrane where cells make contact with one another, suggesting its functions in cell-cell/cell-matrix interactions (Parra et al., 2000).

Most of the studies on Band 4.1B have focused on its potential roles in tumor suppression and progression. Since its original discovery (Tran et al., 1999), Band 4.1B gene expression has been shown to be down-regulated in various tumors, including meningiomas and carcinomas of breast, kidney, colon/rectum, and prostate. Expressing DAL-1 in the non-small cell lung carcinomas that lacked DAL-1 expression resulted in suppression of tumor growth, suggesting its role as a negative growth regulator (Tran et al., 1999). Loss of heterozygosity in the chromosome 18p11.3 where Band 4.1B is located has been reported in 38% of non-small cell lung carcinomas (Tran et al., 1999) and 76% of sporadic meningiomas (Gutmann et al., 2001), further providing evidence for Band 4.1B as a tumor suppressor. Recently, a Band 4.1B knockout mouse model was developed to characterize the functions of Band 4.1B in tumorigenesis. Interestingly, these mice were not prone to develop tumors (Yi et al., 2005). No differences in cell proliferation and apoptosis were found between the Band 4.1B wild type and knockout mice (Yi et al., 2005). However, unlike the 4.1B knockout mice, Band 4.1B deficient transgenic adenocarcinoma of the mouse prostate (TRAMP) mice developed tumors that displayed more aggressive and highly metastatic phenotypes (Wong et al., 2007). These suggest that Band 4.1B is critical for tumor progression and metastasis, rather than tumor formation. Alternatively, Band 4.1B mutations in

combination with other mutations in oncogenes or tumor suppressors may promote tumor formation.

Another member of the protein 4.1 superfamily, merlin, is a well established tumor suppressor protein. Merlin has been demonstrated to negatively regulate several cellular properties that are important for cell-cell and cell-substrate interactions. Merlin impairs cell motility, attachment, and spreading (Gutmann et al., 1999). It has been also suggested that merlin inhibits cell proliferation by modulating cell adhesion (Gutmann et al, 1999). Given the homology between merlin and Band 4.1B, Band 4.1B may function similarly to merlin, regulating various intracellular signaling pathways. Abnormal regulation of these processes in the absence of Band 4.1B may lead to tumor progression and metastasis in tumors lacking Band 4.1B. Indeed, Band 4.1B has been shown to suppress cell proliferation in meningiomas (Gutmann et al., 2001). In addition, metastatic sarcoma cell lines with loss of Band 4.1B expression have displayed increased motility and chemotactic responses (Cavanna et al., 2007).

Despite the proposed roles of Band 4.1B, the mechanisms by which Band 4.1B contributes to various intracellular signaling cascades are not clear. One approach to studying Band 4.1B's functions is to examine the binding partners of Band 4.1B. Each domain of Band 4.1B interacts with a different set of proteins (Bernkopf and Williams, 2008) (Figure 3).

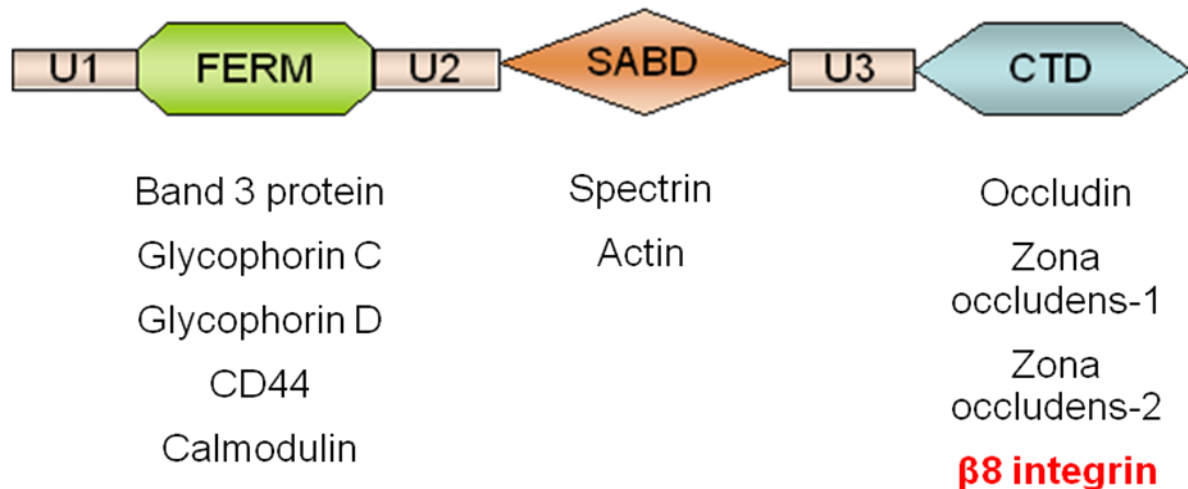


Figure 3. Each conserved domain of Band 4.1B interacts with unique binding partners.

Multiple proteins have been identified to interact with Band 4.1B. Each domain of Band 4.1B binds to a set of molecules without overlaps with other conserved regions. The FERM domain interacts with various transmembrane proteins. The SABD is involved in spectrin-actin complex formation, as the name suggests. The CTD domain appears to be important for interacting with cell surface proteins. Recently, $\beta 8$ integrin was shown to interact with the CTD of Band 4.1B via its cytoplasmic tail (Adopted from Bernkopf and Williams, 2008 with permission from Ashley Publications Ltd).

McCarty and colleagues identified $\beta 8$ integrin as an interacting molecule of Band 4.1B (2005a). The cytoplasmic tail of $\beta 8$ integrin interacts with the CTD of Band 4.1B as demonstrated by the yeast two-hybrid study and co-immunoprecipitation (McCarty et al., 2005a). $\beta 8$ integrin is critical for cell-matrix interactions and intracellular signaling, especially in the central nervous system (CNS). Given the importance of integrins in multiple cellular events, studying the functional links between Band 4.1B and integrins will enhance our understanding of Band 4.1B's functional roles.

1.4. Integrin family

The integrin family of major cell adhesion receptors is comprised of 18α and 8β subunits that form 24 $\alpha\beta$ heterodimeric receptors. Evolutionary studies indicate that both α and β integrin genes are from a common ancestral gene by gene duplications and that these genes are highly conserved in vertebrates (Huhtala et al., 2005). Integrin α and β subunits are consisted of an extracellular domain, a transmembrane helix, and a cytoplasmic tail. The extracellular domain is 700-1000 residues in length (Hynes, 2002). This portion contains a ligand binding site that is comprised of the β propeller and the plexin-semaphorin-integrin domains of α subunit, and the βI (or βA) and the hybrid domains of β subunit (Takada et al., 2007). The α and β cytoplasmic tails are 25-50 residues in size except for the $\beta 4$ tail, which is made of 1000 amino acids (Hynes, 2002). The α cytoplasmic domain has a conserved GFFKR motif that is critical for $\alpha\beta$ cytoplasmic tail interactions

(Harbeger and Calderwood, 2008). The β subunits contain an NPxY motif in their cytoplasmic domains, which is important for integrin activation (Takada et al., 2007).

Integrins can be divided into multiple subgroups based on their ECM ligands: 1) laminin-binding integrins, including $\alpha 1\beta 1$, $\alpha 2\beta 1$, $\alpha 3\beta 1$, $\alpha 6\beta 1$, $\alpha 7\beta 1$, and $\alpha 6\beta 4$; 2) collagen-binding integrins, such as $\alpha 1\beta 1$, $\alpha 2\beta 1$, $\alpha 3\beta 1$, $\alpha 10\beta 1$, and $\alpha 11\beta 1$; 3) leukocyte integrins, including $\alpha L\beta 2$, $\alpha M\beta 2$, $\alpha X\beta 2$, and $\alpha D\beta 2$; and 4) RGD binding integrins, like $\alpha 5\beta 1$, $\alpha V\beta 1$, $\alpha V\beta 3$, $\alpha V\beta 5$, $\alpha V\beta 6$, $\alpha V\beta 8$, and $\alpha IIb\beta 3$ (Hynes, 2002) (Figure 4).

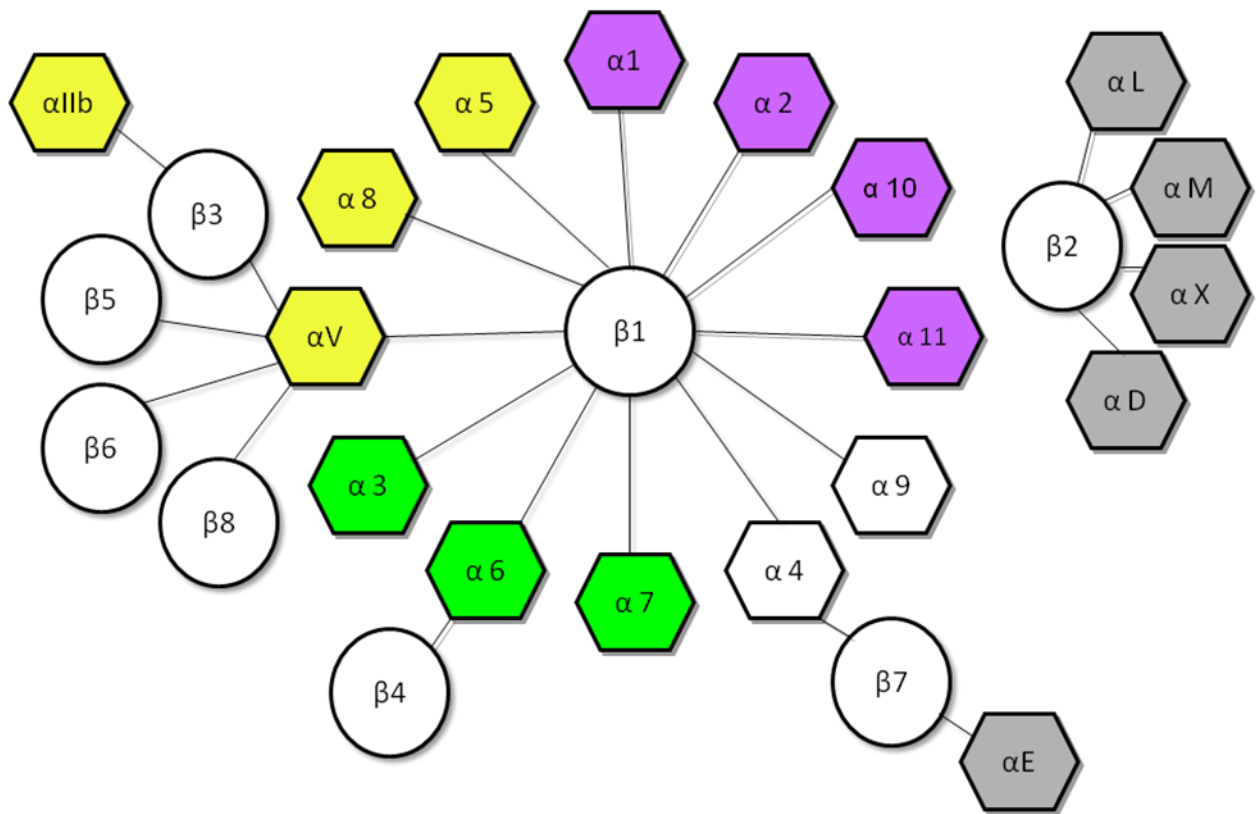


Figure 4. Integrin family.

Figure 4. Integrin family.

The integrin family is comprised of 18 α and 8 β subunits that form 24 $\alpha\beta$ heterodimeric receptors. Integrins can be divided into multiple subgroups based on their ECM ligands: 1) laminin-binding integrins (green); 2) collagen-binding integrins (purple); 3) leukocyte-specific integrins (grey); and 4) RGD binding integrins (yellow). Various integrins have been implicated in development, angiogenesis, lymphangiogenesis, skin integrity, immune response, bone remodeling, and hemostasis (Adopted from Hynes, 2002 with permission from Elsevier).

In addition, integrins can be divided into I, insertion/interaction, domain containing ($\alpha 1$, $\alpha 2$, $\alpha 10$, $\alpha 11$, αL , αM , αX , αD , and αE) and non-containing integrins ($\alpha 3$, $\alpha 4$, $\alpha 5$, $\alpha 6$, $\alpha 7$, $\alpha 8$, $\alpha 9$, αV , αIIb) (Takada et al., 2007). Each integrin has specific and non-redundant roles as shown by the studies of integrin knockout mice. The phenotypes of these knockout mice indicate the importance of various integrins in development (e.g. $\beta 1$), angiogenesis (e.g. $\alpha 1$, αV , $\beta 3$), lymphangiogenesis (e.g. $\alpha 9\beta 1$), skin integrity (e.g. $\alpha 6\beta 4$), immune response (e.g. αL , αM , $\beta 2$, $\beta 7$), bone remodeling (e.g. $\beta 3$), and hemostasis (e.g. αIIb , $\beta 3$, $\alpha 2$) (Barczyk et al., 2010; Harburger and Calderwood, 2008; Hynes, 2002).

Upon activation, integrins mediate cell-ECM interactions. In addition to their role in cell adhesion, they are critical for activation of various intracellular signaling pathways. Many intracellular proteins, such as talin, vinculin, paxillin, actin binding proteins, and other signaling molecules, interact with the cytoplasmic domains of integrins. Through these interactions, integrins modulate diverse cellular events, including cell proliferation, survival, polarity, and motility (Figure 5).

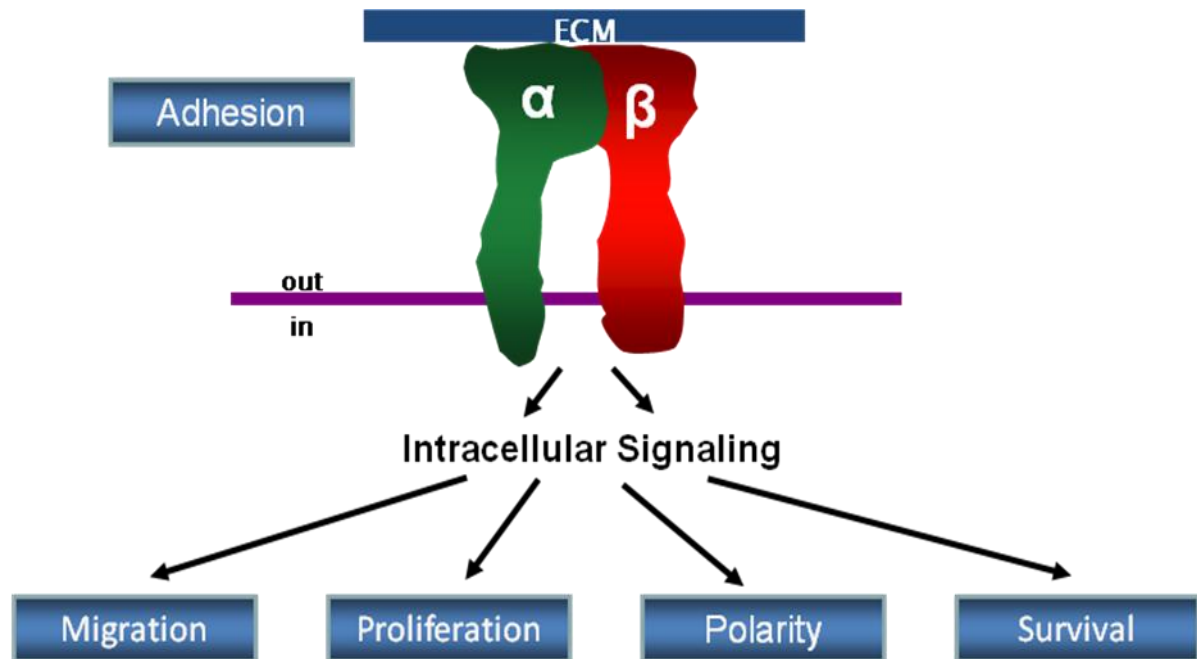


Figure 5. Integrins are involved in various intracellular signaling pathways.

Upon activation, integrins mediate cell-ECM interactions, connecting the ECM to the actin cytoskeleton in the cytoplasm. In addition to functioning as a major adhesion receptor, integrins play critical roles in activation of various intracellular signaling pathways. Many intracellular proteins interact with the cytoplasmic tails of integrins. Through these interactions, integrins modulate diverse cellular events, including cell proliferation, survival, polarity, and motility.

1.5. Integrin activation and signaling

Integrins on cell surfaces are often present in their inactive state, and need to be activated for further signaling. One unique feature of integrin activation is that intracellular signals activate integrins by inducing conformation changes and increasing their affinity to ECM molecules. Thus, this type of activation is termed inside-out activation (Harburger and Calderwood, 2008). The β subunit cytoplasmic tail is important for mediating inside-out activation. The cytoplasmic tails of most α V integrin-binding β subunits, including $\beta 1$, $\beta 3$, $\beta 5$, and $\beta 6$, contain the NPxY motif that is crucial for interactions with an intracellular integrin activator (Calderwood, 2004) (Figure 6).

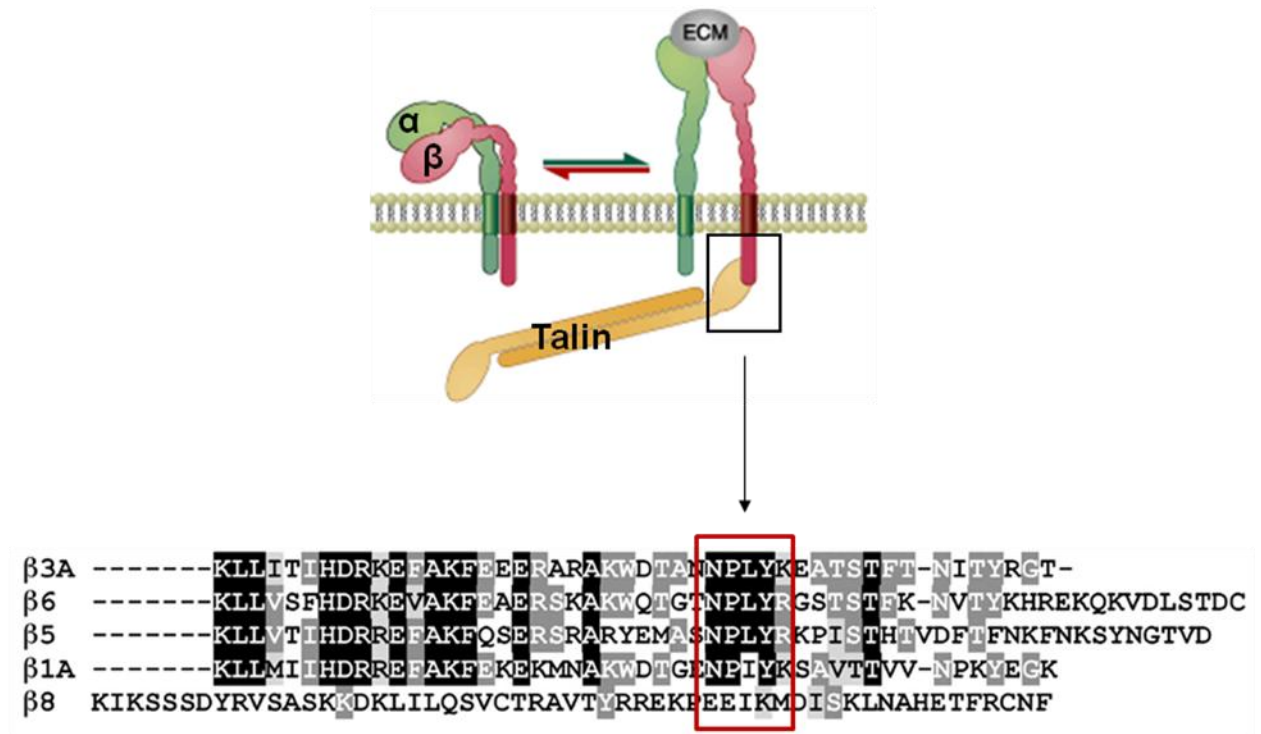


Figure 6. Talin regulates integrin inside-out activation by interacting with the β subunit cytoplasmic domain.

Figure 6. Talin regulates integrin inside-out activation by interacting with the β subunit cytoplasmic domain.

Integrins need to be activated for further signaling. Intracellular signals activate integrins by inducing conformation changes and increasing their affinity to the ECM. Inside-out activation of integrins is mediated by talin, a FERM domain-containing member of the protein 4.1 superfamily. Talin binds to the NPxY motif in the β integrin cytoplasmic tails via its FERM domain to activate integrins. Unlike other β subunits, $\beta 8$ integrin lacks the NPxY motif in its cytoplasmic tail. Therefore, $\beta 8$ integrin cannot be activated by talin. The activator of $\beta 8$ integrin has not been identified (Adopted from Calderwood and Ginsberg, 2003 with permission from Macmillan Publishers Ltd: Nat Cell Biol, copyright 2003 and McCarty et al., 2005a, copyright National Academy of Sciences, U.S.A.).

A common integrin activator, talin, has a FERM domain that can bind to the NPxY motif in its globular head. The FERM domain of talin is divided into F1, F2, and F3 subdomains. The F3 domain contains a PTB that binds the integrin β tails with high affinity (Wegener et al., 2007). Binding of talin appears to be a sufficient final step for activating integrins. In its inactive state, the rod region of talin masks the β subunit binding site in the FERM domain (Calderwood, 2004). The β tail binding site can be exposed when calpain cleaves the FERM domain of talin or PtdIns(4,5)P₂ binds to talin, causing a conformational change (Anthis and Campbell, 2011). Integrin activation by talin can be inhibited by phosphorylation of the NPxY motif of β tails, binding of other proteins to β subunits, or binding of PIPKly-90 to talin (Calderwood, 2004).

The interactions between the membrane proximal regions of the α and β cytoplasmic tails maintain integrins in their inactive state. Binding of talin to integrins results in the disruption of the β tail membrane-proximal region and the dissociation of the α and β tails (Calderwood, 2004). This leads to subsequent conformation changes in the extracellular regions that increase the extracellular binding activity of the integrins. Two models have been proposed for the conformation changes in integrin activation. In the 'deadbolt' model, inactive integrins are in a bent conformation. Upon the binding of talin, the transmembrane regions engage in piston-like movements, causing the α and β extracellular stalks to slide. The interactions between the headpiece and the β stalk, in turn, are disrupted (Arnaout et al., 2005). In the 'switch blade' model, inactive integrins are in a bent form, as well. However, this model suggests that the separation of the cytoplasmic and

transmembrane domains of α and β subunits results in the dislocation of an epidermal growth factor like repeat in the β stalk, causing outward swing of the headpiece like a switchblade (Luo et al., 2007).

1.6. Integrin signaling and Band 4.1B

Among the α V-binding β integrins, β 8 integrin does not share sequence homology with other β subunits (McCarty et al., 2005a) (Figure 6). Because the β 8 cytoplasmic tail lacks the NPxY motif, α v β 8 integrin does not interact with talin. The regulator of α v β 8 integrin activation has not been identified. A recent study has shown the interactions between the cytoplasmic tail of β 8 integrin and the CTD of Band 4.1B (McCarty et al., 2005a). Talin and Band 4.1B share protein sequence homology. Therefore, the binding of Band 4.1B to α v β 8 integrin suggests that Band 4.1B, like talin, may play a role in α v β 8 integrin activation, modulating integrin adhesion and downstream cellular events. Alternatively, Band 4.1B may participate in the α v β 8 integrin-regulated signaling as a downstream signaling molecule.

Cell adhesion, spreading, and motility are some of the cellular events that are regulated by integrins. A crucial component that integrates signaling required for these processes is a focal adhesion complex. Focal adhesion complexes are made up of integrins, signaling molecules, and adaptor proteins (Campbell, 2008). They serve as mechanical links between the ECM and the actin cytoskeleton and provide places for intracellular molecule recruitment and sequestration (Critchley, 2000). Recently, talin was shown to be involved in proper organization of focal adhesions and cell spreading that are mediated by β 1 integrin (Zhang et al., 2008).

Both Band 4.1B and $\beta 8$ integrin have been shown to localize to focal adhesions (McCarty et al., 2005a). Band 4.1B may play a role in focal adhesion formation and cell spreading by interacting with $\beta 8$ or perhaps other β integrins. The interactions of the Band 4.1B FERM domain with β integrins have not been studied. Piao and his colleagues have recently suggested that Band 4.1B may act as a linker between GluR1 and $\beta 1$ integrin (2009). In this study, glioma cell lines overexpressing GluR1 subunit of the α -amino-3-hydroxy-5-methylisoxazole-4-propionic acid glutamate receptor (AMPA) had increased baseline activation of FAK. In addition, overexpression of GluR1 was correlated with increased expression of surface $\beta 1$ integrin, which is a known FAK activator. Although GluR1 did not directly interact with $\beta 1$ integrin, GluR1 was found to bind to Band 4.1B. Therefore, the authors concluded that FAK activation seen in the GluR1 overexpressing glioma cell lines may be due to the effects of integrins and/or Band 4.1B on FAK activity and that GluR1 is likely to interact with $\beta 1$ integrin via Band 4.1B (Piao et al., 2009). FAK is a non-receptor protein tyrosin kinase that contains several protein interaction domains, including the binding sites for Src, FERM proteins, integrins, and paxillin (Hauck et al., 2002). The FAK pathway is one of the early signaling cascades that are activated in focal adhesions (Brown et al., 2005). Multiple protein interactions allow FAK to modulate various signal transduction pathways, such as small GTPase and MAPK signaling that may be critical for cell movement (Hauck et al., 2002). The FAK activity in $\beta 1$ integrin-modulated cell adhesion has been shown to be regulated by talin (Zhang et al., 2008). Band 4.1B and its interactions with integrins have not been associated with FAK signaling. However, it would be interesting to examine

Band 4.1B's roles in FAK regulation, given the similarities between Band 4.1B and talin.

Furthermore, Band 4.1B may play a role in integrin recycling, which is an important step in cell motility (Bel et al., 2009; Caswell and Norman 2008). A recent study has demonstrated that the Band 4.1B-binding domain is necessary for the endocytosis of the neural cell adhesion molecule contactin-associated protein 2 (Caspr2) (Bel et al., 2009). In addition, L1-CAM, another cell adhesion molecule, has been shown to contain a FERM-binding motif at a site that overlaps an endocytosis motif (Bel et al., 2009). Moreover, Numb, an endocytic adaptor that binds directly to β integrins via its FERM domain, has been shown to co-localize with $\beta 1$ integrin in clathrin-coated structures at the leading edge of migrating cells (Caswell and Norman, 2008). Given the prior reports, investigating Band 4.1B's roles in integrin trafficking would be worthwhile.

1.7. Integrins, Band 4.1B, and organogenesis

Because integrins and Band 4.1B can regulate various signaling cascades and cellular behavior, they are likely to contribute to proper organ development and homeostasis regulation during embryogenesis. In fact, integrin-mediated adhesion and signaling are essential for normal heart development (Thiery, 2003). Deletion of αV and $\alpha 5$ integrins causes impaired cardiac development (van der Flier et al., 2010). In addition, deletion of EIIIA and EIIB splice variants of fibronectin, an ECM ligand for integrins, leads to cardiovascular abnormalities and embryonic lethality

(Astrof et al., 2007). In humans, integrins are involved in the pathogenesis of heart disease (Wegener et al., 2007).

Normal development of the cardiovascular system is essential for survival and growth of embryos. The embryonic heart develops as a linear tube and subsequently undergoes looping, trabeculation, and compartmentalization (Jones et al., 2008). In late gastrulation, mesoderm-derived cardiac progenitor cells migrate from the primitive streak and form the early heart tube (Buckingham et al., 2005). During rightward looping of the primitive heart, cardiac chambers are defined and endocardial cushions, the precursors of the mitral and tricuspid valves in atrioventricular (AV) canal as well as the precursors of the aorticopulmonary septum in the outflow tract (OFT), are formed (Harvey, 2002).

The formation of the OFT is contributed by multipotent migratory neural crest cells. Neural crest cells originating from the dorsal neural folds undergo epithelial-to-mesenchymal transition (Jain et al., 2010). They migrate to and invade the OFT, contributing significant mass to the endocardial cushions (Stoller and Epstein, 2005). The migration of neural crest cells requires interactions with various ECM, such as fibronectin, collagen, vitronectin, and laminin, which serve as migratory scaffolds (Delannet et al., 1994). *In vitro* and *in vivo* studies have suggested that integrins are important for neural crest cell-ECM interactions that ensure proper migration of the cell population (Desban and Duband, 1997; Kil et al., 1996; Perris et al., 1989; Bronner-Fraser, 1986). Furthermore, multiple members of the protein 4.1 superfamily have been implicated in neural crest cell delamination and migration (Acloque et al., 2009). The functions of Band 4.1B in cardiac morphogenesis have

not been examined. Given the interactions between Band 4.1B and integrins, known regulators of neural crest, Band 4.1B may also play a role in normal heart development.

1.8. Specific aims

Cell migration is a critical component of normal development, wound healing, and many diseases, including cancer. Therefore, characterizing molecular pathways that are involved in cell migration is crucial for understanding various physiological and pathological processes. Band 4.1B, a cytoskeletal adaptor protein, has been implicated in regulation of cell motility, but the molecular mechanisms by which Band 4.1B contributes to cell migration have not been studied. Band 4.1B, via its CTD, interacts with the integrin $\alpha v \beta 8$. This novel finding has led to the examination of the functional roles for Band 4.1B in integrin-mediated adhesion and signaling that are essential for proper cell migration.

The objective of this study was to determine how Band 4.1B is involved in integrin-modulated adhesion and signaling pathways, and ultimately in cell migration. The central hypothesis of this project was that Band 4.1B regulates integrin-mediated adhesion formation and subsequent signaling cascades that are critical for cell migration. To test the central hypothesis and accomplish the objective of this study, the following two specific aims were pursued:

1. Specific Aim I: Elucidate the roles of Band 4.1B- $\beta 8$ integrin interaction in mouse embryonic development.

The working hypothesis for the first aim was that the absence of Band 4.1B- β 8 integrin interaction impairs cell-ECM adhesion and signaling, resulting in disrupted cardiac neural crest cell migration.

2. Specific Aim II: Determine the functional roles for Band 4.1B in β 1 integrin-mediated cell adhesion and signaling *in vitro*.

The working hypothesis for the second aim was that Band 4.1B regulates adhesion formation and signaling through the interactions between its FERM domain and β 1 integrin during initial cell spreading.

Chapter 2. Materials and Methods

2.1. Experimental mice

Band 4.1B and $\beta 8$ integrin knockout mice have been previously generated and characterized (Yi et al., 2005; Zhu et al., 2002). To produce various single and double gene knockout mice for the *in vivo* study, 4.1B^{-/-} mice with C57BL6/129S4 background and $\beta 8$ ^{+/-} mice with C57BL6/129S4/CD-1 background were crossed. $\beta 8$ ^{+/-};4.1B^{+/-} mice generated from the cross were then interbred to generate $\beta 8$ ^{+/-};4.1B^{+/+} and $\beta 8$ ^{+/-};4.1B^{-/-} mice. Wild type, $\beta 8$ ^{-/-}, 4.1B^{-/-}, and $\beta 8$ ^{-/-};4.1B^{-/-} mice were obtained by crossing $\beta 8$ ^{+/-};4.1B^{+/+} or $\beta 8$ ^{+/-};4.1B^{-/-} mice. Embryos were staged based on timed matings. Noon on the plug date was defined as E0.5. To generate wild type and 4.1B^{-/-} mice with the same genetic background, 4.1B^{-/-} mice with C57BL6/129S4 background were backcrossed with wild type C57BL6 mice. 4.1B^{+/-} mice obtained from the cross were then interbred to generate wild type and 4.1B^{-/-} littermates.

The genotypes of progeny were determined using PCR based methods described previously (Yi et al., 2005; Zhu et al., 2002). Briefly, tail DNA was isolated from digesting the tissue in STE containing proteinase-K (100 μ g/ml, USB Scientific, Cleveland, OH) for 16 hours at 55°C and precipitating DNA in 100% ethanol. The extracted DNA was dissolved in TE (pH 8) at 37°C by using Thermomixer R (Eppendorf, Westbury, NY). The samples for the PCR were prepared using MangoMix (Bioline, Tauton, MA) according to the manufacturer's protocol. The primer sequences used for the $\beta 8$ gene amplification are as follows: 5'-ATTATCTGGTTGATGTGTCAGC-3', 5'-GGAGGCATACAGTCTAAATTGT-3', 5'-

AGAGGCCACTTGTGTAGCGCCAAG-3', and 5'-AGAGAGGAACAAATATCCTTC
CC-3'. The PCR conditions for the $\beta 8$ gene amplification are as follows: 95°C for 5
minutes x1 cycle, 95°C for 45 seconds, 58°C for 30 seconds, 72°C for 1 minute x30
cycles, 72°C for 10 minutes x1 cycle, and 4°C hold. The primer sequences used for
the 4.1B gene amplification are as follows: 5'-CGCACCTGGTGCATGACC-3', 5'-
CGCCACCGTCTGAGCAGC-3', and 5'-GCACGTTTGGTAGCAGTTCCC-3'. The
PCR conditions for the 4.1B gene amplification are as follows: 94°C for 5 minutes x1
cycle, 94°C for 1 minute, 61°C for 1 minute, 72°C for 1 minute x30 cycles, 72°C for
10 minutes x1 cycle, and 4°C hold.

2.2. Astrocyte isolation

Wild type and 4.1B^{-/-} primary astrocytes that express $\beta 1$ integrin were
isolated from wild type and 4.1B^{-/-} mice between postnatal days 0-3. The brains
were removed from the neonates, and the cortices were dissected out by removing
the olfactory bulbs, hippocampi, other internal structures, and meninges. The
cortices were diced into 1mm² cubes and digested in low glucose Dulbecco's
modified Eagle's medium (DMEM) (1000mg/L glucose, Sigma, St. Louis, MO)
containing collagenase type I (Worthington, Lakewood, NJ) and deoxyribonuclease
I (Sigma, St. Louis, MO) for 30 minutes at 37°C. The digested tissues were
homogenized, filtered, and plated on laminin (Sigma, St. Louis, MO) coated T-75
flasks. The growth medium was consisted of low glucose DMEM, 10% bovine calf
serum (Thermo Scientific, Rockford, IL), and 1% penicillin-streptomycin (Sigma, St.

Louis, MO). After one week of growth, astrocytes were prepared for immediate use by shaking the plates at 200rpm for 16 hours at 37°C.

2.3. Immunoblotting

Yolk sacs, hearts, and primary astrocytes were lysed in 50 mM Tris, pH7.4, 150 mM NaCl, 1% NP40, 2.5 mM EDTA, and a complete mini protease inhibitor cocktail tablet (Roche, Mannheim, Germany). The concentrations of the lysates were determined using a BCA protein assay kit (Thermo Scientific, Rockford, IL). Detergent-soluble lysates were resolved by SDS-PAGE and blotted with appropriate antibodies. The anti-4.1B, anti- β 8 integrin, and anti- α v integrin antibodies have been described previously (McCarty et al., 2005a; McCarty et al., 2005b; Mobley et al., 2009; Tchaicha et al., 2010). Rabbit anti-4.1G and rabbit anti-4.1N antibodies were purchased from Protein Express (Chiba, Japan). Rabbit anti-actin antibody was obtained from Sigma (St. Louis, MO). Peroxidase-conjugated goat anti-rabbit IgG was purchased from Jackson ImmunoResearch (West Grove, PA).

2.4. Biotinylation and immunoprecipitation

Primary astrocytes growing on laminin were labeled with 0.1 μ g/ml of sulfo-NHS-biotin (Thermo Scientific, Rockford, IL) for 30 minutes at 37°C. After washing the cells with PBS and TBS twice each, the cells were lysed in 50 mM Tris, pH7.4, 150 mM NaCl, 1% NP40, 2.5 mM EDTA, and a complete mini protease inhibitor cocktail tablet. The concentrations of the lysates were determined using the Thermo BCA protein assay kit. The lysates were pre-cleared with goat anti-rabbit-agarose

(Sigma, St. Louis, MO), rabbit anti-goat IgG-agarose (RDI, Flanders, NJ), or goat anti-rat IgG-agarose (Sigma, St. Louis, MO) for 1 hour at 4°C. Then various integrins were immunoprecipitated for 16 hours at 4°C with one of the following antibodies: rabbit anti- α 1 (Millipore, Billerica, MA), rat anti- α 2 (Emfret Analytics, Eibelstadt, Germany), rabbit anti- α 3 (Millipore, Billerica, MA), rat anti- α 4 (Millipore, Billerica, MA), rat anti- α 5 (Emfret Analytics, Eibelstadt, Germany), rat anti- α 6 (Millipore, Billerica, MA), goat anti- α 8 (Millipore, Billerica, MA), rabbit anti- α v, rat anti- β 1 (Millipore, Billerica, MA). The secondary antibodies conjugated with agarose beads were added to the lysates for 1 hour at 4°C. The beads were washed with 50 mM Tris, pH7.4, 150 mM NaCl, 1% NP40, 2.5 mM EDTA, and a complete mini protease inhibitor cocktail tablet, and then boiled in Laemmli buffer for 5 minutes. The samples were resolved by SDS-PAGE and subsequently transferred to Immobilon-P membrane (Millipore, Billerica, MA). The membrane was blocked with 3% BSA and incubated with the Vectastain ABC mix (Vector Laboratories, Burlingame, CA) in 3% BSA. The membrane was developed using ECL reagents (Amersham, Piscataway, NJ).

2.5. Immunohistochemistry

E10.5 embryos and yolk sacs were fixed in 4% PFA-PBS for 16 hours at 4°C and embedded in paraffin. The sections were blocked with 10% swine or horse serum in PBS for 1 hour at room temperature followed by incubation with appropriate primary antibodies for 16 hours at 4°C. Then, they were washed with PBS containing 0.1% Tween-20 and PBS. Endogenous peroxidase activity was

blocked with 0.3% hydrogen peroxide in PBS for 10 minutes at room temperature. The sections were incubated with appropriate secondary antibodies for 30 minutes at room temperature. After washing with PBS containing 0.1% Tween-20 and PBS, the sections were developed using Vectastain ABC and DAB kits (Vector Laboratories, Burlingame, CA). Hematoxylin counterstaining was used according to the manufacturer's protocol (Vector Laboratories, Burlingame, CA). The following antibodies were utilized: rabbit anti-laminin (1:100, Sigma, St. Louis, MO), mouse anti- α smooth muscle actin (1:500, Sigma, St. Louis, MO), rabbit anti-desmin (1:200, Abcam, Cambridge, CA), biotinylated swine anti-rabbit IgG (1:250, DAKO, Carpinteria, CA), and biotinylated horse anti-mouse IgG (1:250, Vector Laboratories, Burlingame, CA). The sections were analyzed and imaged using a Zeiss Axio Imager Z1 microscope.

2.6. Immunofluorescence

E10.5 embryos and yolk sacs were fresh-frozen in Tissue-Tek OCT compound (Sakura Finetek, Torrance, CA). Cells were fixed with 4% PFA and permeabilized with PBS containing 0.5% NP40. The samples were blocked with 10% goat serum for 1 hour at room temperature. Appropriate primary antibodies were then added to the samples for 16 hours at 4°C. Then the samples were incubated with secondary antibodies for 1 hour at room temperature. The samples were analyzed and imaged using a Zeiss Axio Imager Z1 microscope. The following antibodies were used for immunofluorescence analyses: rabbit anti-4.1B (5 μ g/ml), rabbit anti-4.1G (5 μ g/ml), rabbit anti-4.1N (5 μ g/ml), rabbit anti- α v (1:250), mouse

anti-paxillin (1:50, BD Biosciences, Sparks, MD), rat anti- β 1 (1:100), mouse anti-myc (1:100, Invitrogen, Carlsbad, CA), phalloidin-Texas Red (1:50, Sigma, St. Louis, MO), Alexa Flour 488 goat anti-rabbit IgG, Alexa Flour 488 goat anti-mouse IgG, Alexa Flour 594 goat anti-mouse IgG, Alexa Flour 488 goat anti-rat IgG, and Alexa Flour 594 goat anti-rat IgG (Molecular Probes, Carlsbad, CA).

2.7. Whole-mount immunostaining

Embryos were fixed in methanol:DMSO (4:1) for 2 hours at 4°C. Yolk sacs and hearts were fixed in 4% PFA-PBS for 2 hours at 4°C. They were dehydrated in 15% methanol, 50% methanol, and 100% methanol, and stored in 100% methanol at -20°C until use. The tissues were rehydrated, incubated in 1% H₂O₂ in PBS for 1 hour, and blocked in PBSMT (2% skim milk powder, 0.1% Triton X-100 in PBS) for 2 hours at room temperature. They were then incubated with rat anti-CD31 (1:100, BD Biosciences, San Jose, CA), mouse anti-neurofilament 2H3 (3 μ g/ml, University of Iowa Hybridoma Bank), rabbit anti-4.1B (5 μ g/ml), rabbit anti- β 8 integrin (1:250), or rabbit anti- α v integrin (1:250) for 16 hours at 4°C. The samples were washed five times in PBSMT at room temperature for 1 hour each and incubated with peroxidase-conjugated AffiniPure goat anti-rat IgG, goat anti-mouse IgG, or goat anti-rabbit IgG (1:500, Jackson ImmunoResearch, West Grove, PA). They were washed five times in PBSMT at room temperature for 1 hour each and in PBT (0.2% BSA, 0.1% Triton X-100 in PBS) for 16 hours at 4°C. The samples were developed using DAB kit (Vector Laboratories, Burlingame, CA) and cleared in 100% glycerol.

2.8. Adhesion assays

Glass coverslips were coated with fibronectin (Sigma, St. Louis, MO) for 16 hours at 4°C. Primary astrocytes were plated onto the coverslips and allowed to adhere and spread for 30 minutes, 1 hour, 2 hours or 24 hours. The cells were then fixed with 4% PFA and permeabilized with PBS containing 0.5% NP40 for further immunohistochemical analysis.

Wild type and 4.1B^{-/-} astrocytes were also plated onto a laminin-coated 96 well plate for 30 minutes. The cells were washed with PBS for three times to remove any non-adherent cells. The adherent cells were then stained with crystal violet, and absorbance at 560nm was read using EL800 ELISA reader (BioTek Instruments, Vienna, VA).

COS7 and 293T cells were transiently transfected with myc-tagged 4.1B FERM, full length 4.1B, and LacZ constructs (McCarty et al., 2005a) using Effectene transfection reagents (Qiagen, Valencia, CA). 48 hours after the transfection, the cells were plated onto fibronectin-coated coverslips and allowed to adhere and spread for 30 minutes, 1 hour, 2 hours, or 24 hours. In parallel, the transfected cells were treated with P5D2 mouse anti- β 1 antibody (R&D system, Minneapolis, MN) prior to being plated onto the fibronectin-coated coverslips to block β 1 integrin. After 30 minutes of the antibody treatment, these cells were plated and allowed to adhere and spread for 30 minutes, 1 hour, 2 hours, or 24 hours. The cells were then fixed with 4% PFA and permeabilized with PBS containing 0.5% NP40 for further immunohistochemical analysis. After staining the adherent cells with mouse anti-myc antibody, myc-positive cells were imaged using a Zeiss Axio Imager Z1

microscope. The area of cell spreading was analyzed and quantified using ImageJ (NIH).

2.9. Statistical analysis

All data were analyzed using student's t-test to determine statistically significant differences. P value less than 0.05 was considered statistically significant.

Chapter 3. Specific Aim I

3.1 Introduction

Proper development of the cardiovascular system is key for the development and physiology of all organs and tissues. Cardiac neural crest cells play important roles in normal morphogenesis of the heart. During embryogenesis, neural crest cells migrate into developing heart and get incorporated into various compartments of the cardiovascular system. Multiple ECM, including fibronectin, collagen, vitronectin, and laminin, function as migratory scaffolds for neural crest cells (Delannet et al., 1994). Therefore, integrin-mediated adhesion and signaling are crucial for normal development of the heart. Integrins are cell adhesion receptors that mediate cell-ECM interactions. By participating in neural crest cell-ECM interactions, integrins modulate proper migration of the neural crest cells (Desban and Duband, 1997; Kil et al., 1996; Perris et al., 1989; Bronner-Fraser, 1986). Interestingly, members of the protein 4.1 superfamily have been also implicated in neural crest cell delamination and migration (Acloque et al., 2009). Considering the involvement of integrins and Band 4.1B in a wide range of signaling cascades and cellular behavior (Wang et al., 2010; Dafou et al., 2010; Horresh et al., 2010; Ohno et al., 2009; Kang et al., 2009; Cavanna et al., 2007; Wong et al., 2007), these molecules are likely to be important for organogenesis, especially for cardiovascular development.

In particular, $\beta 8$ integrin has been found to interact with the CTD of Band 4.1B via its cytoplasmic domain (McCarty et al., 2005a). $\beta 8$ integrin plays a crucial role in vascular development. As evident in $\beta 8$ knockout mice, $\beta 8$ integrin's main

function is to regulate vascular development in the CNS (Zhu et al., 2002). However, a small percentage of $\beta 8$ integrin knockout mice were shown to have other cardiovascular phenotypes, such as poorly vascularized yolk sacs and enlarged pericardial cavity (Zhu et al., 2002). Unlike $\beta 8$ integrin knockout mice, Band 4.1B knockout mice do not exhibit obvious cardiovascular phenotypes (Yi et al., 2005). Studies on the roles of other protein 4.1 family members in cardiac function have just started to emerge. Recently, 4.1R has been implicated in the regulation of cardiac ion channels (Baines et al., 2009).

The functional roles for $\beta 8$ integrin-Band 4.1B interactions *in vivo* have not been explored. In this chapter, cooperative functions for $\beta 8$ integrin and Band 4.1B in embryonic development were elucidated by using molecular genetic approaches. The working hypothesis was that the absence of $\beta 8$ integrin-Band 4.1B interactions impairs cell-ECM adhesion and signaling, which leads to disrupted cardiac morphogenesis.

3.2. Results

3.2.1. Genetic knockouts of $\beta 8$ integrin and Band 4.1B demonstrate lethal phenotypes by E11.5.

To study functional roles of $\beta 8$ integrin and Band 4.1B in embryogenesis, various $\beta 8$ integrin, Band 4.1B single and double knockout mutants were generated. Mice lacking the Band 4.1B gene (4.1B^{-/-}) were initially crossed with mice with a $\beta 8$ integrin heterozygous null allele ($\beta 8^{+/-}$). $\beta 8^{+/-};4.1B^{+/-}$ mice, the F1 progeny, were born in the expected Mendelian ratios. They were viable and fertile with no obvious

phenotypes. $\beta 8^{+/-};4.1B^{+/-}$ mice were then interbred to generate $\beta 8^{+/-};4.1B^{-/-}$ and $\beta 8^{+/-};4.1B^{+/+}$ mice. $4.1B^{-/-}$ and $\beta 8^{-/-};4.1B^{-/-}$ mice were obtained by interbreeding $\beta 8^{+/-};4.1B^{-/-}$ pairs. Wild type and $\beta 8^{-/-}$ mice were produced by intercrossing $\beta 8^{+/-};4.1B^{+/+}$ pairs. Genotypes of all mice were determined by PCR-based gene amplification methods. Band 4.1B wild type and knockout bands were 310 and 670 bp, respectively. The sizes of $\beta 8$ wild type and knockout bands were 330 and 450 bp, respectively (Figure 7).

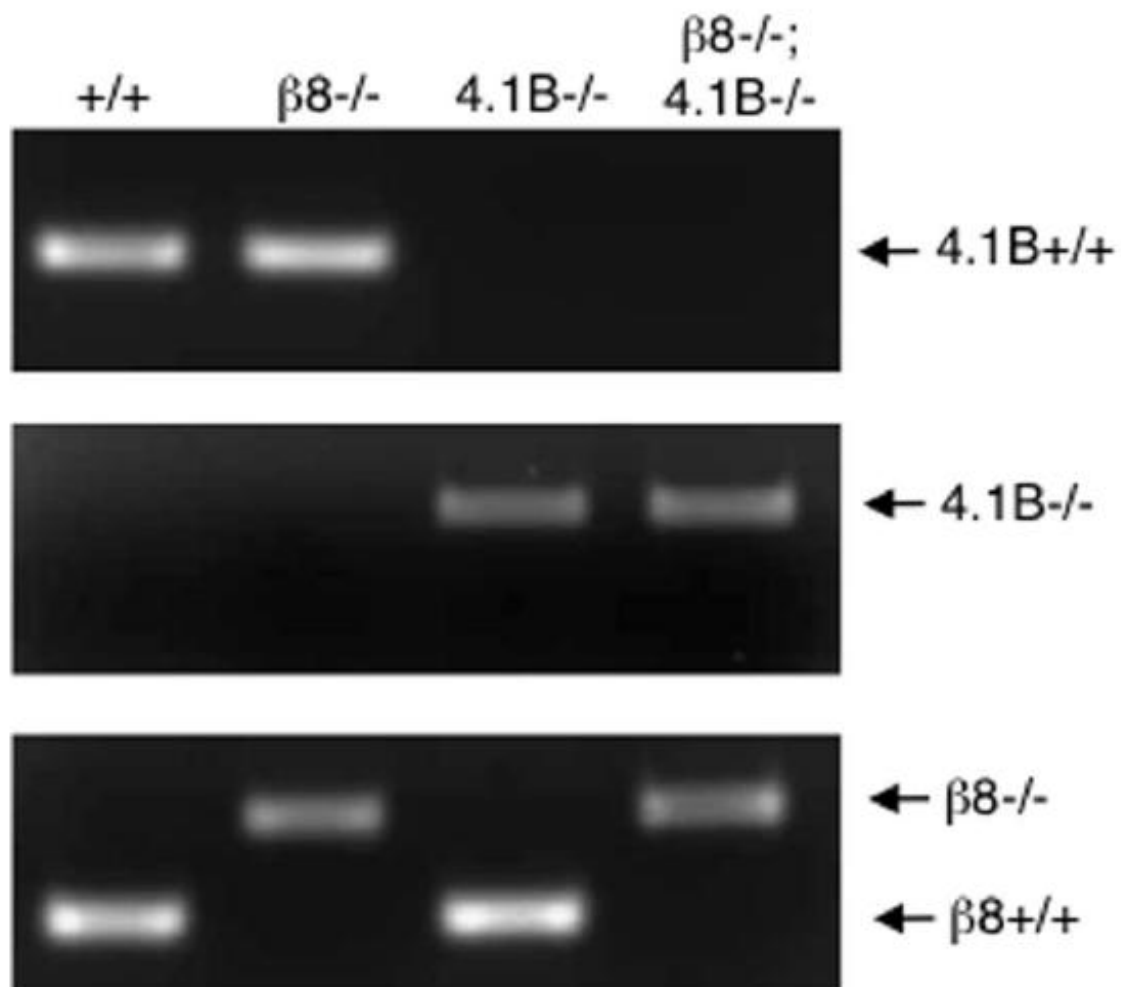


Figure 7. The genotypes of embryos are determined by PCR-based gene amplification methods.

Figure 7. The genotypes of embryos are determined by PCR-based gene amplification methods.

Genotypes of all mice were determined by PCR-based gene amplification methods using tail DNA. The $\beta 8$ primer sequences are as follows: 5'-ATTATCTGGTTGATGTGTCAGC-3', 5'-GGAGGCATACAGTCTAAATTGT-3', 5'-AGAGGCCACTTGTGTAGCGCCAAG-3', 5'-AGAGAGGAACAAATATCCTTCCC-3'. The 4.1B primer sequences are as follows: 5'-CGCACCTGGTGCATGACC-3', 5'-CGCCACCGTCTGAGCAGC-3', 5'-GCACGTTTGGTAGCAGTTCCC-3'. Gene amplification products for each mouse strain are shown here. Band 4.1B wild type and knockout bands were 310 and 670 bp, respectively. The sizes of $\beta 8$ wild type and knockout bands were 330 and 450 bp, respectively.

Examining neonatal mice at postnatal day 0 (P0) demonstrated that wild type mice and 4.1B^{-/-} were born in higher than expected Mendelian ratios (43/139 or 31% and 60/224 or 27%, respectively vs. the expected 25%) (Table 2). However, slightly lower than expected β 8^{-/-} mice were present at P0 (28/139 or 20% vs. the expected 25%) (Table 2). The percentage of β 8^{-/-};4.1B^{-/-} being born (23/244 or 10%) was strikingly lower than the expected 25% (Table 2). The smaller numbers of β 8^{-/-} and β 8^{-/-};4.1B^{-/-} neonates found at P0 suggested embryonic or early postnatal lethality in these mice. The analysis of mice at birth is summarized in Table 2.

Table 2. Genotype distribution of mice

Genotype	E10.5	E11.5	P0
+/+; +/+	34/163 (21%)	19/61 (31%)	43/139 (31%)
β 8 ^{-/-} ; +/+	35/163 (22%)	17/61 (28%)	28/139 (19%)
+/+; 4.1B ^{-/-}	43/182 (24%)	20/78 (26%)	60/224 (27%)
β 8 ^{-/-} ;4.1B ^{-/-}	42/182 (23%)	6/78 (8%)	23/224 (10%)

At P0, wild type and 4.1B^{-/-} mice did not display any abnormal phenotypes, including no CNS pathologies (Figure 8E, G). However, both β 8^{-/-} and β 8^{-/-};4.1B^{-/-} mice demonstrated intracerebral hemorrhage at birth (Figure 8F, H). These findings were similar to the previous reports of cerebral hemorrhage in β 8^{-/-} mice (Zhu et al., 2002; Mobley et al., 2009). No differences in the severity of hemorrhage were observed between β 8^{-/-} and β 8^{-/-};4.1B^{-/-} mice.

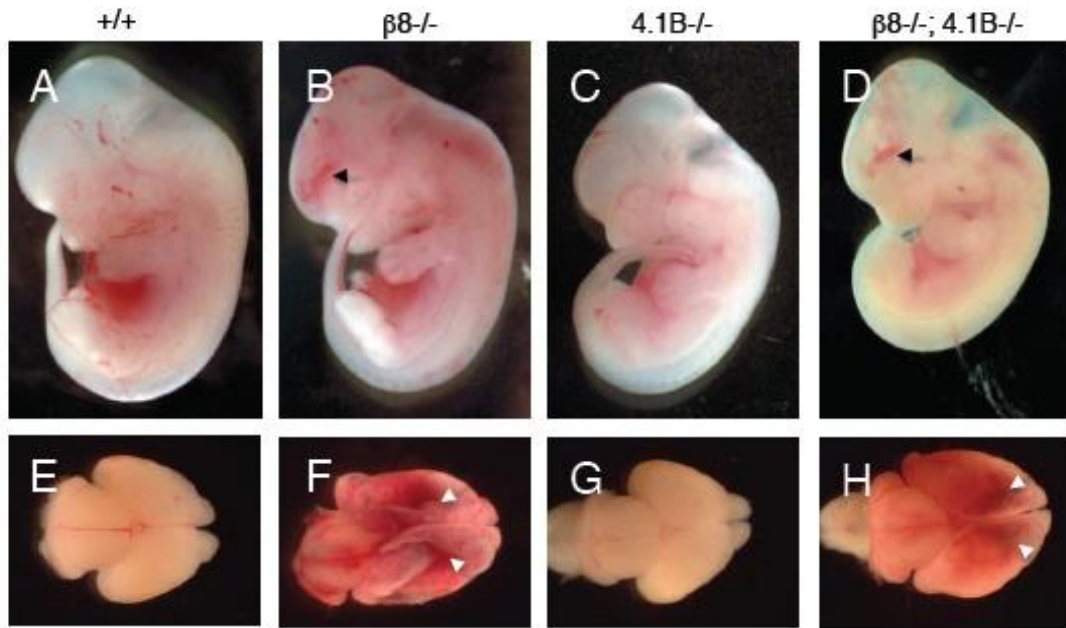


Figure 8. $\beta 8^{-/-}$ and $\beta 8^{-/-}; 4.1B^{-/-}$ mice develop intracerebral hemorrhage after E11.5.

Intracerebral hemorrhage is observed in both embryonic and adult brains of $\beta 8^{-/-}$ and $\beta 8^{-/-}; 4.1B^{-/-}$ mice. A-D: Images of E12.5 wild type (A), $\beta 8^{-/-}$ (B), $4.1B^{-/-}$ (C), and $\beta 8^{-/-}; 4.1B^{-/-}$ (D) embryos showing intracerebral hemorrhage in $\beta 8^{-/-}$ (B) and $\beta 8^{-/-}; 4.1B^{-/-}$ (D), but not in wild type (A) and $4.1B^{-/-}$ (C) embryos. E-H. Images of wild type (E), $\beta 8^{-/-}$ (F), $4.1B^{-/-}$ (G), and $\beta 8^{-/-}; 4.1B^{-/-}$ (H) brains from P0 pups. Intracerebral hemorrhage in $\beta 8^{-/-}$ (F) and $\beta 8^{-/-}; 4.1B^{-/-}$ (H) is indicated in white arrow heads.

All mice that survived beyond P0 were followed for survival analysis. Both wild type (n=20) and 4.1B^{-/-} (n=20) mice lived without any obvious abnormalities during the period that the survival analysis was performed. However, β 8^{-/-} (n=16) and β 8^{-/-};4.1B^{-/-} mice (n=18) started to die in the third and fourth week of the postnatal period (Figure 9).

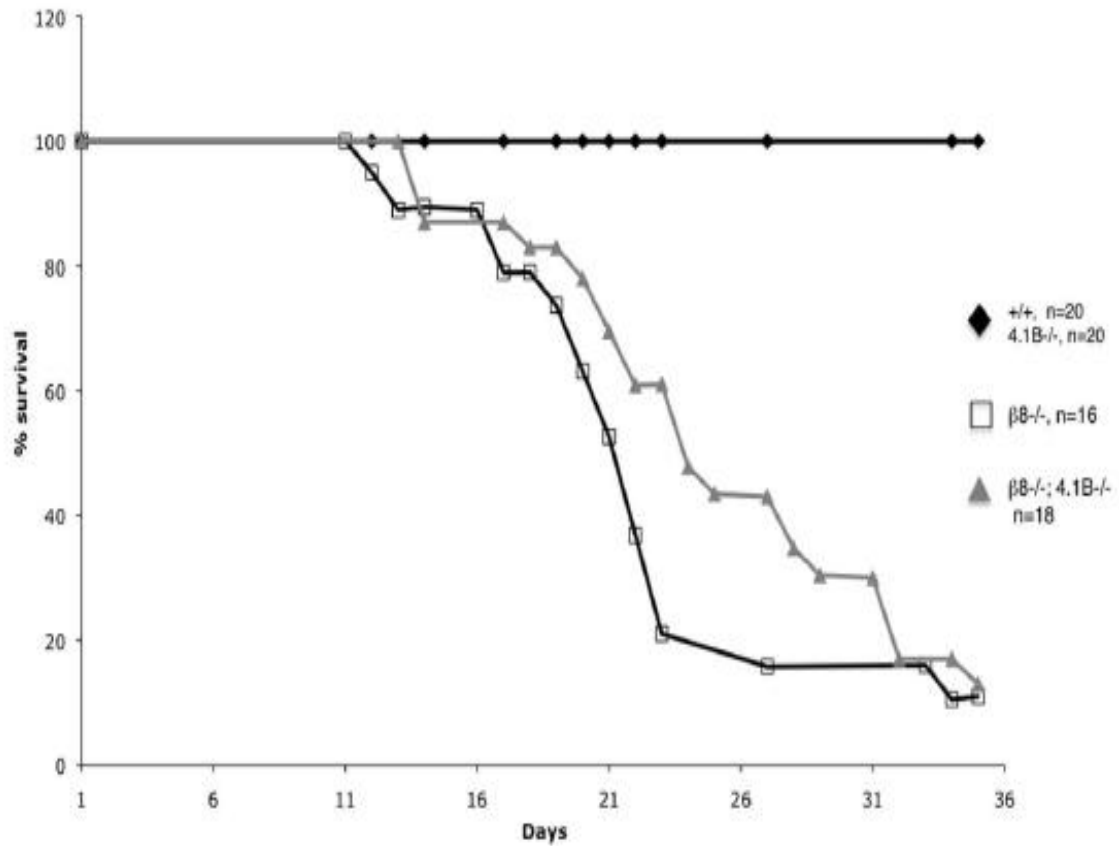


Figure 9. Kaplan-Meier survival analysis.

Postnatal survival of wild type, $\beta 8^{-/-}$, 4.1B $^{-/-}$, and $\beta 8^{-/-}; 4.1B^{-/-}$ mice was examined using Kaplan-Meier survival analysis. Black diamond, wild type and 4.1B $^{-/-}$ (n=20 each); white square, $\beta 8^{-/-}$ (n=16); grey triangle, $\beta 8^{-/-}; 4.1B^{-/-}$ (n=18). Most $\beta 8^{-/-}$ and $\beta 8^{-/-}; 4.1B^{-/-}$ mice died in the third and fourth week of their lives. None of these mice survived beyond P40.

Unlike wild type and 4.1B^{-/-} mice, β 8^{-/-} and β 8^{-/-};4.1B^{-/-} mice demonstrated hunched posturing, abnormal gait, and seizure activity by the third week of their lives (Figure 10A, B). None of these mice survived beyond P40. The lethality shown in β 8^{-/-} and β 8^{-/-};4.1B^{-/-} adult mice were likely due to hydrocephalus secondary to the intracerebral hemorrhage. Postmortem dissection of their brains revealed thinning of the cortices and enlargement of the ventricles that resulted from severe hydrocephalus (Figure 10D, F). Although the phenotypes of β 8^{-/-} and β 8^{-/-};4.1B^{-/-} were severe enough to cause early lethality in these mice, these two strains did not exhibit obvious phenotypic differences in the postnatal period.

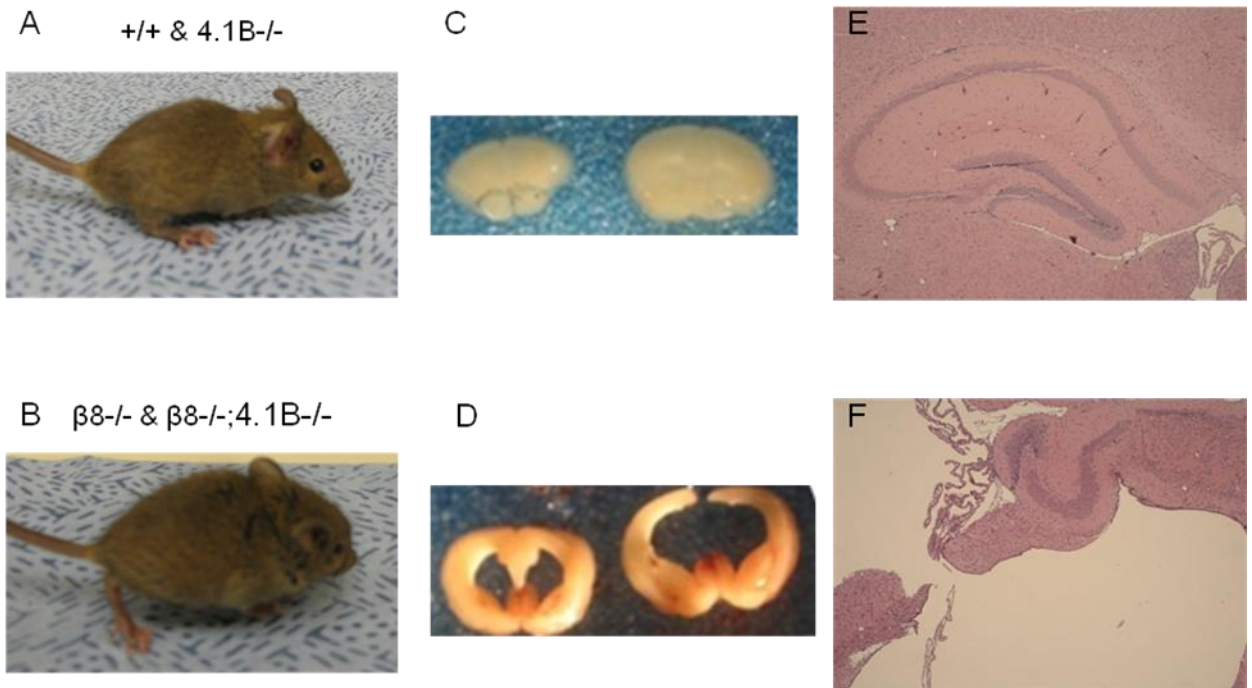


Figure 10. Adult $\beta 8^{-/-}$ and $\beta 8^{-/-}; 4.1B^{-/-}$ mice develop hydrocephalus.

Figure 10. Adult $\beta 8^{-/-}$ and $\beta 8^{-/-};4.1B^{-/-}$ mice develop hydrocephalus.

Both $\beta 8^{-/-}$ and $\beta 8^{-/-};4.1B^{-/-}$ mice develop hydrocephalus postnatally. A-B. Images of wild type / 4.1B^{-/-} (A) and $\beta 8^{-/-}$ / $\beta 8^{-/-};4.1B^{-/-}$ (B) mice at 3 weeks of age. $\beta 8^{-/-}$ and $\beta 8^{-/-};4.1B^{-/-}$ mice demonstrated hunched posturing, abnormal gait, and seizure activity by the third week of their lives (B). C-D. Images of dissected brains of wild type / 4.1B^{-/-} (C) and $\beta 8^{-/-}$ / $\beta 8^{-/-};4.1B^{-/-}$ (D) mice. In $\beta 8^{-/-}$ and $\beta 8^{-/-};4.1B^{-/-}$, grossly thin cortices and enlarged ventricles are seen postmortem (D). E-F. Images of brain H&E sections from wild type / 4.1B^{-/-} (E) and $\beta 8^{-/-}$ / $\beta 8^{-/-};4.1B^{-/-}$ (F) mice. Note enlarged ventricles secondary to hydrocephalus in $\beta 8^{-/-}$ and $\beta 8^{-/-};4.1B^{-/-}$ mouse brains (F). V, ventricle.

It was noted that the differences of embryonic lethality between $\beta 8^{-/-}$ and $\beta 8^{-/-};4.1B^{-/-}$ were significant. Only 23 of 224 pups born from $\beta 8^{+/-};4.1B^{-/-}$ intercrosses were $\beta 8^{-/-};4.1B^{-/-}$ (Table 2). This indicated 60% embryonic lethality in $\beta 8^{-/-};4.1B^{-/-}$ mice. On the other hand, 28 of 139 pups obtained from $\beta 8^{+/-};4.1B^{+/+}$ breeding were $\beta 8^{-/-}$. This represented less than 20% embryonic lethality in $\beta 8^{-/-}$ (Table 2).

To determine the time window of embryonic lethality in $\beta 8^{-/-};4.1B^{-/-}$ mice, embryos from $\beta 8^{+/-};4.1B^{+/+}$ and $\beta 8^{+/-};4.1B^{-/-}$ intercrosses were analyzed at different developmental stages. At E10.5, wild type, $\beta 8^{-/-}$, $4.1B^{-/-}$, and $\beta 8^{-/-};4.1B^{-/-}$ embryos were present in expected Mendelian ratios (34/163 or 21%, 35/163 or 22%, 43/182 or 24%, 42/182 or 23%, respectively) (Table 2). Wild type, $\beta 8^{-/-}$, and $4.1B^{-/-}$ embryos at E10.5 appeared healthy without obvious abnormalities (Figure 11A-C, E-G). However, of 42 $\beta 8^{-/-};4.1B^{-/-}$ embryos, 11 showed severe growth retardation and hypovascularity (Figure 11D, H). Of these 11 embryos, 6 had enlarged pericardial cavity (Figure 11H). In addition, two embryos were dead with no detectable heartbeat and widespread necrosis.

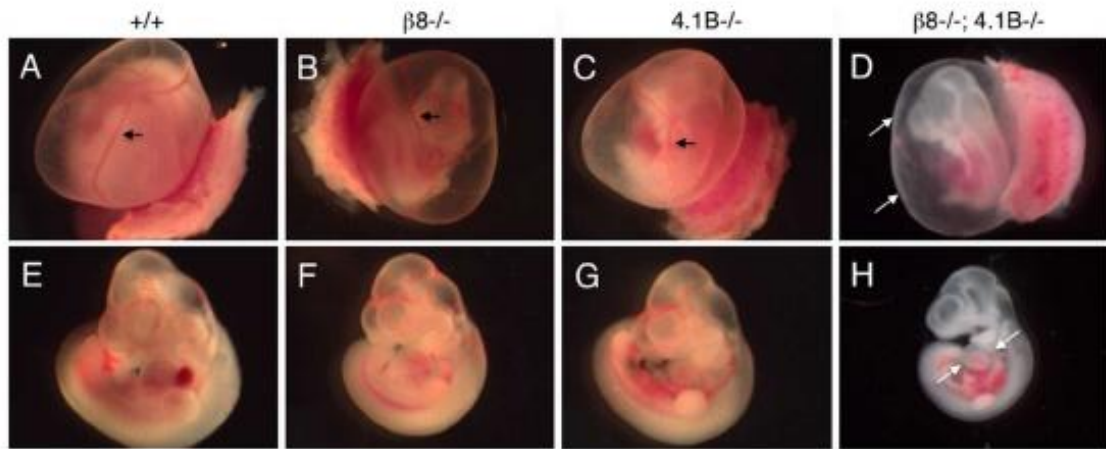


Figure 11. Double knockout embryos develop lethal cardiovascular phenotypes.

Double knockout embryos develop lethal cardiovascular phenotypes. A–H: Images of E10.5 wild type, $\beta 8^{-/-}$, $4.1B^{-/-}$, and $\beta 8^{-/-}; 4.1B^{-/-}$ embryos within yolk sacs (A–D) or removed from yolk sacs (E–H). Note the normal blood vessel patterning in the wild type (A, E) and single knockout embryos and yolk sacs (B, C, F, G). In contrast, most double knockouts are hypovascular (arrows in D) with embryos displaying pericardial edema (arrows in H).

By E11.5, the viability of $\beta 8^{-/-};4.1B^{-/-}$ embryos was significantly decreased. Only 6 of the 78 analyzed embryos were $\beta 8^{-/-};4.1B^{-/-}$ (8% vs. the expected 25%) (Table 2). This represents 68% fewer than expected $\beta 8^{-/-};4.1B^{-/-}$ embryos. The 8% viability at E11.5 is nearly identical to the 10% viability of $\beta 8^{-/-};4.1B^{-/-}$ neonates at P0. This suggests that nearly all death of $\beta 8^{-/-};4.1B^{-/-}$ occurs between E10.5 and E11.5. The remaining 32% of $\beta 8^{-/-};4.1B^{-/-}$ were viable. However, they exhibited intracerebral hemorrhage that was similar to that of $\beta 8^{-/-}$ mice (Figure 8B, D).

3.2.2. Cardiovascular abnormalities contribute to the lethal phenotype of $\beta 8^{-/-};4.1B^{-/-}$ embryos

The most noticeable feature of $\beta 8^{-/-};4.1B^{-/-}$ embryos at E10.5 was their hypovascularity (Figure 11D). Therefore, sagittal sections of E10.5 embryos were stained with H&E or an anti-laminin antibody to further examine the vasculature. Normal vascular morphologies were observed in the neural tubes of wild type (Figure 12A, E) and $4.1B^{-/-}$ embryos (Figure 12C, G). However, $\beta 8^{-/-}$ embryos displayed distended blood vessels in the neural tube (Figure 12B, F). Prior studies also showed that the absence of $\beta 8$ integrin impairs vascular development in the CNS (McCarty et al., 2005b, Proctor et al., 2005). $\beta 8^{-/-};4.1B^{-/-}$ embryos also demonstrated defective blood vessel formation in the neural tube (Figure 12D, H).

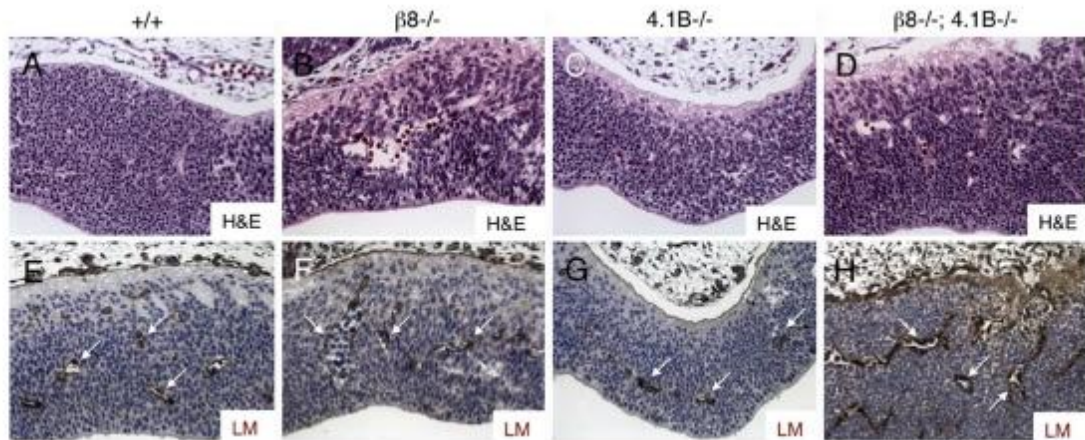


Figure 12. CNS vascular pathologies are seen in $\beta 8^{-/-}$ and $\beta 8^{-/-}; 4.1B^{-/-}$ embryos.

CNS vascular pathologies in $\beta 8$ integrin single knockout and double knockout embryos. A–D: Sagittal sections from E10.5 wild type (A), $\beta 8^{-/-}$ (B), $4.1B^{-/-}$ (C), and $\beta 8^{-/-}; 4.1B^{-/-}$ mutants (D) were stained with H&E. Shown are 200 \times images taken from neural tubes. Note the abnormal vascular patterning in the $\beta 8^{-/-}$ (B) and $\beta 8^{-/-}; 4.1B^{-/-}$ neural tubes (D). E–H: Sagittal sections through wild type (E), $\beta 8^{-/-}$ (F), $4.1B^{-/-}$ (G), and $\beta 8^{-/-}; 4.1B^{-/-}$ mutants (H) were immunolabeled with an anti-laminin antibody to identify blood vessels (white arrows). Note the abnormal neural tube blood vessel patterning in the $\beta 8^{-/-}$ and $\beta 8^{-/-}; 4.1B^{-/-}$ embryos (arrows in F, H).

Upon further examination of $\beta 8^{-/-};4.1B^{-/-}$ vasculature using whole-mount immunostaining with an anti-CD31 antibody, $\beta 8^{-/-};4.1B^{-/-}$ embryos were shown to have a less elaborate vascular network with minimal sprouting and branching (Figure 13D). These findings are consistent with the grossly hypovascular appearance of $\beta 8^{-/-};4.1B^{-/-}$ embryos (Figure 11H). In comparison, wild type, $\beta 8^{-/-}$, and $4.1B^{-/-}$ embryos demonstrated an intricate network of blood vessels accompanied with normal vascular sprouting and branching (Figure 13A-C).

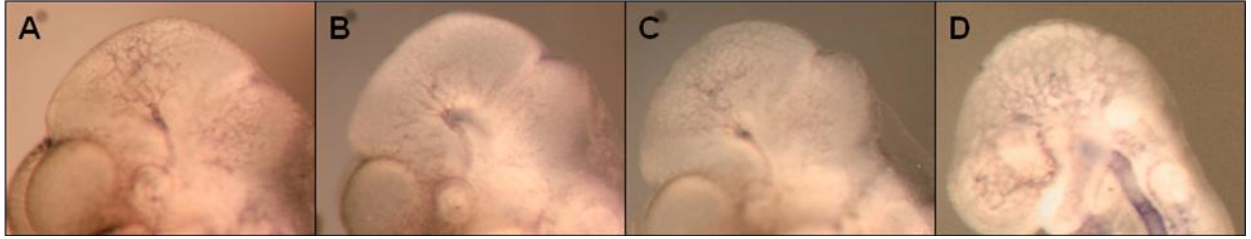


Figure 13. $\beta 8^{-/-};4.1B^{-/-}$ mice lack an elaborate vascular network.

$\beta 8^{-/-};4.1B^{-/-}$ embryos exhibited abnormal vascular patterning in the CNS. A-D. Images of anti-CD31 whole-mount stained embryo head. Note a less elaborate vascular network with minimal branching in $\beta 8^{-/-};4.1B^{-/-}$ (D), compared to wild type (A), $\beta 8^{-/-}$ (B), and $4.1B^{-/-}$ (C).

Hypovascular yolk sacs observed in $\beta 8^{-/-};4.1B^{-/-}$ embryos (Figure 11D) led to the study of the yolk sac vasculature. In order for a better examination of yolk sac blood vessels, E10.5 wild type, $\beta 8^{-/-}$, $4.1B^{-/-}$, and $\beta 8^{-/-};4.1B^{-/-}$ yolk sacs were stained with H&E and an anti-CD31 antibody. Elaborate vascular networks with adequate vessel branching were seen in wild type (Figure 14A top), $\beta 8^{-/-}$ (Figure 14B top), and $4.1B^{-/-}$ (Figure 14C top) yolk sacs. Furthermore, H&E-stained yolk sacs from wild type, $\beta 8^{-/-}$, and $4.1B^{-/-}$ embryos showed closely juxtaposed endodermal and mesodermal layers of blood vessels containing nucleated red blood cells (Figure 14A-C, bottom). On the other hand, yolk sacs from $\beta 8^{-/-};4.1B^{-/-}$ embryos displayed abnormal vascular morphologies with reduced vessel sprouting (Figure 14D top). H&E stained $\beta 8^{-/-};4.1B^{-/-}$ yolk sacs revealed compressed endodermal and mesodermal layers with smaller vessel lumens and fewer erythrocytes (Figure 14D, bottom). These findings are consistent with the grossly hypovascular appearance of $\beta 8^{-/-};4.1B^{-/-}$ yolk sacs.

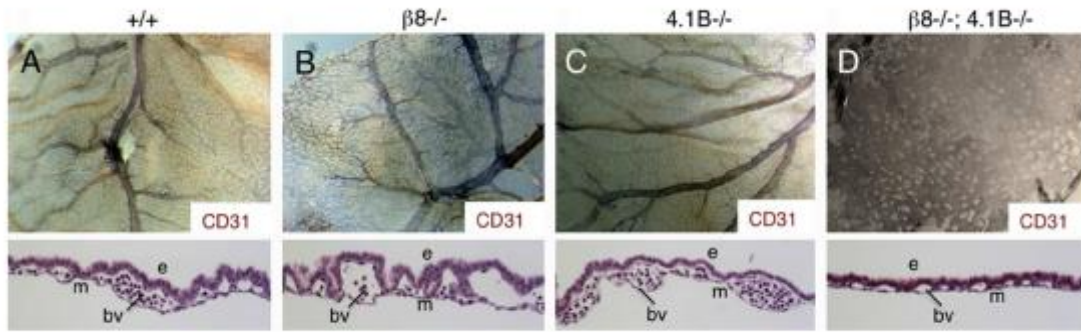


Figure 14. Yolk sac vascular pathologies in $\beta 8^{-/-}; 4.1B^{-/-}$ embryos.

Yolk sac vascular pathologies in double knockout embryos. A–D: Yolk sacs from E10.5 wild type (A), $\beta 8^{-/-}$ (B), $4.1B^{-/-}$ (C), and $\beta 8^{-/-}; 4.1B^{-/-}$ compound mutants (D) were immunostained with an anti-CD31 antibody to reveal blood vessels. Note the abnormal vascular patterning in the yolk sacs of double knockouts (D). Representative H&E-stained microscopic images (400 \times) of yolk sacs from E10.5 wild type, $\beta 8^{-/-}$, $4.1B^{-/-}$, and $\beta 8^{-/-}; 4.1B^{-/-}$ E10.5 embryos are shown in the bottom panels (A–D). e, endoderm; m, mesoderm; bv, blood vessel.

The abnormal findings in yolk sac vasculature suggested possible functional importance of $\beta 8$ integrin and Band 4.1B in yolk sacs. To examine the protein expression of $\beta 8$ integrin and Band 4.1B in yolk sacs, detergent-soluble E10.5 wild type yolk sac lysates were used for immunoblotting. Interestingly, no detectable $\beta 8$ integrin expression was present in yolk sacs (Figure 15D). However, αV integrin, the sole α subunit partner of $\beta 8$ integrin, was expressed in yolk sacs. In addition, high Band 4.1B expression was detected in yolk sacs (Figure 15D). The immunohistochemical examination revealed that Band 4.1B localized to cell-cell contact in the endodermal layer (Figure 15C) whereas αV integrin was found in the cell membrane of both endodermal and mesodermal layers (Figure 15B).

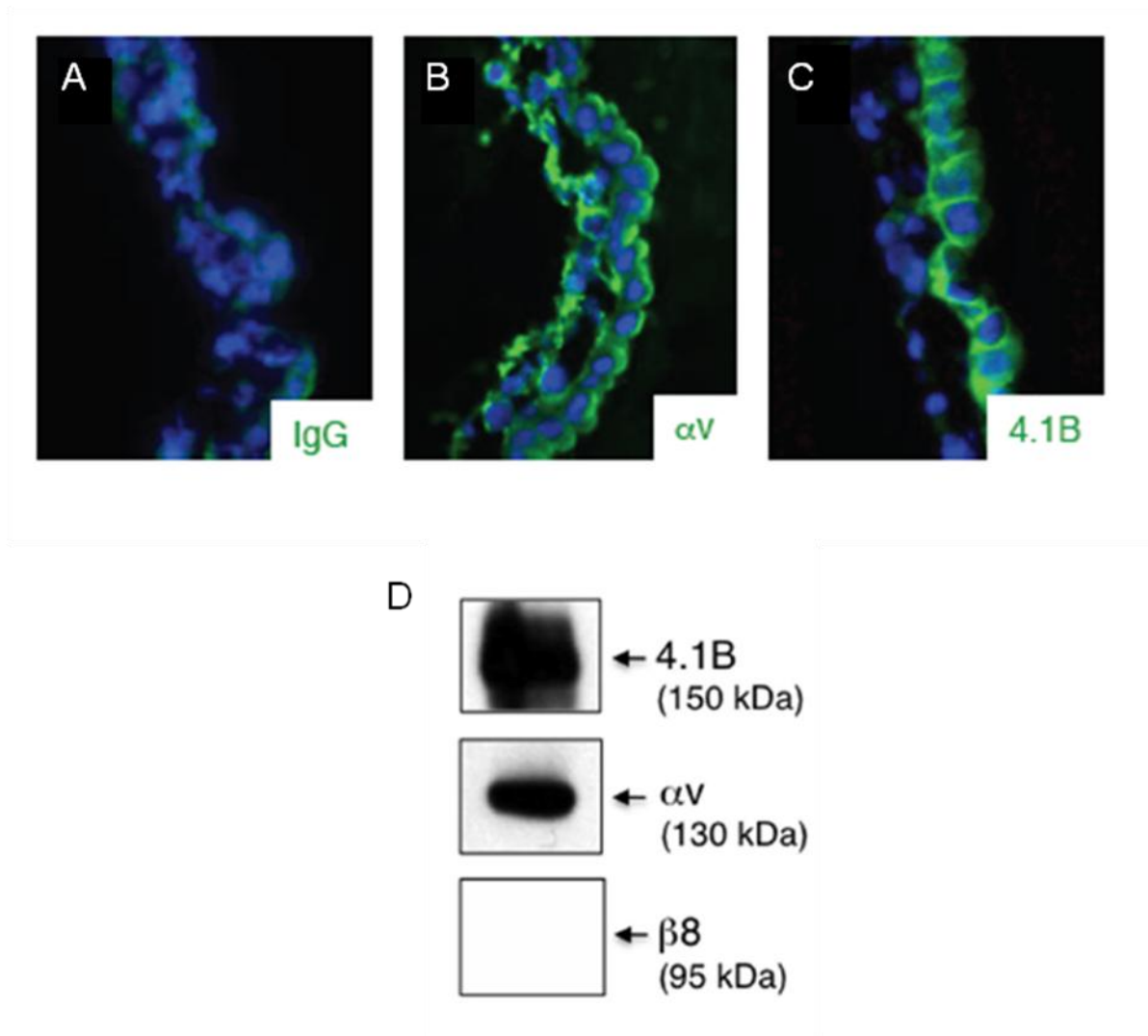


Figure 15. The expression of Band 4.1B and $\alpha v \beta 8$ integrin in yolk sacs.

Figure 15. The expression of Band 4.1B and $\alpha\text{v}\beta 8$ integrin in yolk sacs.

A-C: Yolk sacs from E10.5 wild type embryos were immunostained with control IgG (A), an anti- αv (B), or an anti-4.1B (C) antibody. Note αv integrin is expressed in both the endodermal and mesodermal layers (B) whereas Band 4.1B localizes to the endodermal layer only. D: Detergent-soluble lysates prepared from E10.5 yolk sacs were immunoblotted with an anti- αv , an anti- $\beta 8$, or anti-4.1B rabbit polyclonal antibody, revealing lack of detectable $\beta 8$ integrin protein expression in yolk sacs.

Lack of $\beta 8$ integrin in yolk sacs ruled out cooperative functions of $\beta 8$ integrin and Band 4.1B in yolk sacs. The yolk sac phenotypes observed in $\beta 8^{-/-};4.1B^{-/-}$ were likely to be secondary to systemic cardiovascular abnormalities. Thus, the expression of $\beta 8$ integrin and Band 4.1B was analyzed in the heart using immunoblot analysis of detergent-soluble E10.5 wild type heart lysates. Unlike yolk sacs, $\beta 8$ protein expression was detected in the heart (Figure 16I). αV integrin and Band 4.1B were also present in the heart (Figure 16I). To determine protein localization in different cardiac compartments, whole-mount immunohistochemical analysis of the heart was performed. The hearts dissected from E10.5 wild type embryos were immunostained with anti- αV integrin and anti-4.1B antibodies. Various cardiac chambers expressed both αV integrin and Band 4.1B, supporting the findings of immunoblot analysis. Band 4.1B and αV integrin were mostly expressed in the ventricles and OFT, although less intense expression of these proteins was present in the atria (Figure 16B-H). These findings indicate that the extraembryonic vascular pathologies found in $\beta 8^{-/-};4.1B^{-/-}$ are most likely due to other cardiovascular defects.

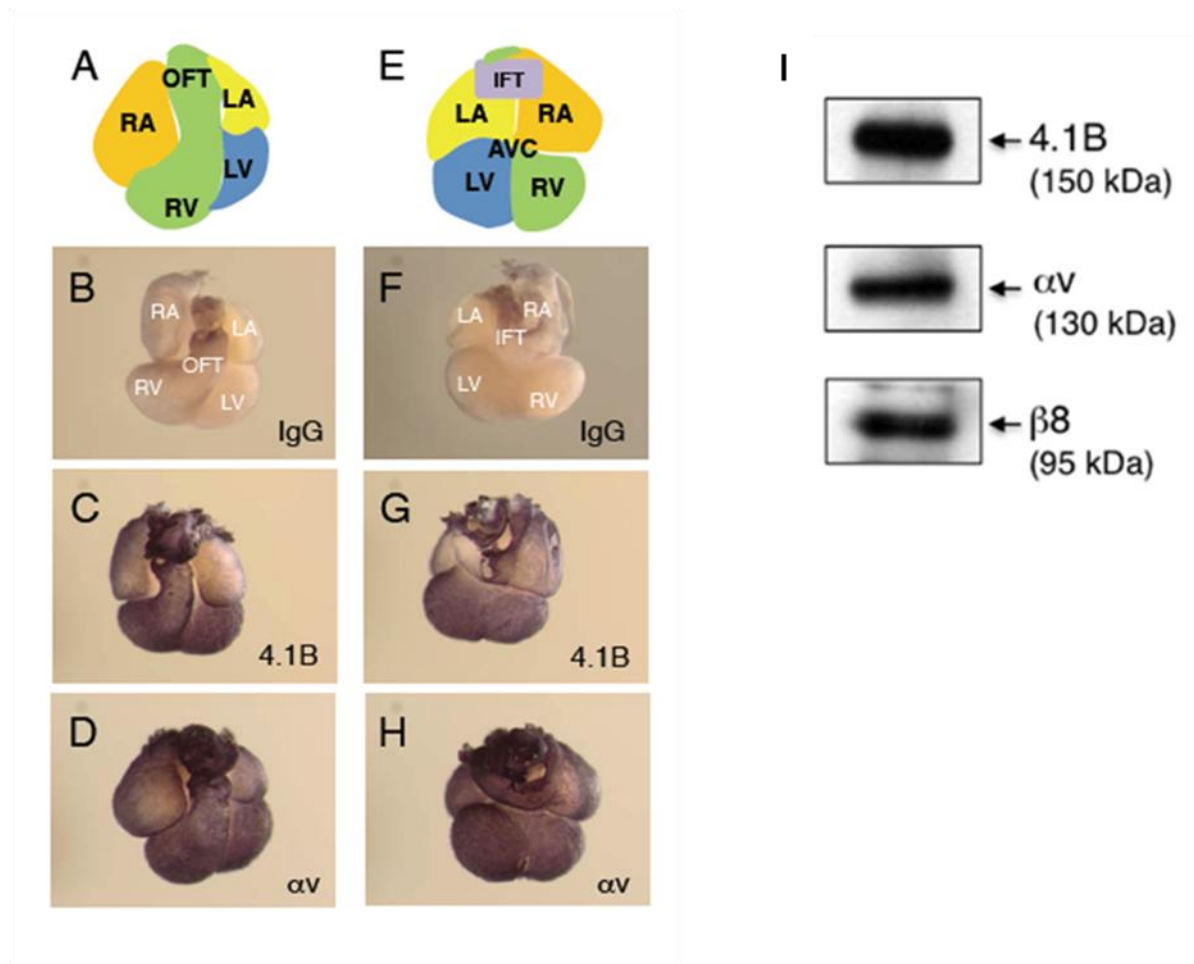


Figure 16. The expression of Band 4.1B and $\alpha v\beta 8$ integrin in the embryonic heart.

Figure 16. The expression of Band 4.1B and $\alpha\text{v}\beta 8$ integrin in the embryonic heart.

A, E: Schematic diagrams of anterior (A) and posterior (E) views of the E10.5 embryonic mouse heart. B-D, F-H: E10.5 mouse hearts were whole-mount immunostained with control IgG (B, F), an anti- αv (C, G), or an anti-4.1B (D, H) antibody. Anterior (B-D) and posterior (F-H) views of the immunostained hearts revealed co-expression of αV integrin and Band 4.1B proteins. I: Detergent-soluble protein lysates prepared from microdissected E10.5 hearts were immunoblotted with anti- αv , anti- $\beta 8$, and anti-4.1B antibodies revealing expression of all three proteins. RA, right atrium; RV, right ventricle; LA, left atrium; LV, left ventricle; OFT, outflow tract; IFT, inflow tract; AVC, atrioventricular canal.

3.2.3. $\beta 8^{-/-};4.1B^{-/-}$ embryos display abnormal morphogenesis of the outflow tract and myocardium of the heart.

The morphologies of the E10.5 wild type, $\beta 8^{-/-}$, $4.1B^{-/-}$, and $\beta 8^{-/-};4.1B^{-/-}$ hearts were carefully examined by immunostaining histological sections with H&E. The heart of $\beta 8^{-/-};4.1B^{-/-}$ was significantly smaller than the wild type, $\beta 8^{-/-}$, and $4.1B^{-/-}$ hearts. This was expected given the growth retardation observed in E10.5 $\beta 8^{-/-};4.1B^{-/-}$ embryos. Structurally, severe hypotrophy of endocardial cushions in the AV junction and the OFT was seen in the $\beta 8^{-/-};4.1B^{-/-}$ heart (Figure 17D), compared to the normal appearing wild type, $\beta 8^{-/-}$, and $4.1B^{-/-}$ hearts (Figure 17A-C). Furthermore, thinning of the myocardium and the OFT vessel wall was observed in the $\beta 8^{-/-};4.1B^{-/-}$ heart (Figure 17D).

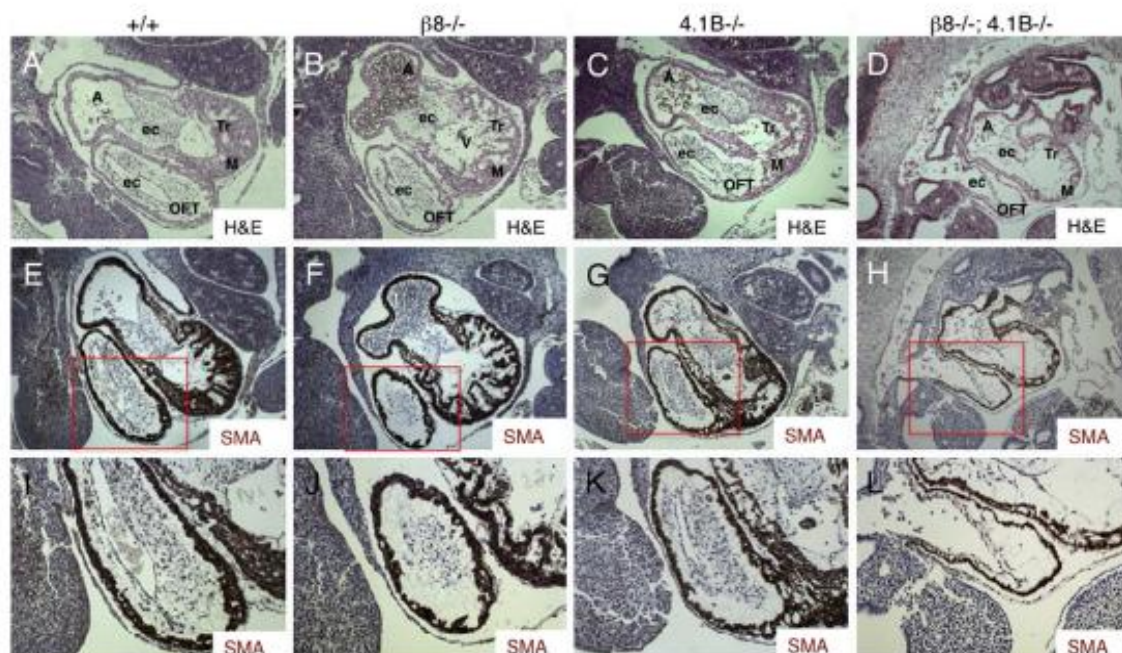


Figure 17. Defective heart morphogenesis in $\beta 8^{-/-}; 4.1B^{-/-}$ embryos.

Figure 17. Defective heart morphogenesis in $\beta 8^{-/-};4.1B^{-/-}$ embryos.

A–D: Sagittal sections cut at the level of the aorticopulmonary septum from wild type (A), $\beta 8^{-/-}$ (B), $4.1B^{-/-}$ (C), and $\beta 8^{-/-};4.1B^{-/-}$ (D) embryos (E10.5) stained with H&E (100 \times magnification). Note the size-reduced heart and conotruncal cushion hypotrophy in the $\beta 8^{-/-};4.1B^{-/-}$ mutant embryo (D). E–H: Sagittal sections from wild type (E), $\beta 8^{-/-}$ (F), $4.1B^{-/-}$ (G), and $\beta 8^{-/-};4.1B^{-/-}$ (H) embryos (E10.5) were immunostained with an anti- α SMA antibody. Note the decreased expression of α SMA at the level of the OFT in the double knockout embryo, shown at 100 \times magnification. I–L: Higher magnification images of boxed areas in E–H (200 \times) showing the OFT from wild type (I), $\beta 8^{-/-}$ (J), $4.1B^{-/-}$ (K), and $\beta 8^{-/-};4.1B^{-/-}$ (L) embryos (E10.5), highlighting reduced expression of α SMA in double knockout embryos. A, atrium; V, ventricle; ec, endocardial cushion; M, myocardium; Tr, trabeculae; OFT, outflow tract.

Neural crest cells that express smooth muscle markers, in part, contribute to the formation of endocardial cushions of the AV junction and OFT. Therefore, the wild type, $\beta 8^{-/-}$, 4.1B $^{-/-}$, and $\beta 8^{-/-};4.1B^{-/-}$ hearts were stained with an anti- α smooth muscle actin (SMA) for further analysis. In comparison to the wild type (Figure 17E, I), $\beta 8^{-/-}$ (Figure 17F, J) and 4.1B $^{-/-}$ (Figure 17G, K) embryonic hearts, the $\beta 8^{-/-};4.1B^{-/-}$ heart showed decreased α SMA expression in the OFT mesenchyme and myocardium (Figure 17H, L). In addition, the expression of desmin, another smooth muscle marker, was reduced in the OFT and myocardium of $\beta 8^{-/-};4.1B^{-/-}$ embryos (Figure 18D), compared to normal desmin expression in wild type (Figure 18A), $\beta 8^{-/-}$ (Figure 18B), and 4.1B $^{-/-}$ (Figure 18C) embryos.

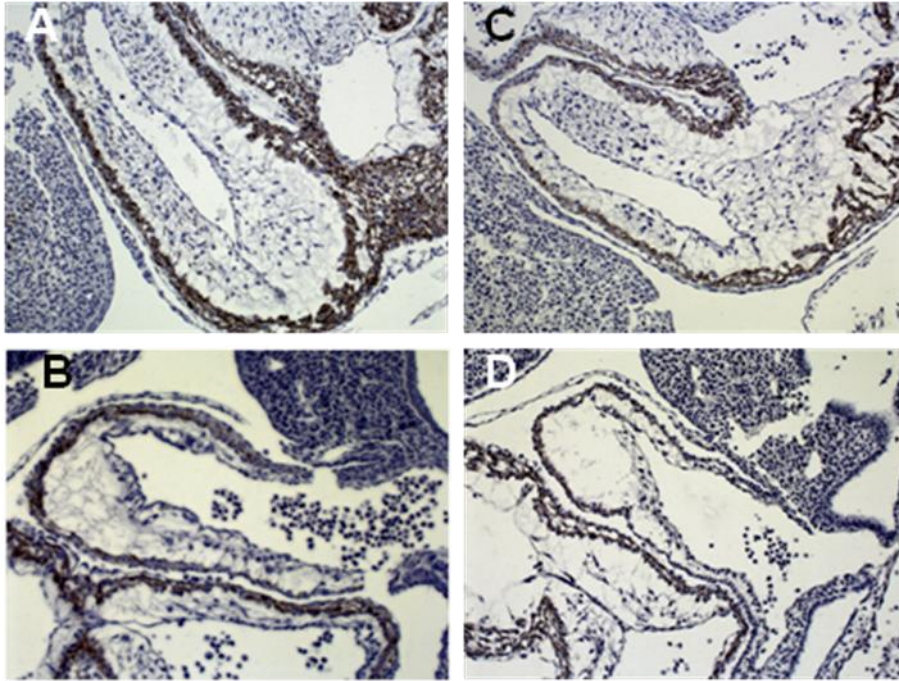


Figure 18. Reduced expression of desmin in $\beta 8^{-/-};4.1B^{-/-}$ embryos.

A–D: Sagittal sections cut at the level of the aorticopulmonary septum from wild type (A), $\beta 8^{-/-}$ (B), $4.1B^{-/-}$ (C), and $\beta 8^{-/-};4.1B^{-/-}$ (D) embryos (E10.5) immunostained with an anti-Desmin antibody. Shown at 200 \times . Note the reduced expression of desmin protein in double knockout embryos (D).

Given the abnormal morphologies of the $\beta 8^{-/-};4.1B^{-/-}$ OFT and myocardium, the protein expression patterns of αV integrin and Band 4.1B in these structures were examined. Fresh-frozen E10.5 wild type embryo was immunofluorescently labeled with an anti- αV integrin or an anti-4.1B antibody. Both αV integrin and Band 4.1B were detected in endocardial cushions of the AV junction and OFT as well as in the myocardium (Figure 19). Subcellularly, these proteins were present in cell-cell contact (Figure 19).

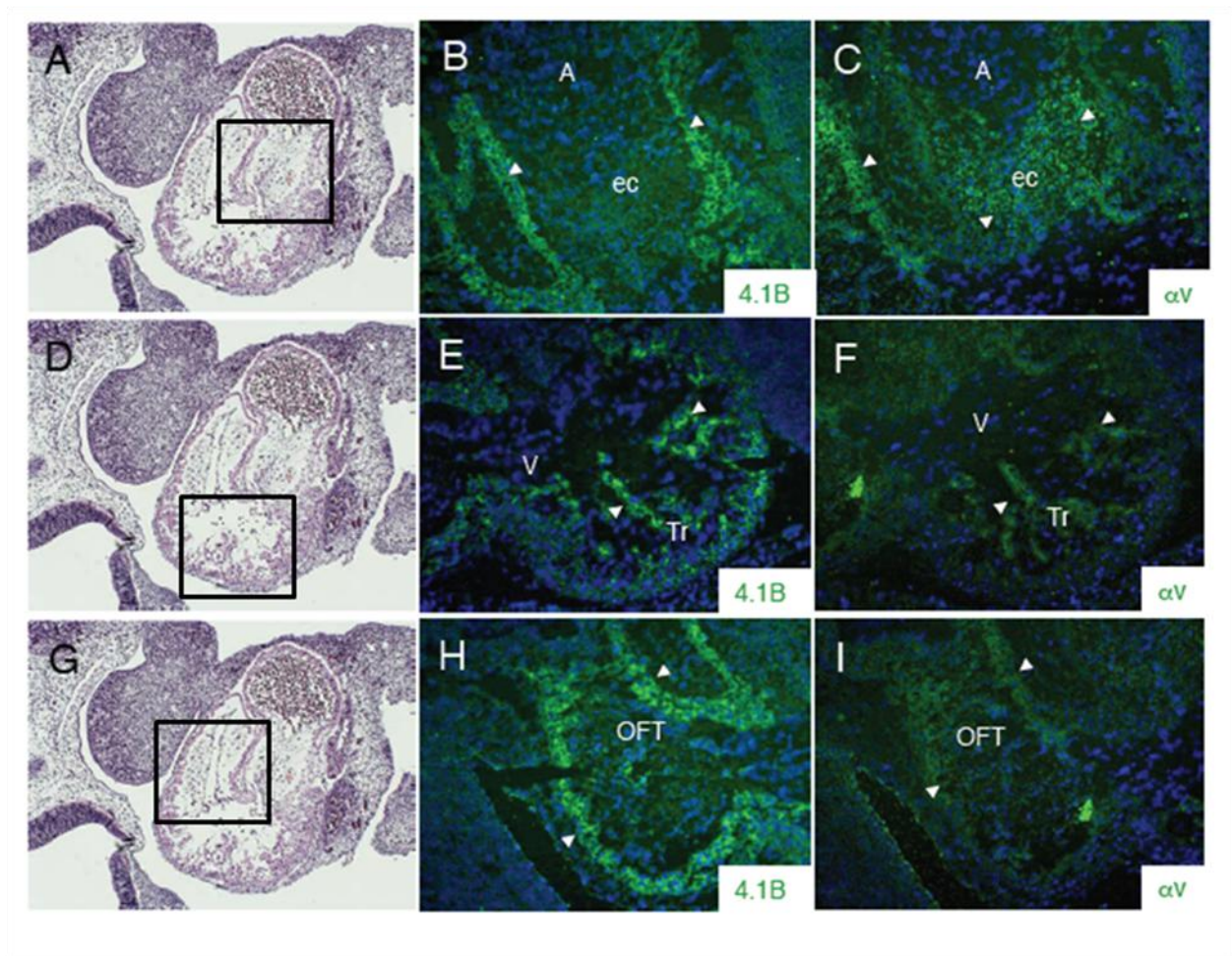


Figure 19. α V integrin and Band 4.1B proteins are co-expressed in the embryonic heart.

Figure 19. α V integrin and Band 4.1B proteins are co-expressed in the embryonic heart.

A, D, G: H&E stained E10.5 wild type heart shown at 100x. Boxed areas correspond with immunofluorescently labeled areas of the heart shown adjacent to the H&E sections. B-C, E-F, H-I: Frozen sagittal sections from E10.5 wild type embryos were immunofluorescently labeled with an anti-4.1B (B, E, H) or an anti- α v (C, F, I) antibody. Shown at 200x. Note that α v integrin and 4.1B protein are co-expressed in the myocardium and mesenchyme of the AV canal and OFT. A, aorta; V, ventricle; OFT, outflow tract; M, myocardium; Tr, trabeculae; ec, endocardial cushion.

$\beta 8$ integrin exclusively pairs with αV integrin (Moyle et al., 1991). Since $\beta 8$ integrin expression in the heart was confirmed by immunoblotting, it is safe to conclude that αV integrin localization patterns seen in the immunofluorescently labeled heart reflect $\beta 8$ integrin expression patterns.

3.2.4. Neural crest cell migration is impaired in $\beta 8^{-/-};4.1B^{-/-}$ embryos.

The migration of cardiac neural crest cells is critical for the morphogenesis of the heart (Snarr et al., 2008). Given the contribution of neural crest cells in OFT formation and the defective OFT morphologies observed in the $\beta 8^{-/-};4.1B^{-/-}$, neural crest patterning in embryos was examined. E10.5 wild type (n=6), $\beta 8^{-/-}$ (n=4), $4.1B^{-/-}$ (n=7), and $\beta 8^{-/-};4.1B^{-/-}$ (n=5) embryos were stained with an anti-neurofilament antibody 2H3 using whole-mount immunostaining methods. Wild type, $\beta 8^{-/-}$, and $4.1B^{-/-}$ embryos displayed an elaborate network of neurofilament positive projections (Figure 20A-C). However, 3 out of 5 $\beta 8^{-/-};4.1B^{-/-}$ embryos that were examined exhibited a defective neurofilament network throughout the body (Figure 20D).

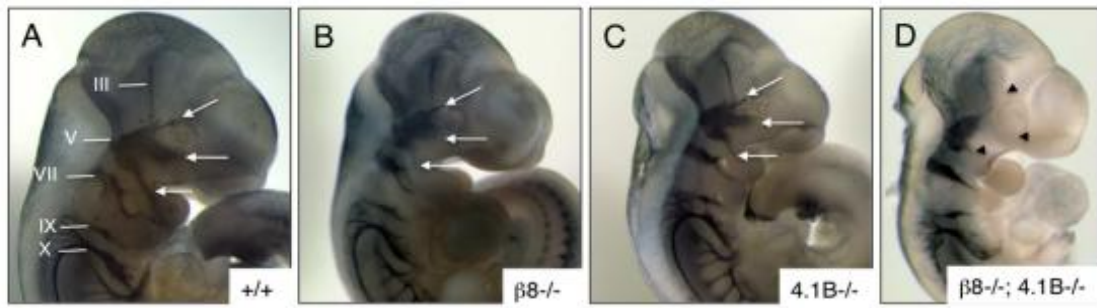


Figure 20. Abnormal patterns of neurofilament expression in $\beta 8^{-/-}; 4.1B^{-/-}$ embryos.

A–D: Wild type (A), $\beta 8^{-/-}$ (B), $4.1B^{-/-}$ (C), or $\beta 8^{-/-}; 4.1B^{-/-}$ (D) embryos (E10.5) were whole-mount immunostained with an anti-neurofilament monoclonal antibody, 2H3. The axonal projections from the trigeminal ganglion are prominent in wild type and single knockouts (white arrows in A–C). In contrast, the lack of distal projections from the trigeminal nerves (upper black arrowheads in D) and the shortened distal projections into the pharyngeal arches (bottom arrowhead, D) were noted in double knockout mice.

In $\beta 8^{-/-};4.1B^{-/-}$ embryos, the size of the trigeminal ganglion of cranial nerve V was reduced (Figure 20D). In addition, the ophthalmic, maxillary, and mandibular branches of cranial nerve V showed shortened projections. Furthermore, neurofilament-positive projections of cranial nerves into the pharyngeal arches were lacking in $\beta 8^{-/-};4.1B^{-/-}$ embryos (Figure 20D). Abnormal neurofilament patterning was also observed in the trunks of $\beta 8^{-/-};4.1B^{-/-}$ embryos (Figure 21 D).

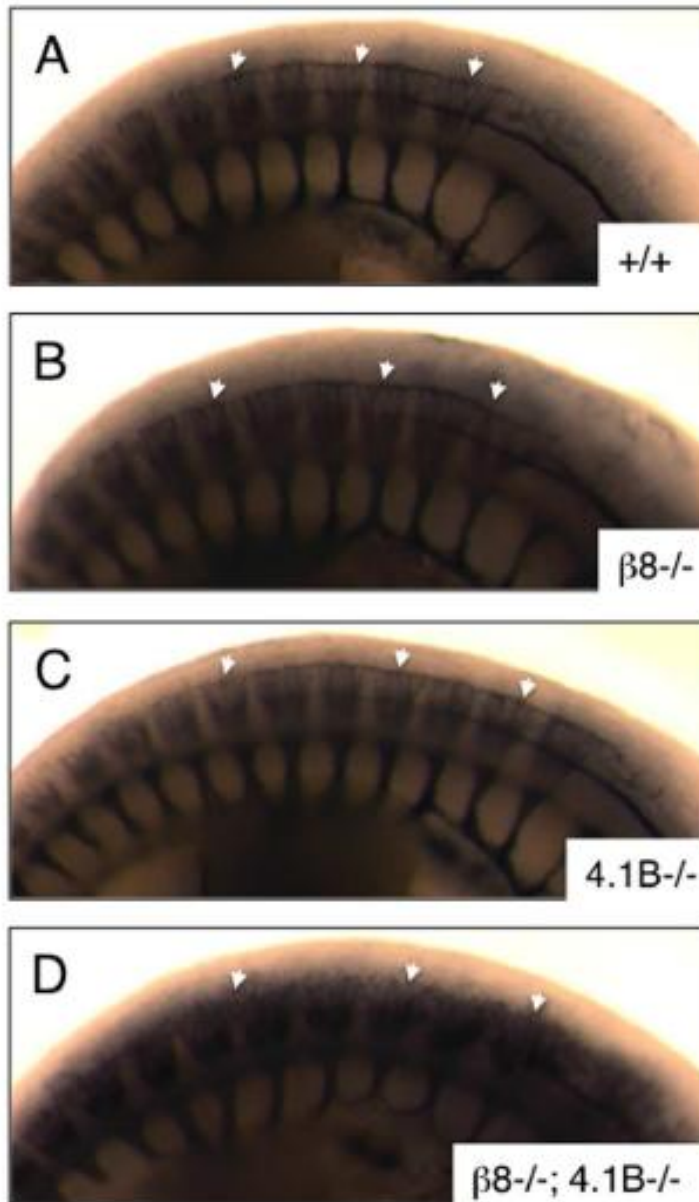


Figure 21. Neurofilament expression patterns are abnormal in $\beta 8^{-/-}$;4.1B $^{-/-}$ trunks.

Figure 21. Neurofilament expression patterns are abnormal in $\beta 8^{-/-};4.1B^{-/-}$ trunks.

A–D: Images of trunk regions from E10.5 wild type (A), $\beta 8^{-/-}$ (B), 4.1B $^{-/-}$ (C), and $\beta 8^{-/-};4.1B^{-/-}$ (D) embryos. Note the normal neural crest patterning in wild type and single knockouts (white arrows in A–C). In contrast, note the abnormal patterning of neurofilament-expressing cells in the double knockout embryo (white arrows in D).

3.3. Discussion

Various *in vitro* studies have shown the direct binding of $\beta 8$ integrin and Band 4.1B (McCarty et al., 2005a). However, cooperative functions for these two proteins have not been determined. This study was the first to demonstrate *in vivo* functional links between $\beta 8$ integrin and Band 4.1B using gene knockout strategies. The data presented here show that ablation of $\beta 8$ integrin and Band 4.1B results in embryonic lethality by E11.5 and that this is likely secondary to abnormal cardiac morphogenesis. $\beta 8$ integrin's roles in CNS vascular development have been well documented in multiple previous reports (Zhu et al., 2002; Mobley et al., 2009; Tchaicha et al., 2010). However, this study established that $\beta 8$ integrin regulates non-CNS vascular development by cooperatively signaling with Band 4.1B.

Interestingly, the lethal cardiovascular phenotypes of $\beta 8^{-/-};4.1B^{-/-}$ embryos were partially penetrant. The lethality seen in these mice may be affected by their background strain variation. In fact, strain-dependent phenotypes of $\beta 8^{-/-}$ mice have been documented. In the study done by Zhu and colleagues, over 50% of $\beta 8^{-/-}$ mice with C57BL6/129S4 background died at mid-gestation, owing to placenta defects (2002). However, another study reported that $\beta 8^{-/-}$ mice with C57BL6/129S4/CD1 background were born alive without displaying embryonic lethality (Mobley et al., 2009). These differences indicate that genetic modifiers of the lethal phenotypes might be present in a strain-specific manner. $\beta 8^{-/-}$ and $\beta 8^{-/-};4.1B^{-/-}$ mice used in this study were generated by crossing parental strains with C57BL6/129S4 and C57BL6/129S4/CD1 backgrounds. Indeed, these mice did not exhibit placental abnormalities.

Grossly, the most striking feature of $\beta 8^{-/-};4.1B^{-/-}$ at E10.5 was hypovascularity of the yolk sac and embryo proper. The yolk sac is the first site of erythrocyte generation (McGrath et al., 2003). The connection of the yolk sac and systemic vasculature establishes functional circulation in embryos (McGrath et al., 2003). Therefore, functional abnormalities in the yolk sac can be lethal to embryos. Indeed, abnormal vascular morphologies with reduced vessel sprouting were observed in $\beta 8^{-/-};4.1B^{-/-}$ yolk sacs. These yolk sacs also exhibited compressed endodermal and mesodermal layers with smaller vessel lumens and fewer erythrocytes. These findings were consistent with the grossly hypovascular appearance of $\beta 8^{-/-};4.1B^{-/-}$ yolk sacs. However, no detectable expression of $\beta 8$ integrin was measured in $\beta 8^{-/-};4.1B^{-/-}$ yolk sacs, indicating that cooperative signaling of $\beta 8$ integrin and Band 4.1B does not occur in yolk sacs. Therefore, the abnormalities displayed in $\beta 8^{-/-};4.1B^{-/-}$ yolk sacs are not likely the primary cause of embryonic death. They are rather likely to be the secondary effects of impairments elsewhere.

Defective systemic circulation can lead to vascular abnormalities in extraembryonic tissues and multiple organ systems. In addition to the abnormal findings in $\beta 8^{-/-};4.1B^{-/-}$ yolk sacs, blood vessels in the neural tube of $\beta 8^{-/-};4.1B^{-/-}$ embryos were found to be impaired. The neural tube contained distended blood vessels and showed a less elaborate vascular network with minimal branching. These vascular phenotypes were consistent with the grossly hypovascular appearance of $\beta 8^{-/-};4.1B^{-/-}$ embryos. Multiple defects in the vasculatures of extraembryonic and embryonic tissues indicated impaired cardiac structures and/or

functions. Cardiovascular defects causing early embryonic lethality include abnormal heart specification and/or poor cardiac function (Conway et al., 2003). In fact, pericardial edema was notable in multiple $\beta 8^{-/-};4.1B^{-/-}$ embryos upon careful examination. Pericardial edema is a sign of poorly functioning heart (Conway et al., 2003). Multiple knockout mice with pericardial edema, such as PDGF α receptor knockouts, have been shown to have OFT and AV septal defects (Soriano, 1997). Similarly, $\beta 8^{-/-};4.1B^{-/-}$ embryos displayed hypotrophic endocardial cushions of the AV junction and OFT with diminished expression of neural crest cell makers.

The generation and incorporation of mesenchymal cells, including neural crest cells, are crucial for proper heart development (Snarr et al., 2008). AV and OFT cushions are two main cardiac mesenchymal structures. AV cushions contribute to the formation of AV valves and septa whereas OFT cushions generate aorticopulmonary septum (Snarr et al., 2008). Cardiac neural crest cells are especially important for the development of the OFT. Neural crest cells are located between the otic placode and the third/fourth somite (Stoller and Epstein, 2005). These cells migrate through the third, fourth, and sixth pharyngeal arches to the heart (Snarr et al., 2008). Ablating neural crest cells resulted in impairments of the OFT and aortic arch (Kirby et al., 1983). Given that similar OFT abnormalities in other mouse models are caused by cardiac neural crest migration defects (Conway et al., 2003), the abnormal cardiac morphogenesis seen in $\beta 8^{-/-};4.1B^{-/-}$ embryos might also be due to impaired neural crest migration. Most E10.5 $\beta 8^{-/-};4.1B^{-/-}$ embryos, indeed, demonstrated a defective network of neurofilament throughout the body with shortened projections of the ophthalmic, maxillary, and mandibular

branches of cranial nerve V and absent projections of cranial nerves to the pharyngeal arches. Therefore, $\beta 8$ integrin and Band 4.1B are likely to cooperatively function to support neural crest cell migration to the OFT and possibly other regions of the developing heart. In fact, multiple αV -binding β integrins have been implicated in neural crest cell adhesion and migration *in vitro* (Delannet et al., 1994).

Bone morphogenetic proteins (BMP) and transforming growth factor beta (TGF β) have been demonstrated to be important for cardiac morphogenesis (Monzen et al., 2002; Sanford et al., 1997). The disruption of BMP and TGF β signaling has been shown to induce impairments of cardiac neural crest-mediated OFT formation. $\beta 8$ integrin is involved in signaling of the TGF β family members. Therefore, it is possible that $\beta 8$ integrin and Band 4.1B may cooperatively regulate TGF β signaling in neural crest cells. In addition to cardiac morphogenesis, neural crest cells participate in palate development (Smith and Tallquist, 2010). Interestingly, mice genetically null for αV , $\beta 8$, or TGF $\beta 3$ all have impaired palate formation (Bader et al., 1998; Zhu et al., 2002; Proetzel et al., 1995). Furthermore, cleft palate and structurally abnormal OFT are seen with selective ablation of TGF β receptors or Smads in neural crest cells (Wurdak et al., 2005; Nie et al., 2008). Collectively, it is highly possible that $\beta 8$ integrin and Band 4.1B exert their effects on neural crest cells by modulating TGF β signaling pathways.

Alternatively, $\beta 8$ integrin and Band 4.1B may work together to promote cardiac neural crest cell growth and survival after cardiac neural crest cells get incorporated into the OFT. Thinning of the OFT and cardiac chamber walls were observed in $\beta 8^{-/-}; 4.1B^{-/-}$ embryos. However, increased apoptosis or decreased cell

proliferation were not seen in the $\beta 8^{-/-};4.1B^{-/-}$ heart. Normal OFT development also involves mesoderm-derived endocardial cells (Acloque et al., 2009). Thus, $\beta 8$ integrin and Band 4.1B may play roles in regulating other cell types as well. Neural crest cells undergo endothelial-to-mesenchymal transformation (EMT) before beginning their migration to the heart (Stoller and Epstein, 2005). Therefore, the involvement of $\beta 8$ integrin and Band 4.1B in EMT is also possible.

The cardiovascular phenotypes seen in $\beta 8^{-/-};4.1B^{-/-}$ embryos occur in the absence of both $\beta 8$ integrin and Band 4.1B. This suggests cooperative functions of these two proteins. Another possibility, however, is that $\beta 8$ integrin and Band 4.1B may act in parallel and/or redundant signaling pathways. In case Band 4.1B regulates downstream signaling pathways of $\beta 8$ integrin and other cell surface receptors, Band 4.1B's functions would be unaltered in the absence of $\beta 8$ integrin. Lethal cardiovascular phenotypes have been demonstrated in mice that are genetically null for αV and $\alpha 5$ integrins (van der Flier et al., 2010). This opens up the possibility that Band 4.1B may function as an intracellular signaling link between multiple integrins. The FERM domain of Band 4.1B may interact with β subunits and other cell surface receptors while the CTD binds to $\beta 8$ integrin (McCarty et al., 2005a), enabling Band 4.1B to incorporate multiple signaling pathways.

Defective OFT is a common feature of congenital heart disease, the most frequently occurring birth defect in humans. One example of congenital heart disease is DiGeorge syndrome. Individuals with DiGeorge syndrome have abnormalities in many structures derived from neural crest cells, including the OFT and aortic arch (Stoller and Epstein, 2005). $\beta 8$ integrin and Band 4.1B have not

been studied in human heart diseases. Given the cardiac defects seen in $\beta 8^{-/-}$;4.1B $^{-/-}$ embryos, it would be interesting to see if $\beta 8$ integrin and Band 4.1B play roles in human congenital heart disease.

Chapter 4. Specific Aim II

4.1. Introduction

The members of the protein 4.1 superfamily function as links between the cell membrane and the actin cytoskeleton, but also play important roles in cell adhesion, proliferation, and motility, and other intracellular signaling pathways (Diakowski et al., 2006). Band 4.1B, a cytoskeletal adaptor protein, has been implicated in regulation of various cellular events, but the molecular mechanisms by which Band 4.1B contributes to these signaling cascades have not been determined. Efforts have been made to identify binding partners of Band 4.1B to better understand the functional roles for Band 4.1B. The discovery of the interaction between $\beta 8$ integrin and Band 4.1B (McCarty et al., 2005a) has led to the examination of Band 4.1B's roles in integrin-mediated adhesion and signaling that are essential for a variety of cellular events.

Cell adhesion, spreading, and motility are some events regulated by integrins. Integrins are also important for coordinating cell-ECM interactions, adhesion formation, and cytoskeleton organization during cell movement (Barczyk et al., 2010; Legate et al., 2009; Harburger and Calerwood, 2009). A focal adhesion complex is a crucial component that integrates signaling required for cell motility. Several molecules that belong to the protein 4.1 superfamily have been shown to modulate focal adhesion formation and cell migration that are mediated by integrins. In particular, talin, a protein that shares sequence homology with Band 4.1B, has been demonstrated to regulate $\beta 1$ integrin-mediated focal adhesion assembly and cell spreading (Zhang et al., 2008). Given the structural similarity between talin and

Band 4.1B, Band 4.1B may also play a role in focal adhesion formation and cell spreading by interacting with $\beta 8$ or perhaps other β integrins. Previously, the association between Band 4.1B and $\beta 1$ integrin has been postulated (Piao et al., 2009), but the interaction between these two proteins has never been examined. Given the importance of the FERM domain in integrin binding and activation, Band 4.1B may help proper localization of $\beta 1$ integrin to newly forming adhesions through physical interactions and/or influence intracellular signaling of $\beta 1$ integrin at the adhesion sites.

In this chapter, the *in vitro* functional roles for Band 4.1B in integrin-mediated cell adhesion and signaling were investigated. The working hypothesis was that Band 4.1B regulates $\beta 1$ integrin-mediated cell-ECM interaction and signaling via its FERM domain during initial cell spreading.

4.2. Results

4.2.1. Lack of Band 4.1B expression does not affect integrin expression in astrocytes.

To characterize the expression of Band 4.1B and other members of the protein 4.1 family in astrocytes, detergent-soluble wild type and 4.1B^{-/-} astrocyte lysates were immunoblotted with anti-4.1B, anti-4.1G, and anti-4.1N antibodies. As expected, Band 4.1B is highly expressed in wild type, but not in 4.1B^{-/-} astrocytes (Figure 22). The size of Band 4.1B was 145 kDa, which was similar to previously reported molecular weight (Sun et al., 2002). Bands 4.1G and 4.1N were strongly expressed in both wild type and 4.1B^{-/-} astrocytes (Figure 22).

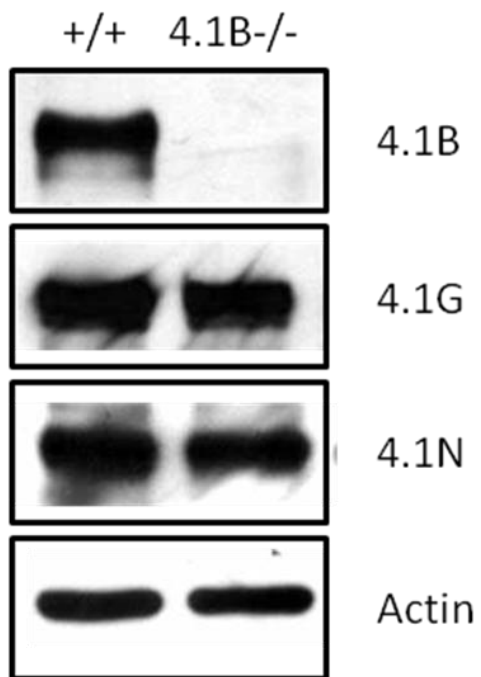


Figure 22. Protein 4.1 expression in astrocytes.

Figure 22. Protein 4.1 expression in astrocytes.

Detergent-soluble wild type and 4.1B^{-/-} astrocytes were immunoblotted with anti-4.1B, anti-4.1G, and anti-4.1N antibodies. As expected, 145 kDa Band 4.1B was highly expressed in wild type, but not in 4.1B^{-/-} astrocytes. Bands 4.1G and 4.1N were expressed in both wild type and 4.1B^{-/-} astrocytes. The sizes of 4.1G and 4.1N were 150 kDa and 100 kDa, respectively. The levels of 4.1G and 4.1N expression were not different between wild type and 4.1B^{-/-} astrocytes.

The sizes of Bands 4.1G and 4.1N were 150 kDa and 100 kDa, respectively. No significant differences in the expression of these proteins were observed between wild type and 4.1B^{-/-} astrocytes.

Next, integrin expression in wild type and 4.1B^{-/-} astrocytes was examined. Astrocytes were labeled with sulfo-NHS-biotin and immunoprecipitated with various integrin antibodies, including anti- α 1, anti- α 2, anti- α 3, anti- α 4, anti- α 5, anti- α 6, anti- α 8, anti- α V, and anti- β 1 antibodies, to detect integrins that are expressed on the cell surface. Both wild type and 4.1B^{-/-} astrocytes showed similar integrin expression profiles (Figure 23). Because sulfo-NHS-biotin labeled $\alpha\beta$ heterodimeric pairs and these associations are maintained through the experimental manipulations, immunoprecipitation of α subunits also revealed their β binding partners, and vice versa. In other words, immunoprecipitation of α 2, α 3, α 5, α 6 and α V demonstrated pairing with the predicted β subunits (Figure 23). Since β 1 integrin pairs with multiple α subunits (Figure 4), immunoprecipitation of β 1 also pulled-down α 1, α 2, α 3, α 5, α 6, and α V integrins (Figure 23). The presence of Band 4.1B in astrocytes did not affect cell surface integrin expression, i.e., the profiles of integrin expression did not differ between wild type and 4.1B^{-/-} astrocytes.

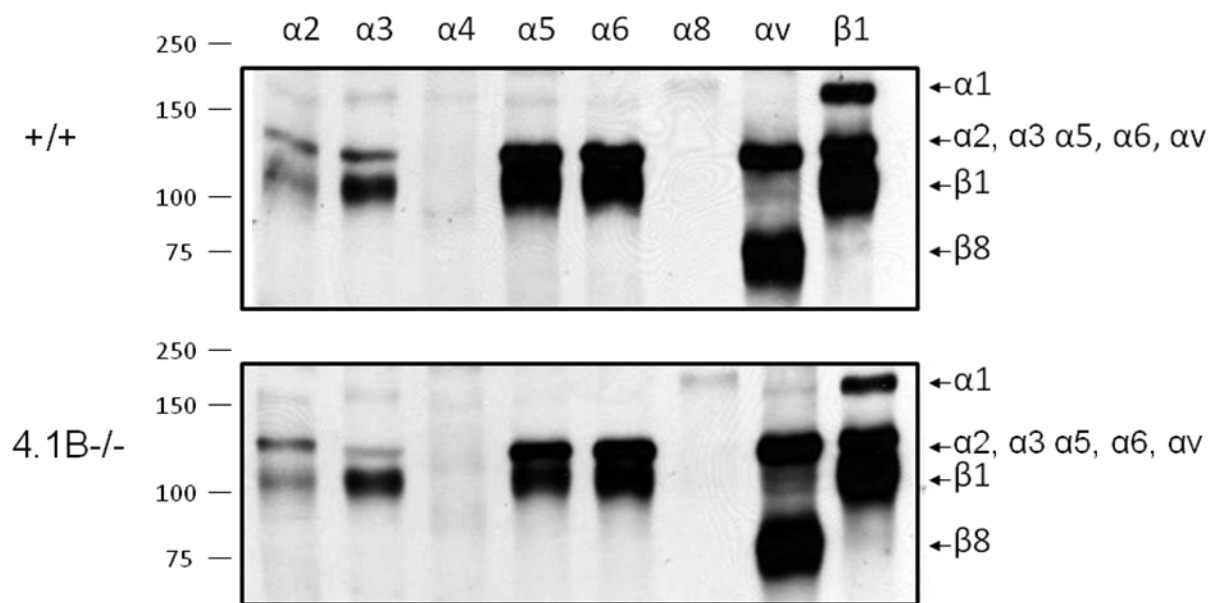


Figure 23. Integrin expression in astrocytes.

Figure 23. Integrin expression in primary mouse astrocytes.

The astrocytes were cell surface-labeled with sulfo-NHS-biotin and immunoprecipitated with various integrin antibodies. Both wild type and 4.1B-/- astrocytes showed similar integrin expression profiles. Because sulfo-NHS-biotin labeled $\alpha\beta$ heterodimeric pairs, immunoprecipitation of α subunits also revealed their β binding partners, and vice versa. Pull-down of $\alpha 2$, $\alpha 3$, $\alpha 5$, $\alpha 6$ and αV showed $\alpha 2\beta 1$, $\alpha 3\beta 1$, $\alpha 5\beta 1$, $\alpha 6\beta 1$, $\alpha V\beta 1$, and $\alpha V\beta 8$ integrin heterodimers, respectively. Since $\beta 1$ integrin pairs with multiple α subunits, immunoprecipitation of $\beta 1$ also pulled-down $\alpha 1$, $\alpha 2$, $\alpha 3$, $\alpha 5$, $\alpha 6$, and αV integrins. The absence of Band 4.1B in astrocytes did not affect cell surface integrin expression.

4.2.2. Band 4.1B shows time-dependent changes in its subcellular localization.

In many cell types, Band 4.1B has been shown to localize to the plasma membrane where cell-cell contacts are formed (Parra et al., 2000). However, Band 4.1B's expression patterns in astrocytes had not been determined. Therefore, subcellular localization of Band 4.1B and other protein 4.1 was explored in astrocytes. Wild type and 4.1B^{-/-} astrocytes were allowed to adhere to fibronectin, an ECM molecule, for 30 minutes. These adherent cells were then immunostained with anti-4.1B, anti-4.1G, and anti-4.1N antibodies. Immunofluorescent analysis of protein 4.1's revealed that Bands 4.1B and 4.1G localized to adhesions during early spreading. Bands 4.1B and 4.1G's localization to adhesions were confirmed by co-localization of these proteins with paxillin, a focal adhesion marker (Figure 24A-D). Unlike Bands 4.1B and 4.1G, Band 4.1N did not localize to adhesions, as apparent in co-labeling analysis with paxillin (Figure 24E, F). However, Band 4.1N was concentrated in the nucleus as it co-localized with DAPI which binds to DNA. In the absence of Band 4.1B, astrocytes were still able to form adhesions, as demonstrated with paxillin-positive contacts in 4.1B^{-/-} astrocytes (Figure 24B). No differences in localization patterns of Bands 4.1G and 4.1N were demonstrated between wild type (Figure 24C, E) and 4.1B^{-/-} (Figure 24D, F) astrocytes.

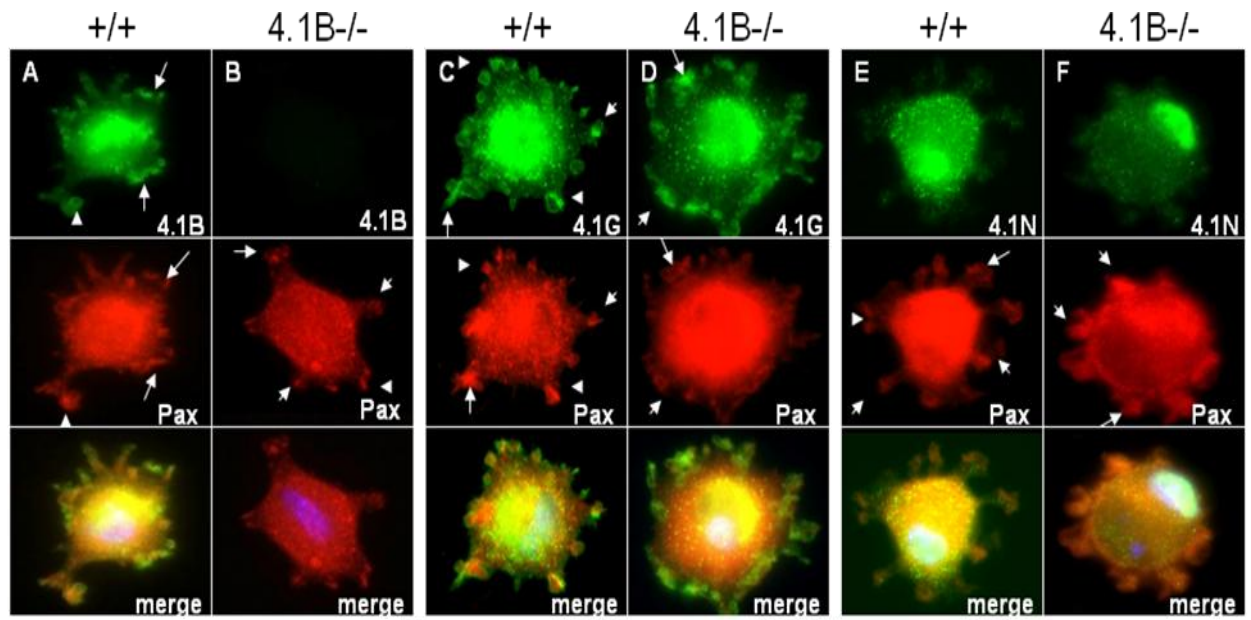


Figure 24. Protein 4.1B and 4.1G, but not 4.1N, localize to cell-ECM contact sites.

Figure 24. Protein 4.1B and 4.1G, but not 4.1N, localize to cell-ECM contact sites.

A-F: Wild type and 4.1B^{-/-} astrocytes were allowed to adhere to fibronectin for 30 minutes and immunostained with anti-4.1B (A, B), anti-4.1G (C, D), and anti-4.1N (E, F) antibodies. 4.1B (arrows in A) and 4.1G (arrows in C, D) co-localized with paxillin in adhesions. Band 4.1N did not co-localize with paxillin, rather it co-localized with DAPI, a nucleus label (E, F). 4.1B^{-/-} astrocytes were still able to form adhesions, as demonstrated with paxillin-positive contacts (arrows in B). No differences in localization patterns of 4.1G and 4.1N were seen between wild type (C, E) and 4.1B^{-/-} (D, F) astrocytes. Images are shown at 400x.

Interestingly, Bands 4.1B, 4.1G, and 4.1N became more diffusely expressed 24 hours after fibronectin adhesion (Figure 25A-C). Further analysis of the protein expression revealed that Band 4.1B and Band 4.1G became concentrated at cell-cell junctions when cells contacted with one another (Figure 25D, E). However, Band 4.1N remained diffusely expressed even when cell-cell contacts were formed (Figure 25F). No differences in the localization patterns of Band 4.1G (Figure 25B, E) and Band 4.1N (Figure 25 C, F) were seen between wild type and 4.1B^{-/-} astrocytes.

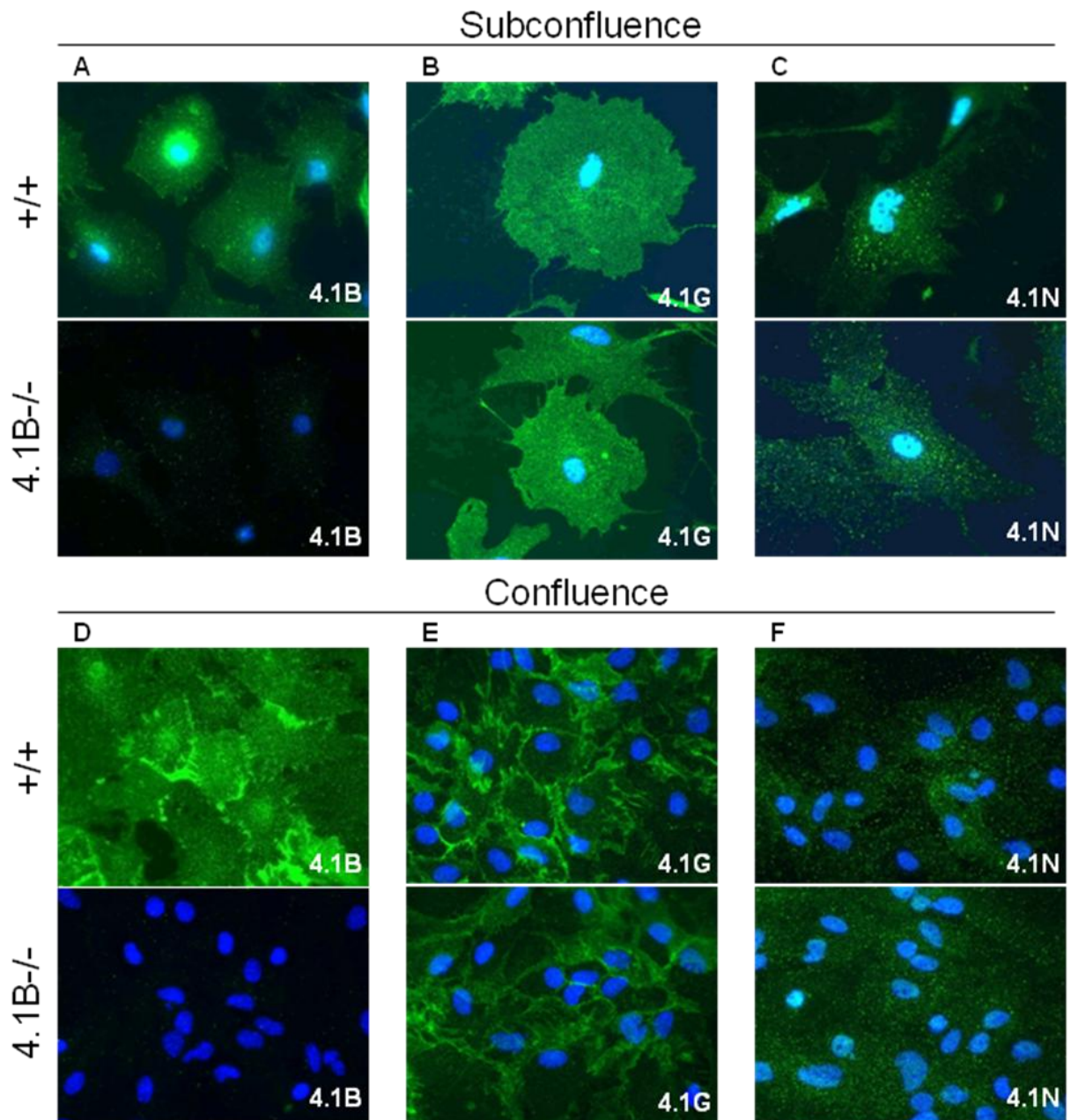


Figure 25. Protein 4.1 sub-cellular localization changes as cell-cell contacts are formed.

Figure 25. Protein 4.1 sub-cellular localization changes as cell-cell contacts are formed.

A-F: The expression of 4.1 proteins was examined 24 hours after astrocyte adhesion to fibronectin. 4.1B (A), 4.1G (B), and 4.1N (C) became diffusely expressed at 24 hours. Interestingly, 4.1B (D) and 4.1G (E) became concentrated at cell-cell junctions when cells contacted with one another, although 4.1N remained diffusely expressed (F). No differences in the localization patterns of 4.1G (B, E) and 4.1N (C, F) were seen between wild type and 4.1B^{-/-} astrocytes. Images are shown at 400x.

4.2.3. Band 4.1B and $\beta 1$ integrin co-localize to cell-ECM contact sites.

$\beta 1$ integrin is a major fibronectin receptor. Given the importance of integrins in cell-ECM adhesion, the localization patterns of Band 4.1B and $\beta 1$ integrin were compared in astrocytes adhering to fibronectin. Wild type astrocytes were allowed to interact with fibronectin for 1 hour or 24 hours. The adherent cells were then immunolabeled with anti-4.1B, anti- $\beta 1$, and anti-paxillin antibodies. In early hours, both Band 4.1B (Figure 26A) and $\beta 1$ integrin (Figure 26B) co-localized with paxillin, indicating their localizations at the adhesion sites. However, after 24 hours, Band 4.1B became diffusely expressed (Figure 26C) whereas $\beta 1$ integrin remained co-localized with paxillin (Figure 26D). As evident by the presence of paxillin-labeled focal contacts, the appearance of focal adhesions did not change when Band 4.1B was absent from the adhesion sites (Figure 26C).

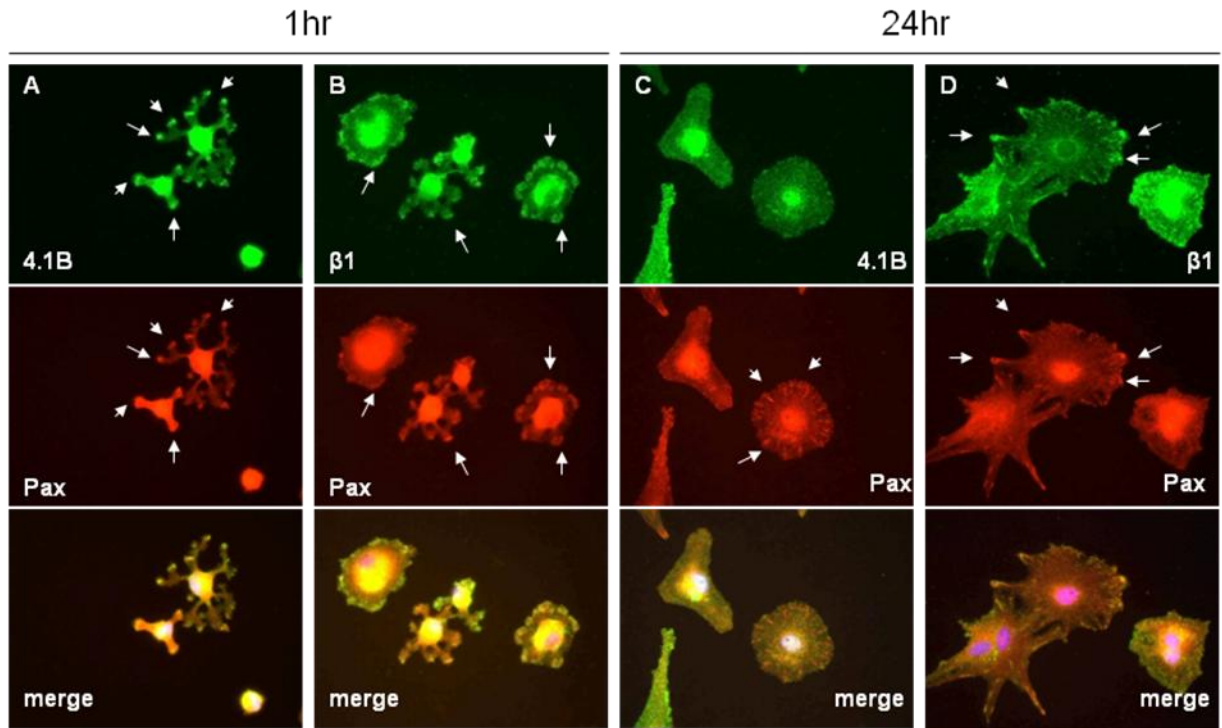


Figure 26. Band 4.1B and $\beta 1$ integrin localize to adhesions during early stages of cell adhesion and spreading.

Figure 26. Band 4.1B and β 1 integrin localize to adhesions during early stages of cell adhesion and spreading.

A-D: Wild type and 4.1B^{-/-} astrocytes adhering to fibronectin were labeled with anti-4.1B (A, C), anti- β 1 (B, D), and anti-paxillin (A-D) antibodies. At one hour, Band 4.1B (arrows in A) and β 1 integrin (arrows in B) co-localized with paxillin, indicating their localization to the adhesion sites. At 24 hours, however, Band 4.1B became diffusely expressed (C) whereas β 1 integrin remained co-localized with paxillin (D arrows). Paxillin-labeled adhesion sites were still present when Band 4.1B was no longer expressed in the adhesion sites (arrows in C). Images shown at 400x.

Based on the co-localization of both Band 4.1B and $\beta 1$ integrin with paxillin, we postulated that these two proteins might co-localize, as well. Therefore, fibronectin-adherent wild type and 4.1B^{-/-} astrocytes were immunostained with anti-4.1B and anti- $\beta 1$ antibodies. As expected, Band 4.1B and $\beta 1$ integrin co-localized during early spreading (Figure 27A), but did not stay co-localized at 2 hours (Figure 27C). The localization of $\beta 1$ integrin to adhesions was not altered by the changes in Band 4.1B expression (Figure 27 A, C). Furthermore, the lack of Band 4.1B expression in 4.1B^{-/-} astrocytes did not affect $\beta 1$ integrin's localization to focal adhesions (Figure 27B, D).

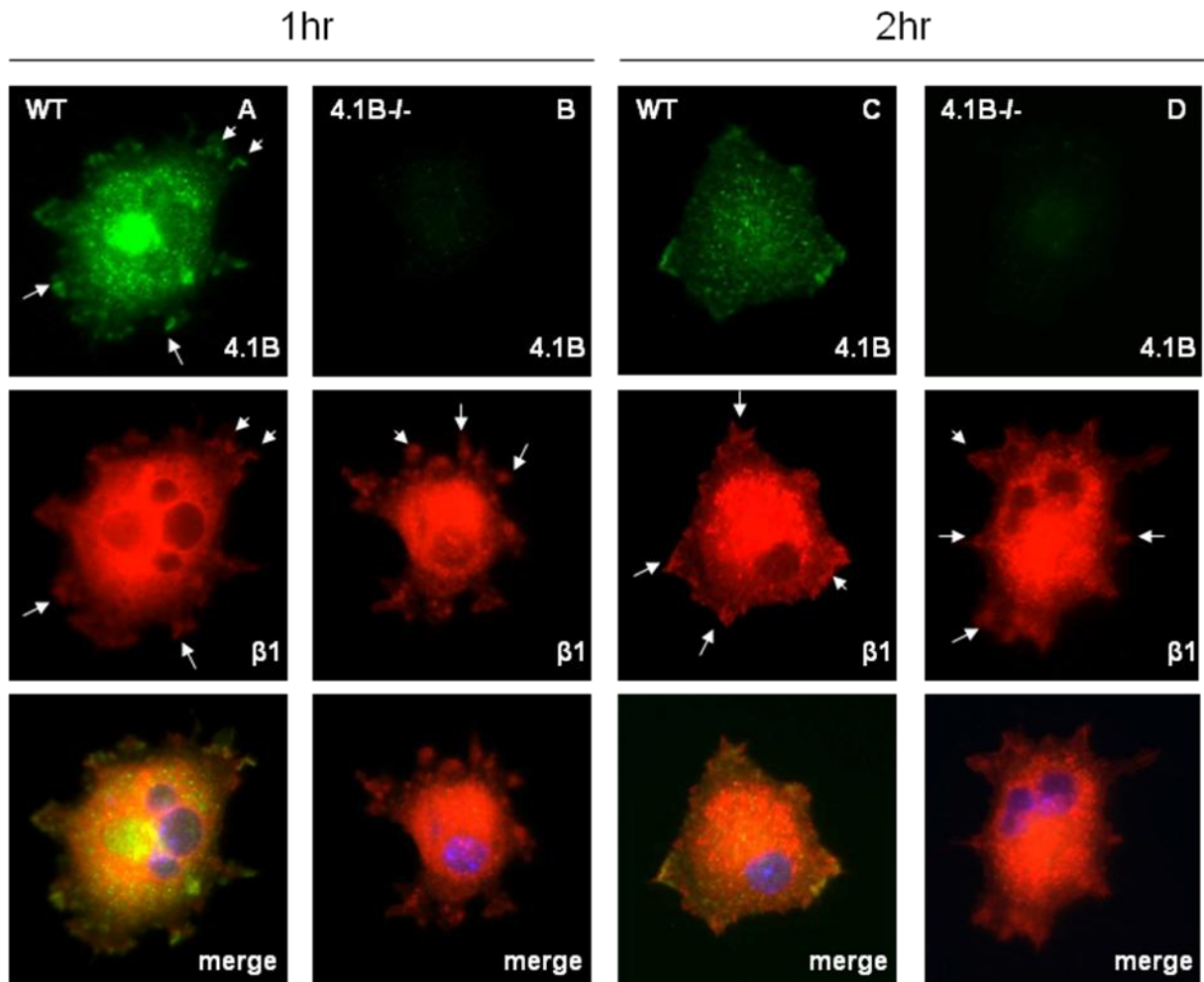


Figure 27. Band 4.1B and $\beta 1$ integrin co-localize during early cell spreading.

Figure 27. Band 4.1B and $\beta 1$ integrin co-localize during early cell spreading.

A-D: Fibronectin-adherent wild type (A, C) and 4.1B^{-/-} (B, D) astrocytes were immunostained with anti-4.1B and anti- $\beta 1$ antibodies. Band 4.1B and $\beta 1$ integrin co-localized one hour after fibronectin adhesion (arrows in A), but did not stay co-localized at 2 hours (C). $\beta 1$ localization to focal adhesions was unaffected by loss of Band 4.1B expression in adhesions (arrows in C). The absence of Band 4.1B expression in 4.1B^{-/-} astrocytes did not influence $\beta 1$ integrin's localization to focal adhesions (arrows in B, D). Images are shown at 400x.

In vivo expression of Band 4.1B and $\beta 1$ integrin was also determined using E11.5 wild type embryos. Fresh-frozen embryo sections were immunofluorescently labeled with anti-4.1B and anti- $\beta 1$ antibodies. Band 4.1B and $\beta 1$ integrin co-localized to the plasma membrane at regions of cell-cell contact, especially in the neural tube (Figure 28). In addition, $\beta 1$ integrin was strongly expressed in blood vessels (arrows in Figure 28).

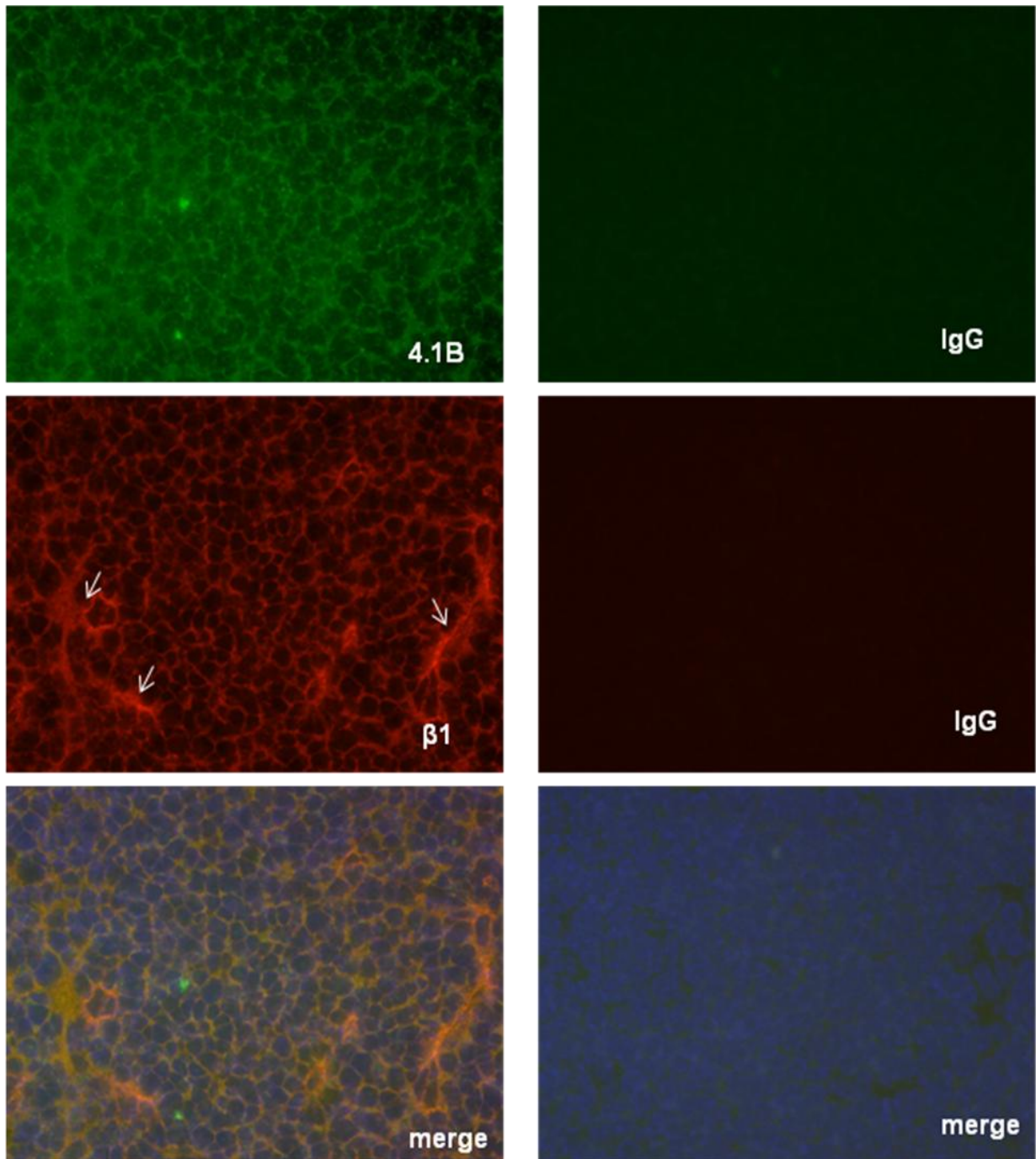


Figure 28. Band 4.1B and $\beta 1$ integrin co-localize in the neuroepithelium.

Figure 28. Band 4.1B and $\beta 1$ integrin co-localize in the neuroepithelium.

In vivo expression of Band 4.1B and $\beta 1$ integrin was determined in E11.5 wild type embryos. Fresh-frozen embryo sections were immunofluorescently labeled with anti-4.1B and anti- $\beta 1$ integrin antibodies and IgG controls. Band 4.1B and $\beta 1$ integrin co-localized to the plasma membrane at regions of cell-cell contact. $\beta 1$ integrin, but not Band 4.1B, was also strongly expressed in blood vessels (arrows). Images are shown at 400x.

4.2.4. Band 4.1B is not necessary for cell adhesion to the ECM.

The localization of Band 4.1B to cell-ECM contacts led to the examination of Band 4.1B's role in cell adhesion. Wild type and 4.1B^{-/-} astrocytes were plated on a 96-well plate coated with laminin, an ECM molecule for 30 minutes. The cells adhering to laminin were stained with crystal violet. The crystal violet-positive cells were quantified using an ELISA reader. The numbers of wild type and 4.1B^{-/-} adherent cells were not significantly different (Figure 29A), indicating Band 4.1B does not influence initial adhesion of cells to the ECM.

Morphologies of wild type and 4.1B^{-/-} astrocytes were also examined after adhesion to laminin. Again, these astrocytes were plated onto laminin-coated coverslips for 30 minutes and labeled with phalloidin, a cytoskeleton marker. Careful examination of the attached cells revealed that the morphologies of wild type and 4.1B^{-/-} astrocytes after initial adhesion were not significantly different from one another (Figure 29B).

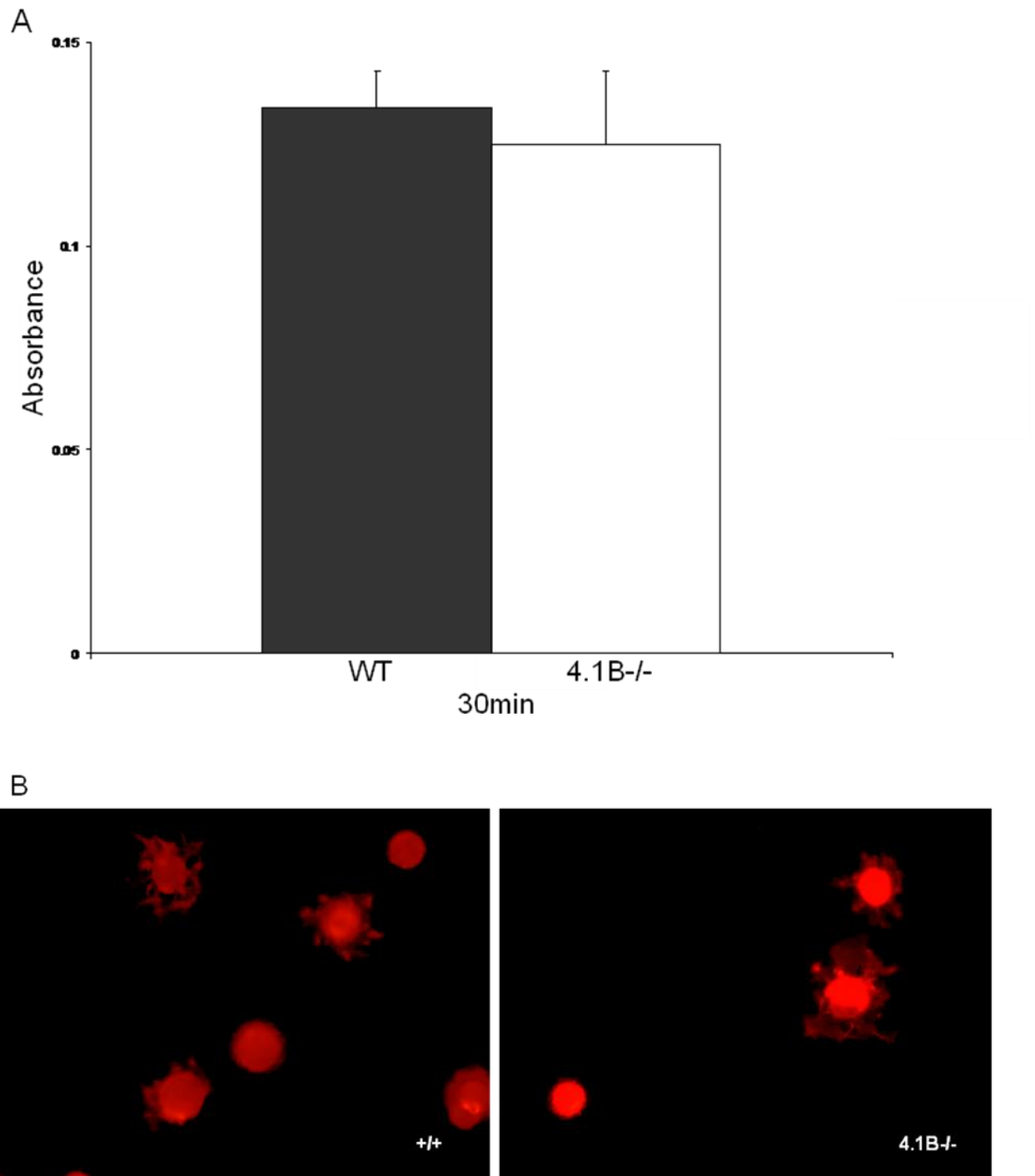


Figure 29. Band 4.1B is not necessary for cell adhesion to the ECM.

Figure 29. Band 4.1B is not necessary for cell adhesion to the ECM.

A: Wild type and 4.1B^{-/-} astrocytes were plated on a 96-well plate coated with laminin for 30 minutes. After staining the adherent cells with crystal violet, the differences in cell adhesion in these cells were quantified. The numbers of wild type and 4.1B^{-/-} adherent cells were not significantly different ($p>0.05$). B: Wild type and 4.1B^{-/-} astrocytes were also examined for their morphologies after a brief interaction with laminin. The cells were stained with phalloidin, a cytoskeleton marker. The morphologies of wild type and 4.1B^{-/-} astrocytes were not significantly different from one another. Images are shown at 400x.

4.2.5. The FERM domain of Band 4.1B enhances cell spreading on fibronectin.

The FERM domain is thought to be crucial for mediating cell spreading. To determine the effects of the 4.1B FERM domain on cell spreading, COS7 cells were transiently transfected with myc-tagged 4.1B FERM, full length 4.1B, and LacZ constructs (McCarty et al., 2005a) for 48 hours. These cells were allowed to adhere to fibronectin and stained with an anti-myc antibody. The areas of cell spreading were quantified by a software analysis of captured images of myc-labeled cells. Strikingly, COS7 cells that were transfected with 4.1B FERM and full length 4.1B constructs displayed enhanced spreading on fibronectin (Figure 30B, C), compared to the cells transfected with LacZ control (Figure 30A). These spreading differences were statistically significant ($p < 0.01$) (Figure 30D). A similar analysis using vitronectin adherent cells did not show spreading differences in cells transfected with these constructs (data not shown).

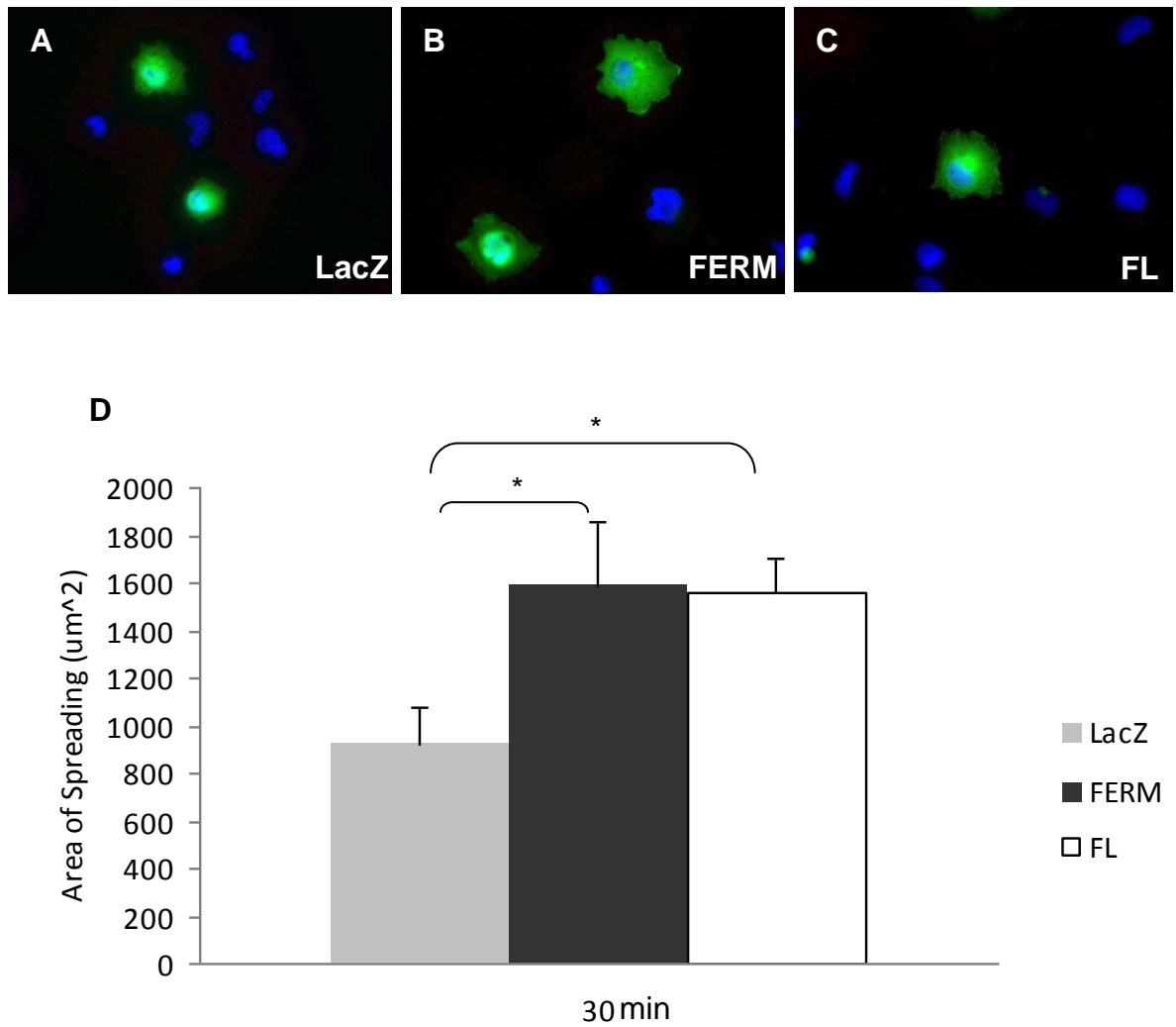


Figure 30. The FERM domain of Band 4.1B enhances cell spreading on fibronectin.

Figure 30. The FERM domain of Band 4.1B enhances cell spreading on fibronectin.

A-C: COS7 cells were transiently transfected with myc-tagged LacZ (A), 4.1B FERM (B), and full length 4.1B (C) constructs for 48 hours and stained with an anti-myc antibody. Images are shown at 400x. 4.1B FERM (B) and full length 4.1B (C) transfected cells displayed enhanced spreading on fibronectin, compared to the LacZ control (A). D: The areas of cell spreading were quantified by a software analysis of captured images of the myc-labeled cells. 4.1B FERM and full length 4.1B transfected cells showed statistically significant ($p < 0.01$) enhancement of spreading, compared to the LacZ control.

Since the increased spreading in 4.1B transfected cells was only observed in cells interacting with fibronectin, it was speculated that Band 4.1B, especially the Band 4.1B FERM domain, promotes cell spreading mediated by $\beta 1$ integrin. Therefore, cells that were transfected with the 4.1B FERM, full length 4.1B, and LacZ constructs were treated with a $\beta 1$ integrin blocking antibody prior to being plated on fibronectin. Again, cells transfected with 4.1B FERM (Figure 31B) and full length 4.1B (Figure 31C) constructs showed enhanced spreading on fibronectin without blocking, in comparison to the LacZ control (Figure 31A). However, the enhanced cell spreading in these cells was abolished after blocking $\beta 1$ (Figure 31D-F).

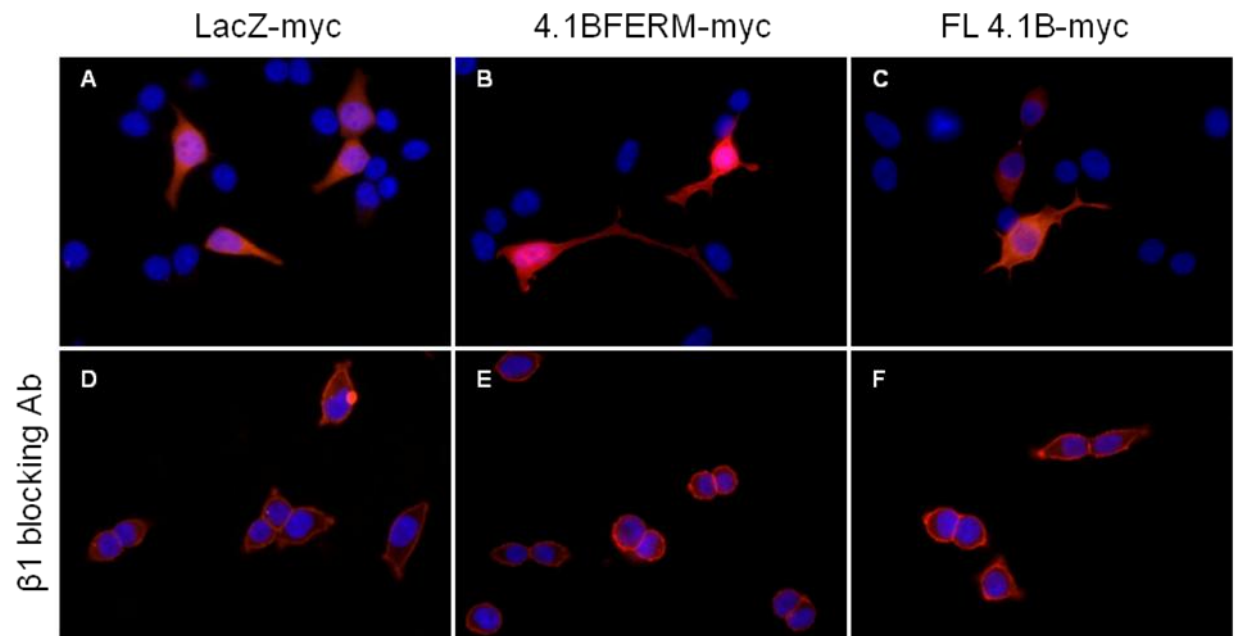


Figure 31. Band 4.1B FERM domain promotes cell spreading mediated by $\beta 1$ integrin.

Figure 31. Band 4.1B FERM domain promotes cell spreading mediated by β 1 integrin.

A-F: 293T cells that were transfected with 4.1B FERM, full length 4.1B, and LacZ constructs were treated with a β 1 integrin blocking antibody P5D2 prior to being plated on fibronectin. Again, cells transfected with 4.1B FERM (B) and full length 4.1B (C) constructs showed enhanced spreading on fibronectin, in comparison to the LacZ control (A). P5D2 blocked the increased spreading in these cells (D-F).

4.3. Discussion

The functional roles for Band 4.1B in the brain, and especially in astrocytes, have not been identified. This study was the first to show time-dependant localization changes of Band 4.1B expression in astrocytes and to implicate the involvement of Band 4.1B in cell adhesion and spreading. Here, the FERM domain of Band 4.1B was shown to promote $\beta 1$ integrin-mediated early cell spreading by localizing to $\beta 1$ integrin-rich cell-ECM adhesion sites.

Band 4.1B has been previously shown to localize to the plasma membrane at regions of direct cell-cell contact (Parra et al., 2000). Given the subcellular expression, Band 4.1B has been speculated to be involved in cell-cell, cell-ECM interactions. Similar to the previous report, Band 4.1B in astrocytes also localizes to the plasma membrane when cell-cell contacts are formed. However, it is important to note that the localization patterns of Band 4.1B change throughout the stages of cell adhesion and spreading. Interestingly, Band 4.1B localizes to paxillin-labeled adhesions only during early cell spreading, but becomes diffusely expressed in later stages of cell spreading. Although the expression of Band 4.1B is diffuse in sparse cultures of astrocytes, Band 4.1B becomes concentrated at cell-cell junctions when cells form contacts with one another. No differences in the protein expression of Band 4.1B were observed between sparse and confluent cultures of astrocytes, as demonstrated by immunoblot analysis (data not shown). Therefore, the changes in localization of Band 4.1B are not accompanied by the changes in protein expression. These novel findings suggest that Band 4.1B may be important for early adhesion assembly and signaling, but dispensable for the maintenance of focal

adhesions. In addition, Band 4.1B is likely to mediate cell-cell interactions once focal adhesions are well established and cells begin to form contacts with each other. Collectively, the data from this study demonstrate stage-dependant changes in Band 4.1B localization in astrocytes and suggest multiple intracellular roles for Band 4.1B in cell adhesion and signaling.

Interestingly, these unique changes in Band 4.1B localization are seen in astrocytes adherent to fibronectin, an ECM protein ligand for $\beta 1$ integrins. $\beta 1$ integrin binds multiple α subunits (Baczyk et al., 2010; Takada et al., 2007; Hynes, 2002). $\beta 1$ integrin has been shown to participate in various cellular events, including cell-ECM adhesion and cell spreading (Harburger and Calderwood, 2009). As shown in this study, astrocytes express multiple $\beta 1$ containing integrins, such as $\alpha 2\beta 1$, $\alpha 3\beta 1$, $\alpha 5\beta 1$, $\alpha 6\beta 1$, and $\alpha V\beta 1$. Therefore, it was speculated that $\beta 1$ integrin is an important regulator of astrocyte adhesion and signaling. Similar to Band 4.1B, $\beta 1$ integrin localizes to paxillin-containing adhesions during initial cell spreading. However, unlike Band 4.1B, $\beta 1$ integrin remains in focal adhesions even after cells make initial contact with the ECM. These findings suggest that $\beta 1$ integrin is important not only for early adhesion formation, but also for maintenance of focal adhesions.

Co-localization of Band 4.1B and $\beta 1$ integrin occur only during early stages of cell spreading on fibronectin. This suggests that their interactions are likely to be important for early adhesion formation and/or stabilization. Cell-ECM adhesion is the critical first step for various cellular events. Talin, a member of the protein 4.1 superfamily, has been reported to regulate cell adhesion and spreading through its

interaction with $\beta 1$ integrin (Zhang et al., 2008). Talin mediates focal adhesion formation and organization by activating $\beta 1$ integrin, bridging the integrin with the actin cytoskeleton, and modulating intracellular signaling (Zhang et al., 2008). Given the similarities between talin and Band 4.1B, Band 4.1B may perform redundant functions in astrocytes. Alternatively, Band 4.1B may be important for establishing cell adhesion and spreading events before talin takes over regulating these processes. In fact, talin is not involved in initial cell spreading, including primary adhesion formation and early cell-edge extension (Zhang et al., 2008). Therefore, the interactions between $\beta 1$ integrin and Band 4.1B in the early stage of cell spreading may be an initiating event for adhesion formation and membrane extension.

The exact functions of Band 4.1B in $\beta 1$ -rich adhesions have yet to be determined. One possibility is that Band 4.1B may be necessary for proper localization of $\beta 1$ integrin to newly forming adhesions through their physical interactions. Alternatively, Band 4.1B may influence intracellular signaling regulated by $\beta 1$ integrin. In the absence of Band 4.1B, $\beta 1$ integrin were still detectable in adhesions. Furthermore, Band 4.1B did not affect initial cell-ECM contact modulated by $\beta 1$ integrin. Therefore, Band 4.1B is unlikely to recruit $\beta 1$ integrin to newly forming adhesions. Instead, $\beta 1$ integrin may recruit Band 4.1B to early adhesion sites for regulating intracellular signaling or the cytoskeleton.

Several FERM containing proteins have been shown to regulate cell spreading that is a downstream event of integrin-initiated cell adhesion (Gutmann et al., 1999; Zhang et al., 2008). Based on the data from the present study, Band 4.1B

also promotes cell spreading. Interestingly, the expression of Band 4.1B FERM alone is sufficient to increase cell spreading. This indicates that the FERM domain is responsible for modulating signaling pathways altering cell behavior.

Although Band 4.1B CTD's interaction with $\beta 8$ integrin have been studied (McCarty et al., 2005a), other domains of Band 4.1B have not been explored for their integrin binding capabilities. Piao and colleagues have suggested interactions between Band 4.1B and $\beta 1$ integrin in their prior report (2009). Given that enhanced spreading was seen in 4.1B FERM-expressing cells on fibronectin, an ECM ligand for $\beta 1$ integrin, the FERM domain may be an essential region of Band 4.1B for $\beta 1$ interaction. Through this interaction, Band 4.1B may participate in $\beta 1$ integrin-mediated intracellular signaling cascades. Abolishment of enhanced cell spreading with a $\beta 1$ blocking antibody indirectly shows that Band 4.1B FERM- $\beta 1$ interaction induces better cell spreading.

Despite the proposed roles of Band 4.1B in $\beta 1$ -mediated cell adhesion and signaling, 4.1B^{-/-} astrocytes do not behave differently from wild type astrocytes. Even in the absence of Band 4.1B, these cells form normal paxillin-positive adhesions, have $\beta 1$ -containing focal contacts, and display normal cell morphology and spreading. The lack of differences between wild type and 4.1B^{-/-} cells may be contributed by other 4.1 proteins playing redundant functions in the absence of Band 4.1B. Bands 4.1G and 4.1N are highly expressed in 4.1B^{-/-} astrocytes. In particular, Band 4.1G shares similar expression patterns with Band 4.1B: Band 4.1G localizes to primary adhesions during early spreading and to cell-cell junctions upon completion of cell spreading. Band 4.1G may take over the functions of Band

4.1B when Band 4.1B is not present. Clear phenotype differences demonstrated between Band 4.1B-expressing COS7 cells and untransfected cells that lack endogenous protein 4.1 expression strongly support this possibility. In this case, it is still possible that Band 4.1B may play a role in recruitment of $\beta 1$ integrin to early adhesions, but this might not be apparent in this study due to the presence of other 4.1 proteins in knockout cells.

In summary, Band 4.1B may be involved in the formation of primary adhesion and/or intracellular signaling through the interaction between its FERM domain and $\beta 1$ integrin during initial cell spreading. However, it is difficult to clearly demonstrate their functions in these cellular processes due to the presence of other 4.1 proteins that might play redundant roles. The examination of Band 4.1B in the absence of other 4.1 proteins using siRNA-mediated approaches would be useful for better characterization of Band 4.1B's functional roles.

Chapter 5. Summary and Future Directions

This study was the first to demonstrate the *in vivo* and *in vitro* functions of Band 4.1B in integrin-mediated cell adhesion and signaling. The key findings of the present study are as follows:

Specific Aim I:

1. *$\beta 8$ and Band 4.1B are expressed in the embryonic heart (Figures 16, 19).*

The expressions of $\beta 8$ integrin and Band 4.1B were detected in endocardial cushions of the AV junction and OFT as well as the myocardium.

2. *Most mice that are genetically null for $\beta 8$ integrin and Band 4.1B die by E11.5 (Table 2).*

The number of $\beta 8^{-/-};4.1B^{-/-}$ mice that were born was 60% less than expected. Although these mice were present in the expected Mendelian ratio at E10.5, they showed 8% viability at E11.5.

3. *$\beta 8^{-/-};4.1B^{-/-}$ mice that survive until adulthood die of hydrocephalus caused by intracerebral hemorrhage (Figures 9, 10).*

$\beta 8^{-/-};4.1B^{-/-}$ mice displayed hunched posturing, abnormal gait, and seizure activity by the third week of their lives and died before P40. The cause of death was severe hydrocephalus secondary to intracerebral hemorrhage. Although striking, these phenotypes were similarly observed in $\beta 8^{-/-}$ mice, suggesting these features were mainly the effects of absent $\beta 8$ integrin.

4. *The defective cardiovascular system contributes to the lethal phenotype of $\beta 8^{-/-};4.1B^{-/-}$ embryos (Figures 11-14).*

Hypovascularity in the yolk sac and embryo proper was the most grossly noticeable feature of the double mutants. Defective blood vessel formation in the yolk sac and neural tube was also seen in these embryos.

5. *Abnormal morphogenesis of the outflow tract is seen the $\beta 8^{-/-};4.1B^{-/-}$ heart (Figures 17, 18).*

Hypotrophy of the OFT endocardial cushion with the diminished expression of multiple neural crest markers and thinning of myocardium were demonstrated in the double mutants.

6. *Neural crest cell migration is impaired in $\beta 8^{-/-};4.1B^{-/-}$ embryos (Figures 20, 21).*

A defective neurofilament network in $\beta 8^{-/-};4.1B^{-/-}$ embryos was evident by aberrant projections of the cranial nerve V branches into the pharyngeal arches and abnormal neurofilament patterning in the trunks.

Functional links between $\beta 8$ integrin and Band 4.1B *in vivo* have never been shown prior to the present study. This study shows cooperative functions for $\beta 8$ integrin and Band 4.1B in embryonic heart development. Given the importance of cardiac neural crest cells in OFT formation and similar OFT abnormalities seen in other mouse models with cardiac neural crest migration defects, $\beta 8$ integrin and Band 4.1B are suspected to work together to support neural crest cell migration to the OFT and possibly other regions of the developing heart. In particular, $\beta 8$ integrin and Band 4.1B may contribute to proper migration of neural crest cells by regulating TGF β signaling pathways since mice lacking various TGF β family members share similar features with the double mutants.

The exact mechanisms by which $\beta 8$ integrin and Band 4.1B affect cardiac morphogenesis are yet to be determined. Selective ablation of these genes in neural crest cells, especially cardiac neural crest cells, would provide better understanding of $\beta 8$ -4.1B signaling in cardiac morphogenesis. In addition, the involvement of Band 4.1B in integrin-mediated TGF β activation and signaling and the roles of these signaling cascades in the development of neural crest-derived structures may be addressed using *in vitro* approaches. Given the abnormal neurofilament projections shown in the double knockout embryos, impaired migration of neural crest cells is strongly suspected. To demonstrate defective neural crest migration, cells isolated from the double mutants can be utilized for *in vitro* migration assays. These cells can also be subject to time-lapse monitoring of cell movement to understand dynamic regulation of cell migration by $\beta 8$ integrin and Band 4.1B. *In vitro* approaches will also allow rescue experiments to monitor the reversibility of the abnormal migration phenotype by re-expressing $\beta 8$ integrin and Band 4.1B in cells. Furthermore, $\beta 8$ integrin and Band 4.1B's regulation of TGF β pathways can be studied by examining downstream molecules of TGF β signaling cascades, such as SMAD2/3 and 4. By utilizing antibodies against these proteins, changes in the levels of expression and activation of TGF β signaling molecules can be detected in double knockout neural crest cells.

Although $\beta 8^{-/-};4.1B^{-/-}$ embryos exhibit striking lethal phenotypes, these phenotypes are partially penetrant. The partial penetrance of lethality in these mice was attributed to their background strain variation. In many mutant mice, including knockout mice of $\beta 8$ integrin and TGF β 's show strain-dependent phenotypes (Zhu

et al., 2002; Mobley et al., 2009; Bonyadi et al., 1997). These differences may be explained by the presence of genetic modifiers in specific strains. Therefore, it would be worthwhile to investigate potential contributions of genetic modifiers to cardiac development by backcrossing the double knockout mutants to 129S4 and C57BL6 backgrounds.

Since impaired OFT is commonly seen in congenital heart disease, $\beta 8$ integrin and Band 4.1B may be important players in human cardiac morphogenesis. In DiGeorge syndrome, neural crest cell derived structures, including the OFT and aortic arch are severely defected (Stoller and Epstein, 2005). $\beta 8$ integrin and Band 4.1B have not been implicated in human heart diseases. Given the cardiac defects seen in $\beta 8^{-/-};4.1B^{-/-}$ embryos, studying the roles of $\beta 8$ integrin and Band 4.1B in DiGeorge syndrome and other congenital heart diseases using animal models and human samples can lead to the discovery of a new therapeutic target.

Specific Aim II:

1. *Astrocytes express multiple 4.1 proteins and $\beta 1$ -containing integrins (Figure 22, 23).*

Bands 4.1B, 4.1G, and 4.1N as well as $\alpha 1\beta 1$, $\alpha 2\beta 1$, $\alpha 3\beta 1$, $\alpha 5\beta 1$, $\alpha 6\beta 1$, and $\alpha V\beta 1$ integrins were detected in astrocytes.

2. *Band 4.1B shows time-dependent changes in its subcellular localization (Figure 24, 25).*

Band 4.1B localized to primary adhesions during early cell spreading. However, the expression of Band 4.1B was seen in the plasma membrane at cell-cell junction when cells formed contacts with one another.

3. *Band 4.1B and $\beta 1$ integrin co-localize to the adhesion sites (Figure 26, 27).*

Band 4.1B and $\beta 1$ integrin co-localized to paxillin-labeled adhesions during early spreading. However, Band 4.1B became diffusely expressed whereas $\beta 1$ integrin remained co-localized with paxillin in late stages of cell spreading.

4. *Band 4.1B is not necessary for cell adhesion to the ECM (Figure 29).*

Astrocytes that lack Band 4.1B adhere to laminin without any differences from wild type cells. In addition, the morphologies of wild type and 4.1B^{-/-} astrocytes after initial adhesion were not significantly different from one another.

5. *The FERM domain of Band 4.1B enhances $\beta 1$ integrin-mediated cell spreading (Figure 30, 31).*

Increased cell spreading was demonstrated in cells expressing 4.1B FERM and full-length 4.1B constructs. However, the enhanced spreading in these cells was abolished by treating the cells with a $\beta 1$ blocking antibody.

This study was the first to demonstrate the localization changes of Band 4.1B during cell spreading and to implicate the involvement of Band 4.1B in $\beta 1$ -mediated cell adhesion and spreading. These novel findings indicate that Band 4.1B may be important for early adhesion assembly and signaling, but dispensable for the maintenance of focal adhesions. It is possible that physical interactions between Band 4.1B and $\beta 1$ integrin may be necessary for proper localization of $\beta 1$ integrin to

newly forming adhesions. Alternatively, Band 4.1B may function as a downstream signaling molecule of $\beta 1$ integrin.

In spite of the proposed roles of Band 4.1B in $\beta 1$ -mediated cell adhesion and signaling, the lack of differences between wild type and 4.1B^{-/-} cells made it difficult to demonstrate the exact roles of Band 4.1B *in vitro*. The presence of redundant functions among 4.1 proteins could not be ruled out in this study. Therefore, it would be critical to examine Band 4.1B's functions in the absence of other 4.1 proteins using siRNA-mediated approaches. As demonstrated here, Bands 4.1G and 4.1N are highly expressed in astrocytes, although their functions in these cells have not been established. Given their subcellular localizations and conserved FERM domain that share sequence homology with Band 4.1B, other 4.1 proteins may play similar roles in cell adhesion and signaling mediated by integrins. Especially, Band 4.1G demonstrated similar sub-cellular localization as Band 4.1B. Therefore, limiting Band 4.1G's expression in early adhesions by silencing Band 4.1G via RNAi-mediated approaches may produce significant disruption in cell adhesion and spreading in cells lacking Band 4.1B. Although Band 4.1N did not localize to cell adhesions in astrocytes, it may become an important regulator of cell adhesion and signaling when Bands 4.1B and 4.1G are both absent. It would be interesting to study if Band 4.1N's localization patterns change in the absence of other 4.1 proteins and if silencing Band 4.1N negatively affects cell adhesion and signaling when Bands 4.1B and 4.1G are not present.

In addition, subtle changes in adhesion formation during early cell spreading would be difficult to be shown by observing cell spreading at fixed time intervals. Since Band 4.1B's expression in adhesions is time-dependant, its regulation of cell adhesion and spreading may also be time sensitive and limited to certain stages of cell spreading. Continuous monitoring of cell adhesion and spreading, therefore, would provide better understanding of time-dependent changes in adhesion formation and organization and cell spreading. Time-lapse monitoring of adhesion assembly/disassembly and cell spreading can be accomplished by transfecting cells with fluorescently labeled proteins and monitoring the movements of these proteins in the cells. Given the co-localizations of Band 4.1B, $\beta 1$ integrin, and paxillin at the adhesion sites, monitoring dynamic cellular changes using cells transfected with fluorescently-labeled Band 4.1B, $\beta 1$ integrin, and paxillin would be a useful first step for understanding their roles in cell adhesion and spreading.

One possible mechanism by which Band 4.1B is involved in cell adhesion and signaling is functioning as a downstream adaptor of $\beta 1$ and other integrins in early adhesions. Adhesions are the sites for sequestering proteins that are important for intracellular signaling (Brown et al., 2005). Many adaptor and signaling proteins play important roles in connecting integrins and the actin cytoskeleton (Legate et al., 2009; Zhang et al., 2008; Cram et al., 2003). Band 4.1B is also a known cytoskeletal adaptor protein that is thought to bind to the actin cytoskeleton via its SABD (Sun et al., 2002). Therefore, Band 4.1B may function as a link between integrins and the actin cytoskeleton. It may also act as a binding partner of other molecules in an adhesion complex, sequestering these proteins for further

intracellular signaling. Thus, the absence of Band 4.1B in cells may influence the actin cytoskeleton dynamics and/or localization of other adhesion proteins. Examining the actin organization and other known integrin/actin binding proteins in adhesions in wild type and 4.1B^{-/-} cells using immunohistochemical approaches would provide insights into the involvement of Band 4.1B in adhesion complex regulation.

Given that enhanced cell spreading mediated by Band 4.1B was observed only on fibronectin, a major ECM ligand for $\beta 1$ integrin, and this effect was abolished by the use of a $\beta 1$ integrin blocking antibody, Band 4.1B was thought to modulate cell spreading mediated by $\beta 1$ integrin. Although co-localization of Band 4.1B and $\beta 1$ integrin *in vitro* and *in vivo* suggests that Band 4.1B and $\beta 1$ integrin are likely to interact with one another, demonstrating direct interactions between Band 4.1B, and $\beta 1$ integrin by co-immunoprecipitation would further emphasize the importance of Band 4.1B in $\beta 1$ integrin signaling. Examining endogenous interactions between these two proteins would be the best way to demonstrate their binding. Since these proteins were shown to co-localize in early adhesions, lysates made from cells attached to fibronectin for a brief period of time can be used for displaying the endogenous interaction. However, the transient interactions between Band 4.1B and $\beta 1$ integrin may make the co-immunoprecipitation difficult to be performed, given the time-dependent changes in Band 4.1B localization. Another way would be to utilize Band 4.1B and $\beta 1$ integrin constructs and monitor for exogenous interactions of these proteins. Given the importance of the talin FERM domain and the β cytoplasmic tails in talin-integrin interactions, the Band 4.1B

FERM domain that is overexpressed in cells can be allowed to bind to $\beta 1$ cytoplasmic tail that is attached to a resin.

This study demonstrated several crucial *in vivo* and *in vitro* functions for Band 4.1B in integrin-mediated cell adhesion and signaling. However, the mechanisms by which Band 4.1B is involved in these cellular events still need to be determined. The knowledge obtained from the present study would provide a solid foundation for further analysis of Band 4.1B's roles. The proposed future studies would strengthen our understanding of the functions for Band 4.1B in integrin-mediated adhesion and signaling.

References

- Acloque H, Adams MS, Fishwick K, Bronner-Fraser M, Nieto MA. 2009. Epithelial-mesenchymal transitions: the importance of changing cell state in development and disease. *J Clin Invest* 119:1438-49.
- Anthis NJ, Campbell ID. 2011. The tail of integrin activation. *Trends Biochem Sci Epub*.
- Astrof S, Crowley D, Hynes RO. 2007. Multiple cardiovascular defects caused by the absence of alternatively spliced segments of fibronectin. *Dev Biol* 311:11-24.
- Arnaout MA, Mahalingam B, Xiong JP. 2005. Integrin structure, allostery, and bidirectional signaling. *Annu Rev Cell Dev Biol* 21:381-410.
- Bader BL, Rayburn H, Crowley D, Hynes RO. 1998. Extensive vasculogenesis, angiogenesis, and organogenesis precede lethality in mice lacking all alpha v integrins. *Cell* 95:507-19.
- Baines AJ, Bennett PM, Carter EW, Terracciano C. 2009. Protein 4.1 and the control of ion channels. *Blood Cells Mol Dis* 42:211-5.
- Barczyk M, Carracedo S, Gullberg D. 2010. Integrins. *Cell Tissue Res* 339:269-80.
- Bel C, Oguievetskaia K, Pitaval C, Goutebroze L, Faivre-Sarrailh C. Axonal targeting of Caspr2 in hippocampal neurons via selective somatodendritic endocytosis. *J Cell Sci*, 2009 122:3403-13.
- Belkina NV, Liu Y, Hao JJ, Karasuyama H, Shaw S. LOK is a major ERM kinase in resting lymphocytes and regulates cytoskeletal rearrangement through ERM phosphorylation. 2009. *Proc Natl Acad Sci* 106:4707-12.

- Bernkopf DB, Williams ED. 2008. Potential role of EPB41L3 (protein 4.1B/Dal-1) as a target for treatment of advanced prostate cancer. *Expert Opin Ther Targets* 7:845-53.
- Bonyadi M, Rusholme SA, Cousins FM, SU HC, Bironn CA, Farrall M, Akhurst RJ. 1997. Mapping of a major genetic modifier of embryonic lethality in TGF beta 1 knockout mice. *Nat Genet* 15:207-11.
- Bretscher A, Edwards K, Fehon RG. 2002. ERM proteins and merlin: integrators at the cell cortex. *Nat Rev Mol Cell Biol* 3:586-599.
- Bronner-Fraser M. 1986. An antibody to a receptor for fibronectin and laminin perturbs cranial neural crest development in vivo. *Dev Biol* 117: 528–36.
- Brown MC, Cary LA, Jamieson JS, Cooper, JA, Turner CE. 2005. Src and FAK kinases cooperate to phosphorylate paxillin kinase linker, stimulate its focal adhesion localization, and regulate cell spreading and protrusiveness. *Mol Cell Biol* 16:4316-28.
- Buckingham M, Meilhac S, Zaffran S. 2005. Building the mammalian heart from two sources of myocardial cells. *Nat Rev Genet* 6:826-35.
- Calderwood DA. 2004. Integrin activation. *J Cell Sci* 117:657-66.
- Calderwood DA, Ginsberg MH. 2003. Talin forges the links between integrins and actin. *Nat Cell Biol* 5:694-7.
- Calderwood DA, Shattil SJ, Ginsberg MH. 2000. Integrins and actin filaments: reciprocal regulation of cell adhesion and signaling. *J Biol Chem* 275:22607-10.

- Campbell I.D., Studies of focal adhesion assembly. *Biochem Soc Trans*, 2008. 36:263-66.
- Caswell PT, Chan M, Lindsay AJ, Mccaffrey MW, Boettiger D, Norman JC. 2008. Rab-coupling protein coordinates recycling of $\alpha 5\beta 1$ integrin and EGFR1 to promote cell migration in 3D microenvironments. *J Cell Biol* 183:143-55.
- Caswell, PT, Norman JC. 2008. Endocytic transport of integrins during cell migration and invasion. *Trends Cell Biol* 18:257-63.
- Cavanna T, Pokorna E, Vesely P, Gray C, Zicha D. 2007. Evidence for protein 4.1B acting as a metastasis suppressor. *J Cell Sci* 120:606-16.
- Conway SJ, Kruzynska-Frejtag A, Kneer PL, Machnicki M, Koushik SV. 2003. What cardiovascular defect does my prenatal mouse mutant have, and why? *Genesis* 35:1-21.
- Costa P, Parsons M. 2010. New insights into dynamics of cell adhesions. *Int Cell Rev Mol Biol* 283:57-91.
- Correas I, Speicher DW, Marchesi VT. 1986 Structure of the spectrin-actin binding site of erythrocyte protein 4.1. *J Biol Chem* 261: 13362-13366.
- Cram EJ, Clark SG, Schwarzbauer JE. 2003. Talin loss of function uncovers roles in cell contractility and migration in *C. elegans*. *J Cell Sci* 116:3871-8.
- Critchley DR. 2009. Biochemical and structural properties of integrin-associated cytoskeletal protein talin. *Annu Rev Biophys* 38:235-54.
- Critchley DR. 2000. Focal adhesions - the cytoskeletal connection. *Curr Opin Cell Biol* 12: 133-139.
- Critchley DR, Gingras AR. 2008. Talin at glance. *J Cell Sci* 121:1345-7.

- Dafou D, Grun B, Sinclair J, Lawrenson K, Benjamin EC, Hogdall D, Kruger-Kjaer S, Christensen L, Sowter HM, Al-Attar A, Edmondson R, Darby S, Berchuck A, Laird PW, Pierce CL, Ramus SJ, Jacobs IJ, Gayther SA. 2010. Microcell-mediated chromosome transfer identifies EPB41L3 as a functional suppressor of epithelial ovarian cancer. *Neoplasia* 12:579-89.
- Delannet M, Martin F, Bossy B, Cheresh DA, Reichardt LF, Duband JL. 1994. Specific roles of the $\alpha\beta1$, $\alpha\beta3$ and $\alpha\beta5$ integrins in avian neural crest cell adhesion and migration on vitronectin. *Development* 120:1687-702.
- Desban N, Duband JL. 1997. Avian neural crest cell migration on laminin: interaction of the $\alpha1\beta1$ integrin with distinct laminin-1 domains mediates different adhesive responses. *J Cell Sci* 110: 2729-44.
- Diakowski W, Grzybek M, Sikorski AF. 2006. Protein 4.1, a component of the erythrocyte membrane skeleton and its related homologue proteins forming the protein 4.1/FERM superfamily. *Folia Histochem Cytobiol* 44:231-48.
- Dumin JA, Dickeson SK, Stricker TP, Bhattacharyya-Pakrasi M, Roby JD, Santoro SA, Parks WC. 2001. Pro-collagenase-1 (matrix metalloproteinase-1) binds the $\alpha(2)\beta(1)$ integrin upon release from keratinocytes migrating on type I collagen. *J Biol Chem* 276: 29368-74.
- Ellerbroek SM, Wu I, Overall CM, Stack MS. 2001. Functional interplay between type I collagen and cell surface matrix metalloproteinase activity. *J Biol Chem* 276: 24833-42.
- Fehon RG, McClatchey AI, Bretscher A. 2010. Organizing the cell cortex: the role of ERM proteins. *Nat Rev Mol Cell Biol* 11:276-87.

- Fievet BT, Gautreau A, Roy C, Del Maestro L, Mangeat P, Louvard D, Arpin M. 2004. Phosphoinositide binding and phosphorylation act sequentially in the activation mechanism of ezrin. *J Cell Biol* 164:653-9.
- Friedl P, Wolf K. 2003. Tumour cell invasion and migration: diversity and escape mechanisms. *Nat Rev Cancer* 3:362-74.
- Fukata M, Nakagawa M, Kaibuchi, K. 2003. Roles of Rho family GTPases in cell polarization and directional migration. *Curr Opin Cell Biol* 15:590-7.
- Galvez BG, Matias-Roman S, Yanez-Mo M, Sanchez-Madrid F, Arroyo AG. 2002. EEGM regulates MT1-MMP localization with beta1 or alphavbeta3 integrins at distinct cell compartments modulating its internalization and activation on human endothelial cells. *J Cell Biol.* 159:509-21.
- Gary R, Bretscher A. 1995. Ezrin self-association involves binding of an N-terminal domain to a normally masked C-terminal domain that includes the F-actin binding site. *Mol Biol Cell* 6:1061-75.
- Gascard P, Cohen CM. 1994. Absence of high-affinity band 4.1 binding sites from membranes of glycophorin C- and D-deficient (Leach phenotype) erythrocytes. *Blood* 83: 1102-1108.
- Gimm JA, An X, Nunomura W, Mohandas N. 2002. Functional characterization of spectrin-actin-binding domains in 4.1 family of proteins. *Biochemistry* 41: 7275-7282.
- Gu MX, York JD, Warshawsky I, Majerus PW. 1991. Identification, cloning, and expression of a cytosolic megakaryocyte protein tyrosine phosphatase with

- sequence homology to cytoskeletal protein 4.1. *Proc Natl Acad Sci USA* 88:5867-71.
- Gutmann DH, Hirbe AC, Huang ZY, Haipiek CA. 2001. The protein 4.1 tumor suppressor, DAL-1, impairs cell motility, but regulates proliferation in a cell-type-specific fashion. *Neurobiol Dis* 8:266-78.
- Gutmann DH, Sherman L, Seftor L, Haipiek C, Hoang Lu K, Hendrix M. 1999. Increased expression of the NF2 tumor suppressor gene product, merlin, impairs cell motility, adhesion and spreading. *Hum Mol Gen* 8:267-75.
- Han BG, Nunomura W, Takakuwa Y, Mohandas N, Jap BK. 2000. Protein 4.1R core domain structure and insights into regulation of cytoskeletal organization. *Nature Struct Biol* 7: 871-875
- Hauck CR, Hsia DA, Schlaepfer DD. 2002. The focal adhesion kinase-a regulator of cell migration and invasion. *IUBMB Life* 53:115-9.
- Harburger DS, Calderwood DA. 2008. Integrin signaling at a glance. *J Cell Sci* 122:159-63.
- Harvey RP. 2002. Patterning the vertebrate heart. *Nat Rev Genet* 3:544-56.
- Holzwarth G, Yu J, Steck TL. 1976. Heterogeneity in the conformation of different protein fractions from the human erythrocyte membrane. *J Supramol Struct* 4:161-8.
- Hood JD, Cheresch DA. 2002. Role of integrins in cell invasion and migration. *Nat Rev Cancer* 2:91-100.

- Horresh I, Bar V, Kissil JL, Peles E. 2010. Organization of myelinated axons Caspr and Caspr2 requires the cytoskeletal adaptor protein 4.1B. *J Neurosci* 30:2480-9.
- Hou C-L, Tang C-JC, Roffler SR, Tang TK. 2000. Protein 4.1R binding to eIF3-p44 suggest an interaction between the cytoskeletal network and the translational apparatus. *Blood* 96:747-753.
- Huhtala M, Heino J, Casciari D, de Luise A, Johnson MS. 2005. Integrin evolution: insights from ascidian and teleost fish genomes. *Matrix Biol.* 24:83-95.
- Hynes, RO. 2002. Integrins: bidirectional, allosteric signaling machines. *Cell* 110:673-87.
- Ishiguro H, Furukawa Y, Daigo Y, Miyoshi Y, Nagasawa Y, Nishiwaki T, Kawasoe T, Fujita M, Satoh S, Miwa N, Furii Y, Nakamura Y. 2000. Isolation and characterization of human NBL4, a gene involved in the beta-catenin/tcf signaling pathway. *Jpn J Cancer Res* 91: 597-603.
- Jain R, Rentschler S, Epstein JA. 2010. Notch and cardiac outflow tract development. *Ann NY Acad Sci* 1188:184-90.
- Jones EAV, Yuan L, Breant C, Watts RJ, Eichmann A. 2008. Separating genetic and hemodynamic defects in neuropilin 1 knockout embryos. *Development* 135:2479-88.
- Kang Q, Wang T, Zhang H, Mohandas N, An X. 2009. A golgi-associated protein 4.1B variant is required for assimilation of proteins in the membrane. *J Cell Sci* 122:1091-9.

- Kil SH, Lallier T, Bronner-Fraser M. 1996. Inhibition of cranial neural crest adhesion in vitro and migration in vivo using integrin antisense oligonucleotides. *Dev Biol* 179: 91–101.
- Kirby ML, Gale TF, Stewart DE. 1983. Neural crest cells contribute to normal aorticopulmonary septation. *Science* 220:1059-61.
- Krieg J, Hunter T. 1992. Identification of the two major epidermal growth factor-induced tyrosine phosphorylation sites in the microvillar core protein ezrin. *J Biol Chem* 267:19258-65.
- Le Clainche C, Carlier MF. 2008. Regulation of actin assembly associated with protrusion and adhesion in cell migration. *Physiol Rev* 88:489-513.
- Legate KR, Wickstrom SA, Fassler R. 2009. Genetic and cell biological analysis of integrin outside-in signaling. *Genes Dev.* 23:397-418.
- Luo BH, Carman CV, Springer TA. 2007. Structural basis of integrin regulation and signaling. *Annu Rev Immunol* 25:619-647.
- Marfatia SM, Leu RA, Branton D, Chishti AH. 1994. *In vitro* studies suggest a membrane-associated complex between erythroid p55, protein 4.1 and glycophorin C. *J Biol Chem* 269:8631-8634.
- Matsui T, Maeda M, Doi Y, Yonemura S, Amano M, Kaibuchi K, Tsukita S, Tsukita S. 1998. Rho-kinase phosphorylates COOH-terminal threonines of ezrin/radixin/moesin (ERM) proteins and regulates their head-to-tail association. *J Cell Biol* 140:647-57.

- Mattagajasingh SN, Huang SC, Harteistein JS, Benz EJ Jr. 2000. Characterization of the interaction between protein 4.1R and ZO-2. A possible link between the tight junction and the actin cytoskeleton. *J Biol Chem* 275: 30573-30585.
- McCarty, JH, Cook AA, Hynes RO. 2005a. An interaction between $\alpha\beta 8$ integrin and band 4.1B via a highly conserved region of the band 4.1 c-terminal domain. *Proc Natl Acad Sci U S A* 102:13479-83.
- McCarty JH, Lacy-Hulbert A, Charest A, Bronson RT, Crowley D, Housman D, Savill J, Roes J, Hynes RO. 2005b. Selective ablation of $\alpha\text{v}\beta 8$ integrins in the central nervous system leads to cerebral hemorrhage, seizures, axonal degeneration and premature death. *Development* 132:165-72.
- McGrath KE, Koniski AD, Malik J, Palis J. 2003. Circulation is established in a stepwise pattern in the mammalian embryo. *Blood* 101:1669-76.
- Mitra SK, Hanson DA, Schlaepfer DD. 2005. Focal adhesion kinase: in command and control of cell motility. *Nat Rev Mol Cell Biol* 6:56-68.
- Mobley AK, Tchaicha JH, Shin J, Hossain MG, McCarty JH. 2009. $\beta 8$ integrin regulates neurogenesis and neurovascular homeostasis in the adult brain. *J Cell Sci* 122:1842-51.
- Monkley SJ, Zhou XH, Kinston SJ, Giblett SM, Hemmings L, Priddle H, Brown JE, Pritchard CA, Critchley DR, Fassler R. 2000. Disruption of the talin gene arrests mouse development at the gastrulation stage. *Dev Dyn* 219:560-74.
- Monzen K, Nagai R, Komuro I. 2002. A role for bone morphogenetic protein signaling in cardiomyocyte differentiation. *Trends Cardiovasc Med* 12:263-9.

- Moser M, Legate KR, Zent R, Fassler R. 2009. The tail of integrins, talin, and kindlins. *Science* 324:895-9.
- Moyle M, Napier MA, McLean JW. 1991. Cloning and expression of a divergent integrin subunit beta 8. *J Biol Chem* 266:19650-8.
- Nakamura F, Amieva MR, Furthmayr H. Phosphorylation of threonine 558 in the carboxyl terminal actin binding domain of moesin by thrombin activation of human platelets. *J Biol Chem* 270:31377-85.
- Ng T, Parsons M, Hughes WE, Monypenny J, Zicha D, Gautreau A, Arpin M, Gschmeissener S, Verveer PJ, Bastiaens PI, Parker PJ. 2001. Ezrin is a downstream effector of trafficking PKC-integrin complexes involved in the control of cell motility. *EMBO J* 20:2723-41.
- Nie X, Deng CX, Wang Q, Jiao K. 2008. Disruption of Smad4 in neural crest cells leads to mid-gestation death with pharyngeal arch, craniofacial and cardiac defects. *Dev Biol* 316:417-30.
- Nowotschin S, Hadjantonakis AK. 2010. Cellular dynamics in the early mouse embryo: from axis formation to gastrulation. *Curr Opin Genet Dev* 20:420-7.
- Nunomura W, Takakuwa Y, Parra M, Conboy JG, Mohandas N. 2000. Ca(2+)-dependent and Ca(2+)-independent calmodulin binding sites in erythrocyte protein 4.1. Implications for regulation of protein 4.1 interactions with transmembrane proteins. *J Biol Chem* 275: 6360-6367.
- Ohno N, Tereda N, Komada M, Saitoh S, Costantini F, Pace V, Germann PG, Weber K, Yamakawa H, Ohara O, Ohno S. 2009. Dispensable role of protein DAL1/4.1B in rodent adrenal medulla regarding generation of

- pheochromocytoma and plasmalemmal localization TSLC1. *Biochem Biophys Acta* 1793:506-15.
- Parra M, Gascard P, Walensky LD, Gimm JA, Blackshaw S, Chan N, Takakuwa Y, Berger T, Lee G, Chasis JA, Snyder SH, Mohandas N, Conboy JG. 2000. Molecular and functional characterization of protein 4.1B, a novel member of the protein 4.1 family with high level, focal expression in brain. *J Biol Chem* 275:3347-55.
- Peri F. 2010. Breaking ranks: how leukocytes react to developmental cues and tissue injury. *Curr Opin Genet Dev* 20:416-9.
- Perris R, Paulsson M, Bronner-Fraser M. 1989. Molecular mechanisms of avian neural crest cell migration on fibronectin and laminin. *Dev Biol* 136: 222–39.
- Piao Y, Lu L, de Groot J. 2009. AMPA receptors promote perivascular glioma invasion via $\beta 1$ integrin-dependent adhesion to the extracellular matrix. *Neuro Oncol* 11:260-73.
- Proctor JM, Zang K, Wang D, Wang R, Reichardt LF. 2005. Vascular development of the brain requires beta8 integrin expression in the neuroepithelium. *J Neurosci* 25:9940-9948.
- Proetzel G, Pawlowski SA, Wiles MV, Yin M, Boivin GP, Howles PN, Ding J, Ferguson MW, Doetschman T. 1995. Transforming growth factor-beta 3 is required for secondary palate fusion. *Nat Genet* 11:409-14.
- Ridely AJ, Schwartz MA, Burridge K, Firtel RA, Ginsberg MH, Borisy G, Parsons JT, Horwitz RA. 2003. Cell migration: integrating signals from front to back. *Science* 302: 1704-9.

- Rodriguez Fernandez JL, Geiger B, Salomon D, Ben-Zeev A. Overexpression of vinculin suppresses cell motility in BALB/c3T3 cells. *Cell Motil Cytoskeleton* 22:127-34.
- Sanford P, Ormsby I, Gittenberger-de Groot AC, Sariola H, Friedman R, Boivin GP, Lou Cardell E, Doetschman T. 1997. TGFb2 knockout mice have multiple developmental defects that are nonoverlapping with other TGFb knockout phenotypes. *Development* 124, 2659-70.
- Shattil SJ, Kim C, Ginsberg MH. 2010. The final steps of integrin activation: the end game. *Nat Rev Mol Cell Biol* 11:288-300.
- Sherman LS, Gutmann DH. 2001. Merlin: hanging tumor suppression on the Rac. *Trends Cell Biol* 11:442–444.
- Simons PC, Pietromonaco SF, ReczekD, Bretscher A, Elias L. 1998. C-terminal threonine phosphorylation activates ERM proteins to link the cell's cortical lipid bilayer to the cytoskeleton. *Biochem Biophys Res Commun* 253:561-5.
- Smith CL, Tallquist MD. 2010. PDGF function in diverse neural crest cell populations. *Cell Adh Migr* 4:561-66.
- Snarr BS, Kern CB, Wessels A. 2008. Origin and fate of cardiac mesenchyme *Dev Dyn* 237:2804-2819.
- Soriano P. 1997. The PDGF alpha receptor is required for neural crest cell development and for normal patterning of the somites. *Development* 124: 2691–700.
- Stoller JZ, Epstein JA. 2005. Cardiac neural crest. *Semin Cell Dev Biol* 16:704-15.

- Sun CX, Robb VA, Gutmann DH. 2002. Protein 4.1 tumor suppressors: getting a FERM grip on growth regulation. *J Cell Sci* 115:3991-4000.
- Takada Y, Ye X, Simon S. 2007. The integrins. *Genome Biol* 8:215.
- Tchaicha JH, Mobley AK, Hossain MG, Aldape KD, McCarty JH. 2010. A mosaic mouse model of astrocytoma identifies alphavbeta8 integrin as a negative regulator of tumor angiogenesis. *Oncogene* 29:4460-72.
- Teckchandani A, Toida N, Goodchild J, Henderson C, Watts J, Wollscheid B, Cooper JA. 2009. Quantitative proteomics identifies a Dab2/integrin module regulating cell migration. *J Cell Biol* 186:99-111.
- Thiery JP. 2003. Cell adhesion in development: a complex signaling network. *Curr Opin Genet Dev* 13:365-71.
- Tran YK, Bogler O, Gorse KM, Wieland I, Green MR, Newsham IF. 1999. A novel member of the NF2/ERM/4.1 superfamily with growth suppressing properties in lung cancer. *Cancer Res* 59:35-43.
- van der Flier A, Badu-Nkansah K, Whittaker CA, Crowley D, Bronson RT, Lacy-Hulbert A, Hynes RO. 2010. Endothelial alpha5 and alphav integrins cooperate in remodeling of the vasculature during development. *Development* 137:2439-49.
- van Hangel J, D'Hooge P, Hooghe B, Wu X, Libbrecht L, De Vos R, Quondamatteo F, Klempt M, Brakebusch C, van Roy F. 2008. Continuous cell injury promotes hepatic tumorigenesis in cdc42-deficient mouse liver. *Gastroenterology* 134:781-92.

- Walensky LD, Blackshaw S, Liao D, Watkins CC, Weier HUG, Parra M, Huganir RL, Conboy JG, Mohandas N, Snyder SH. 1999. A novel neuron-enriched homolog of the erythrocyte membrane cytoskeletal protein 4.1. *J Neurosci* 19:6457-67.
- Walensky LD, Shi ZT, Blackshaw S, DeVries AC, Demas GE, gascard P, Nelson RJ, Conboy JG, Rubin EM, Snyder SH, Mohandas N. 1998. Neurobehavioral deficits in mice lacking the erythrocyte membrane cytoskeletal protein 4.1. *Curr Biol* 8:1269-72.
- Wang H, Liu C, Debnath G, Baines AJ, Conboy JG, Mohandas N, An X. 2010. Comprehensive characterization of expression patterns of protein 4.1 family members in mouse adrenal gland: implications for functions. *Histochem Cell Biol* 134:411-20.
- Webb DJ, Parsons T, Horwitz AF. 2002. Adhesion assembly, disassembly and turnover in migrating cells-over and over again. *Nat Cell Biol* 4:E97-100.
- Wegener KL, Partridge AW, Han J, Pickford AR, Liddington RC, Ginsberg MH, Campbell ID. 2007. Structural basis of integrin activation by talin. *Cell* 128:171-82.
- Wong SY, Haack H, Kissil JL, Barry M, Bronson RT, Shen SS, Whittaker CA, Crowley D, Hynes RO. 2007. Protein 4.1B suppresses prostate cancer progression and metastasis. *Proc Natl Acad Sci U S A* 104:12784-9.
- Wurdak H, Ittner LM, Lang KS, Leveen P, Suter U, Fischer JA, Karlsson S, Born W, Sommer L. 2005. Inactivation of TGFbeta signaling in neural crest stem cells

- leads to multiple defects reminiscent of diGeorge syndrome. *Genes Dev* 19:530-5.
- Xu W, Coll JL, Adamson ED. 1998. Rescue of the mutant phenotype by reexpression of full-length vinculin in null F9 cells: effects on cell locomotion by domain deleted vinculin. *J Cell Sci* 111:1535-44.
- Yang HS, Hinds PW. 2003. Increased Ezrin expression and activation by CDK5 coincident with acquisition of the senescent phenotype. *Mol Cell* 11:1163-76.
- Yawata, Y. 2003. *Cell membrane: red blood cell as a model*. Weinheim, Germany: Wiley-VCH..
- Yi C, McCarty JH, Troutman SA, Eckman MS, Bronson RT, Kissil JL. 2005. Loss of the putative tumor suppressor band 4.1B/Dal1 gene is dispensable for normal development and does not predispose to cancer. *Mol Cell Biol* 25:10052-9.
- Zamir, E, Geiger B. 2001. Molecular complexity and dynamics of cell-matrix adhesion. *J Cell Sci* 114:3583-90.
- Zhang X, Jiang G, Cai Y, Monkley SJ, Critchley DR, Sheetz MP. 2008. Talin depletion reveals independence of initial cell spreading from integrin activation and traction. *Nat Cell Biol* 9:1062-8.
- Zhu J, Motejlek K, Wang D, Zang K, Schmidt A, Reichardt LF. 2002. $\beta 8$ integrins are required for vascular morphogenesis in mouse embryos. *Development* 129:2891-903.

Vita

Youngsin Jung, the daughter of Hyung Keun Jung and Hea Ran Chang, was born in Seoul, South Korea on November 29, 1981. Upon graduating from Chang Moon High School in Seoul, Youngsin enrolled at University of Portland in Portland, Oregon. She graduated with Maxima Cum Laude, receiving B.S. in Biology. Youngsin then enrolled in the M.D./Ph.D. program at the University of Texas Health Science Center at Houston in August, 2004. She joined the lab of Dr. Joseph McCarty at the University of Texas MD Anderson Cancer Center in July, 2007, where she studied the roles of Band 4.1B in integrin-mediated adhesion and signaling.